

**The Physical Oceanography of
Bridport Inlet, N.W.T.
Volume I of II.
Analysis and Interpretation**

Paul Greisman
Dobrocky Seatech Ltd.
Sidney, B.C. V8L 3S1

Institute of Ocean Sciences
Department of Fisheries and Oceans
Sidney, B.C. V8L 4B2

1983

**Canadian Contractor Report of
Hydrography and Ocean Sciences
No. 9**



Fisheries
and Oceans

Pêches
et Océans

Canada

Canadian Contractor Report of Hydrography and Ocean Sciences

These reports are unedited final reports from scientific and technical projects contracted by the Ocean Science and Surveys (OSS) sector of the Department of Fisheries and Oceans.

The contents of the reports are the responsibility of the contractor and do not necessarily reflect the official policies of the Department of Fisheries and Oceans.

If warranted, Contractor Reports may be rewritten for other publications series of the Department, or for publication outside the government.

Contractor Reports are produced regionally but are numbered and indexed nationally. Requests for individual reports will be fulfilled by the issuing establishment listed on the front cover and title page. Out of stock reports will be supplied for a fee by commercial agents.

Regional and headquarters establishments of Ocean Science and Surveys ceased publication of their various report series as of December 1981. A complete listing of these publications and the last number issued under each title are published in the *Canadian Journal of Fisheries and Aquatic Sciences*, Volume 38: Index to Publications 1981. The current series began with Report Number 1 in January 1982.

Rapport canadien des entrepreneurs sur l'hydrographie et les sciences océaniques

Cette série se compose des rapports non publiés réalisés dans le cadre des projets scientifiques et techniques par des entrepreneurs travaillant pour le service des Sciences et Levés océaniques (SLO) du ministère des Pêches et des Océans.

Le contenu des rapports traduit les opinions de l'entrepreneur et ne reflète pas nécessairement la politique officielle du ministère des Pêches et des Océans.

Le cas échéant, certains rapports peuvent être rédigés à nouveau de façon à être publiés dans une autre série du Ministère, ou à l'extérieur du Gouvernement.

Les rapports des entrepreneurs sont produits à l'échelon régional mais sont numérotés et placés dans l'index à l'échelon national. Les demandes de rapports seront satisfaites par l'établissement auteur dont le nom figure sur la couverture et la page de titre. Les rapports épuisés seront fournis contre rétribution par des agents commerciaux.

Les établissements des Sciences et Levés océaniques dans les régions et à l'administration centrale ont cessé de publier leurs diverses séries de rapports depuis décembre 1981. Vous trouverez dans l'index des publications du volume 38 du *Journal canadien des sciences halieutiques et aquatiques*, la liste de ces publications ainsi que le dernier numéro paru dans chaque catégorie. La nouvelle série a commencé avec la publication du Rapport n° 1 en janvier 1982.

Canadian Contractor Report of
Hydrography and Ocean Sciences
No. 9

1983

The Physical Oceanography of Bridport Inlet, N.W.T.
Volume I of II. Analysis and Interpretation

by

Paul Greisman

Dobrocky Seatech Ltd.
Sidney, B.C. V8L 3S1

for

Institute of Ocean Sciences
Department of Fisheries and Oceans
Sidney, B.C. V8L 4B2

PREFACE

This report is an analysis of data collected in Bridport Inlet in 1979 and 1980 by the Frozen Sea Research Group of the Institute of Ocean Sciences. Previous analyses were performed by R.A. Lake and by the present author and are referred to in the text. The 117 individual CTD profiles measured in 1980 are presented in Volume II. The CTD and recorded current meter data can be obtained on computer tape from the Institute of Ocean Sciences and will be deposited with the Marine Environmental Data Services (DFO-OSS) in Ottawa.

This report was written under contract number OSB 82-00220 for the Frozen Sea Research Group at the Institute of Ocean Sciences.

Copyright Minister of Supply and Services Canada - 1983

Cat. No. Fs 97-17/9

ISSN 0711-6748

Correct citation for this publication:

Greisman, P. 1983. The Physical Oceanography of Bridport Inlet, N.W.T. Volume I of II, Analysis and Interpretation. Can. Contr. Rep. Hydrogr. Ocean Sci. No. 9 (Vol. 1):163p.

TABLE OF CONTENTS

	<u>Page</u>
PREFACE	ii
TABLE OF CONTENTS	iii
TABLES	iv
FIGURE CAPTIONS	v
ABSTRACT	vii
ACKNOWLEDGEMENTS	viii
I INTRODUCTION	1
A. BATHYMETRY	1
B. INSTRUMENTATION	5
1. Current Meters	5
2. CTD's	11
3. Tide Gauges	11
4. Ultrasonic Current Meter	11
II MEASURED MEAN CIRCULATION	13
A. GEOSTROPHIC CURRENTS	13
B. CURRENT METER MEASUREMENTS	18
C. CURRENT PROFILES	33
III INFERRED CIRCULATION	36
IV ESTUARINE CIRCULATION	56
A. DYNAMICS	56
B. SALT FLUX	62
C. COMPARISON WITH 1979	65
V TIDAL OSCILLATIONS	70
VI SOME COMMENTS ON THE EFFECTS OF AN LNG TERMINAL	80
REFERENCES	82
APPENDIX A MEAN CTD PROFILES	85
APPENDIX B ULTRASONIC CURRENT METER PROFILES	129

TABLES

	<u>Page</u>
1. Current Meter Deployments.	3
2. Locations of Current Meters, Tide Gauges and CTD sites.	4
3. CTD Records - Bridport Inlet - April 1980.	7
4. Instrument Specifications.	10
5. Mean Current Vectors and their Associated Precisions.	30
6. 1980 Tidal Height Analyses - both tide gauges.	71
7. Tidal Stream Analyses for Components $> 1 \text{ cm s}^{-1}$.	74

FIGURE CAPTIONS

Page

1. Locations of current meter moorings, CTD profiles and tide gauges in Bridport Inlet, March - April 1980. 2
2. Bottom topography of Bridport Inlet (from Lake, 1979 b). 6
3. Surface geostrophic currents with precisions. The bottom is taken as the reference level where the velocity is zero. 15
4. Profiles of geostrophic shear at the Inlet entrance. 16
5.
 - a - histogram for CM 4 19
 - b - " " CM 5 20
 - c - " " CM 6 21
 - d - " " CM 7 at 12 m depth 22
 - e - " " CM 7 at 50 m depth 23
 - f - " " CM 8 at 12 m depth 24
 - g - " " CM 8 at 50 m depth 25
 - h - " " CM 9 26
 - i - " " CM 10 27
6. Monthly mean vectors recorded at the current meters. The dashed vectors refer to currents at 50 m depth. * = no direction information; ** = mean speed not significant. 29
7.
 - a - horizontal plots of temperature and salinity at 5 m depth 37
 - b - " " " " " " " " 10 m depth 38
 - c - " " " " " " " " 20 m depth 39
 - d - " " " " " " " " 30 m depth 40
 - e - " " " " " " " " 40 m depth 41
8. Vertical salinity section running nearly north-south through the Inlet entrance. 42
9. Vertical north-south section of the difference between in-situ temperature (T) and the freezing point temperature at atmospheric pressure and in-situ salinity (T_f) for 1980 (Millidegrees). 44
10. Average T, S, and σ_t profiles at 80-1. The envelopes about each dotted mean profile span all the values recorded. 48
11. Profile of the Väisälä frequency $\left(\frac{\sqrt{g}}{\rho} \frac{\partial \rho}{\partial z} \right)$ at site 80-1. The horizontal bars indicate the precision of the computed values at several depths. 50
12. The amount of salt required for convection to 50 m depth and the time required for ice growth to reject sufficient brine for convection. Section north-south through the Inlet entrance. 51
13. Vertical section of $T - T_f$ counter clockwise around the periphery of the Inlet (millidegrees). 54

FIGURE CAPTIONS (continued)Page

14. Computed thermohaline velocity profile
 $\left(u = \frac{\sqrt{2\Delta x}}{\rho} \frac{d\rho}{dx} \right)$ unbalanced for continuity. 59
15. Continuity balanced thermohaline flow, u_T . 60
16. Salinity difference, ΔS , between station 80-1 and 80-3 versus depth. 63
17. Profile of computed salt flux, $u_T \Delta S$, versus depth. 64
18. Vertical north-south section of $T - T_f$, 1979 (Millidegrees). 66
19. Mean CTD profiles from sites 80-2 and 1-79. 69
20. Profiles of the first internal mode at tidal frequency at the Inlet entrance. 75

ABSTRACT

Greisman, P. 1983. The Physical Oceanography of Bridport Inlet, N.W.T. Volume I of II: Analysis and Interpretation. Can. Contract. Rep. Hydrogr. Ocean Sci. No. 9.

Time series measurements of currents, water properties and water levels from 1979 and 1980 were analysed. The currents within the Inlet cannot be resolved adequately by direct measurement or by dynamic height computations, while the currents at the Inlet entrance rarely exceed 12 cm s^{-1} . The exchange of salt through the Inlet entrance appears to be driven by densification of the water within the Inlet due to brine rejection from growing sea ice. The convective processes are not clearly indicated by the vertical density profiles, but rather the system is dominated by horizontal advection and probably by intermittent convection. There is a very pronounced interannual variability in the vertical stratification of the Inlet.

Key words: estuarine circulation, brine rejection, convection, Arctic Oceanography, thermohaline processes.

RÉSUMÉ

Greisman, P. 1983. The Physical Oceanography of Bridport Inlet, N.W.T. Volume I of II: Analysis and Interpretation. Can. Contract. Rep. Hydrogr. Ocean Sci. No. 9.

Le présent rapport analyse les mesures par séries chronologiques des courants et des propriétés et niveaux de l'eau, en 1979 et 1980. Les courants à l'intérieur de l'inlet ne peuvent être déterminés par une mesure directe ni par le calcul de la hauteur dynamique; à l'entrée de l'inlet, la vitesse des courants dépasse rarement 12 cm s^{-1} . L'échange de sel à l'entrée de l'inlet semble provenir de la densification de l'eau à l'intérieur de l'inlet, causée par le rejet de saumure contenue dans la glace de mer en croissance. Les processus de convection ne sont pas clairement montrés par les profils verticaux de la densité, mais le système est plutôt dominé par une advection horizontale et probablement par une convection intermittente. Il existe d'une année à l'autre une variabilité très prononcée de la stratification verticale dans l'inlet.

Mots-clés: circulation estuarienne, rejet de saumure, convection, océanographie de l'Arctique, processus thermohalins.

ACKNOWLEDGMENTS

During most of the preparation of this report I shared an office with Humfrey Melling of the Frozen Sea Research Group, I.O.S. Not only did he cheerfully accept my intrusion but he provided uncounted useful suggestions in addition to invaluable inspiration.

Bob Lake patiently corrected all my misapprehensions of the data set and suffered through several verbal drafts.

Andrew Wharton performed the data analysis and tolerantly accepted my misgivings about some of the results. Through his persistence certain inadequacies in programming were rectified.

Dennis Richards drew the figures, Wendy Holmes typed the draft manuscript and Lorena Quay typed the final report.

As usual it was a pleasure to work with the members of FSRG at the Institute of Ocean Sciences.

DISCLAIMER

This report was written under contract and its contents are the responsibility of the author.

I INTRODUCTION

During March and April 1980 personnel of the Institute of Ocean Sciences (R.A. Lake, D. Richards, and R. Cooke) performed a physical oceanographic survey in Bridport Inlet, Melville Island, NWT where an LNG plant had been proposed for the Arctic Pilot Project. Previous surveys had been performed in 1978 (Greisman, 1978; Lake, 1979a) and in 1979 (Lake, 1979b,c). The data from the 1978 survey collected by Innovative Ventures of Calgary, were of doubtful quality which, in part, motivated the later program. In 1979, 2 current meters were installed at each of 3 locations, and CTD measurements were made at 8 locations. The results of the 1979 survey revealed that more intensive measurements at the entrance to Bridport Inlet were required as well as a more dense network of CTD surveys.

In 1980, 9 current meters were deployed at the locations shown in Figure 1. Two current meters were emplaced at 12 m and 50 m depth at locations 7 and 8, while at the other sites current meters were installed at 12 m depth. Table 1 lists the specifics of the current meter deployments, and Table 2 lists their geographic positions. It was hoped that the high density sampling at the Inlet entrance would resolve the details of the flow. In addition, CTD measurements were made at each of the current meter sites plus 4 additional locations (see Figure 1). The CTD measurements at the Inlet entrance were designed to determine the horizontal density gradients for dynamic computations of geostrophic flows. A total of 146 CTD measurements were made with multiple casts performed at each station. Casts were repeated at fixed time intervals at some stations to provide a time series over a tidal cycle. Table 3 lists the times and locations of the CTD casts performed. Two tide gauges were deployed; one just outside the Inlet and the other near the eastern shore. Finally, current profiles with an ultra-sonic current meter were measured at 8 locations.

A. BATHYMETRY

The bottom topography of Bridport Inlet has been described elsewhere. Figure 2 is reproduced from Lake (1979,b).

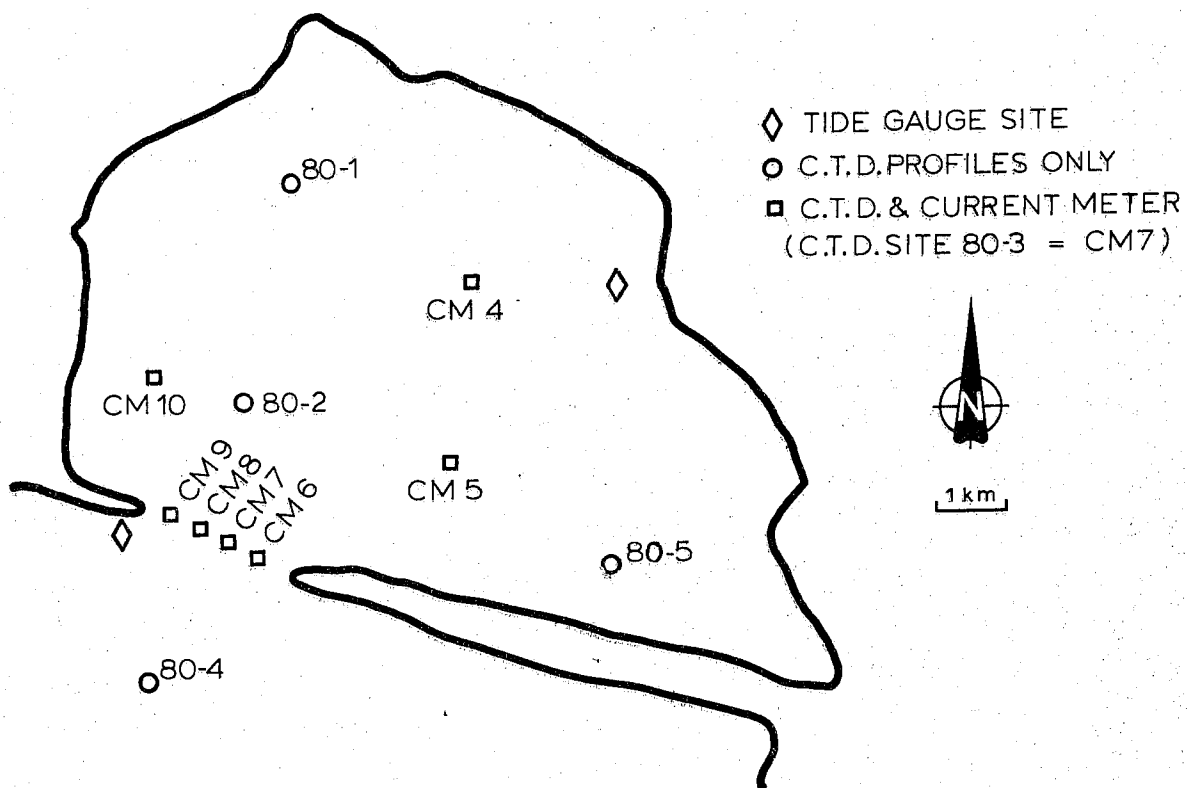


FIGURE 1. Locations of current meter moorings, CTD Profiles and tide gauges in Bridport Inlet, March - April 1980.

TABLE 1

CURRENT METER DEPLOYMENTS

Site	Meter Serial No.	Depth Metres	Deployed Time	Deployed Date	Recovered Time	Recovered Date	Record Length days-hrs;min:sec	Remarks
CM-4	3228	12	00:45:00	27-03-80	13:15:45	28-04-80	32-12:30:45	
CM-5	1936	12	15:30:00	27-03-80	14:45:44	28-04-80	31-23:15:44	Note 3
CM-6	3223	12	19:16:00	27-03-80	16:45:50	28-04-80	31-21:29:50	Note 4
CM-7	1930	50	23:00:00	27-03-80	18:45:22	28-04-80	31-20:45:22	:
CM-7	1932	12	02:45:00	28-03-80	18:30:42	28-04-80	31-15:45:42	
CM-8	2466	50	20:15:00	28-03-80	20:00:32	28-04-80	30-23:45:32	63
CM-8	3387	12	18:45:00	28-03-80	20:15:46	28-04-80	31-01:30:46	
CM-9	1931	12	21:15:00	28-03-80	21:31:04	28-04-80	31-00:16:04	
CM-10	1939	12	00:45:00	29-03-80	15:01:09	29-04-80	31-14:16:09	

Note 1: Dates and times are Universal Coordinated Time (G.M.T.).

Note 2: Times are given for first and last valid record.

Note 3: Direction vane gave unreliable results.

Note 4: Clock lost 4 hours during recording period of 4.72 seconds/scan.

TABLE 2

LOCATIONS OF TIDE GAUGES, CURRENT METERS AND CTD SITES

SITE	UTM COORDINATES ZONE 12		GEOGRAPHIC COORDINATES	
	N	E	N	W
TG - 1	8,324,300	561,050	74°59'54"	108°53'08"
TG - 3	8,328,375	569,250	75°01'54"	108°35'50"
CM - 4	8,328,650	566,550	75°02'06"	108°41'20"
- 5	8,325,300	566,250	75°00'18"	108°42'20"
- 6	8,323,775	562,950	74°59'34"	108°49'18"
- 7	8,323,950	562,525	74°59'40"	108°50'03"
- 8	8,324,100	562,140	74°59'44"	108°50'55"
- 9	8,324,250	561,750	74°59'50"	108°51'40"
-10	8,326,650	561,100	75°01'08"	108°52'52"
80 - 1	8,330,075	563,025	75°02'56"	108°48'40"
- 2	8,326,200	563,225	75°00'51"	108°48'30"
- 3	8,323,950	562,525	74°59'40"	108°50'03"
- 4	8,321,050	561,200	74°58'08"	108°53'02"
- 5	8,323,525	568,600	74°59'18"	108°37'36"
UCM - 1	8,325,500	561,375	75°00'30"	108°52'20"
- 2	8,324,650	564,650	74°59'58"	108°45'35"
- 3	8,326,650	569,225	75°00'58"	108°36'00"

B. INSTRUMENTATION

1. Current Meters

The current meters used in the survey were Aanderaa model RCM-4 equipped with speed and direction sensors as well as temperature and conductivity sensors. Data were recorded internally every 15 minutes on magnetic tape. The instrument counts the number of rotor revolutions during the sampling interval so that an average current speed can be computed. On the other hand, direction, temperature and conductivity are instantaneous values. In the data processing the two direction measurements bracketing the speed averaging interval are averaged to produce a direction coincident with the mid-point of sampling interval.

The Savonius rotors have the unfortunate characteristic of stalling at a current speed of 2.2 cm s^{-1} . While normally insignificant in most of the world's oceans, the current speeds encountered in the Canadian Archipelago often are too weak to be sensed with the Aanderaa instrument. The percentage of records for which the current speeds were below the stall speed of instrument are shown in Table 5 in section II.B. Particularly for current meters 4 and 10, located within the Inlet, the speed records can convey no sense of the flow.

The standard Aanderaa direction vane was replaced with a Hydro Products vane mounted below the current meter pressure case in order to facilitate deployment through the ice. The vane responds to current direction at speeds considerably below the stall speed of the rotor.

CTD casts were taken at each mooring site to calibrate the current meter temperature and conductivity sensors.

The ranges, resolutions and accuracies for the variables measured by the Aanderaa instruments are shown in Table 4.

Moorings for the current meters were required to be torsionally rigid to provide a constant orientation. This is a standard procedure in proximity to the magnetic pole where compasses are useless. The 12 m depth meters were suspended from the sea ice by hydraulic hose

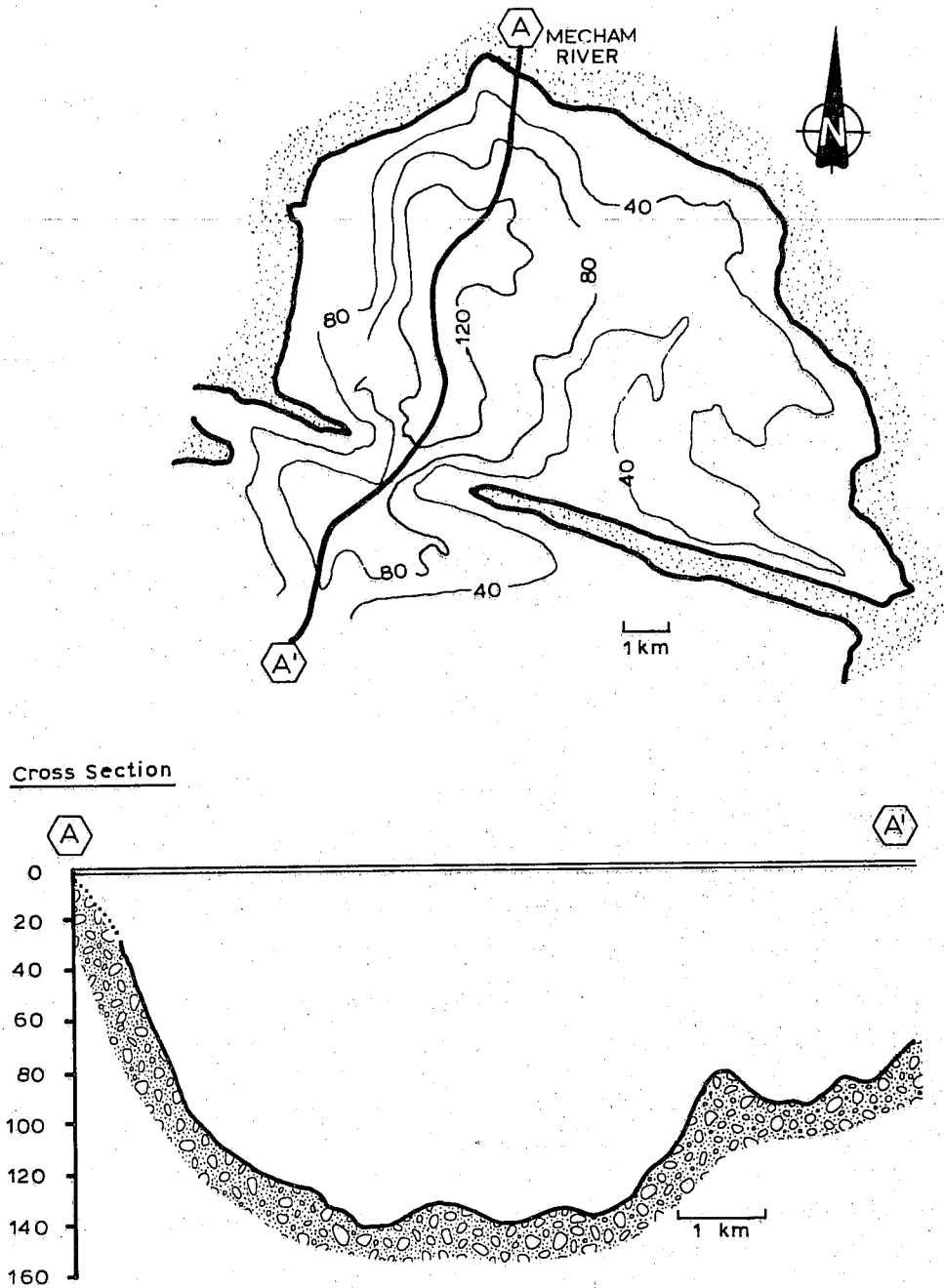


FIGURE 2. Bottom topography of Bridport Inlet (from Lake, 1979 b),

TABLE 3

CTD RECORDS - BRIDPORT INLET - APRIL 1980

<u>NO.</u>	<u>SITE</u>	<u>RANGE</u>	<u>DEPTH</u>	<u>G.M.T.</u>	<u>DATE</u>	<u>REMARKS</u>
3300	CM-10	2-61 m	65 m	18:06	30/03	Bottle sample
3301	CM-10	2-60	65	20:35	30/03	CM-10 Calibr.
3302	CM-10	2-61	65	20:41	30/03	CM-10 Calibr.
3303	CM-9	2-45	50	23:00	30/03	CM-9 Calibr.
3304	CM-9	2-45	50	23:15	30/03	CM-9 Calibr.
3305	CM-9	2-45	50	23:30	30/03	CM-9 Calibr.
3306	CM-8	2-80	80	13:20	31/03	Ice in C cell
3307	CM-8	2-75	80	13:35	31/03	CM-8 Calibr.
3308	CM-8	2-76	80	13:45	31/03	CM-8 Calibr.
3309	CM-7	2-100	109	18:30	31/03	Ice in C cell
3310	CM-7	2-100	109	18:45	31/03	Bottle sample
3311	CM-7	2-100	109	19:00	31/03	CM-7 Calibr.
3312	CM-6	2-20	26	20:00	31/03	Ice in C cell
3313	CM-6	2-20	26	20:15	31/03	CM-6 Calibr.
3314						Delete
3315	CM-6	2-20	26	20:32	31/03	CM-6 Calibr.
3316						Delete
3317	CM-5	2-25	28	17:32	01/04	Ice in C cell
3318	CM-5	2-26	28	17:45	01/04	Ice in C cell
3319	CM-5	2-25	28	17:50	01/04	CM-5 Calibr.
3320	CM-5	2-25	28	17:52	01/04	CM-5 Calibr.
3321	CM-5	2-25	28	18:00	01/04	CM-5 Calibr.
3322	CM-4	2-59	62	15:30	02/04	CM-4 Calibr.
3323	CM-4	2-58	62	15:45	02/04	CM-4 Calibr.
3324	CM-4	2-58	62	16:00	02/04	CM-4 Calibr.
3325	80-1	2-110	(120)	01:45	06/04	Ice in C cell
3326	80-1	2-110	(120)	01:55	06/04	
3327	80-1	2-110	(120)	02:05	06/04	
3328	80-1	2-110	(120)	02:15	06/04	
3329	80-2	2-100	(137)	17:05	07/04	Ice in C cell
3330	80-2	2-101	(137)	17:10	07/04	
3331	80-2	2-125	(137)	17:25	07/04	
3332	80-2	2-130	(137)	17:50	07/04	
3333	80-2	2-130	(137)	19:20	07/04	
3334						Delete
3335	80-2	2-131	(137)	20:23	07/04	
3336	80-2	2-130	(137)	21:23	07/04	
3337	80-2	2-130	(137)	21:40	07/04	
3338	80-2	2-130	(137)	22:00	07/04	
3339	80-2	2-130	(137)	22:20	07/04	
3340	80-2	2-130	(137)	22:40	07/04	Bottle sample
3341	80-2	2-130	(137)	23:00	07/04	
3342	80-2	2-130	(137)	23:20	07/04	
3343	80-3	2-100	109	16:25	08/04	
3344	80-3	2-100	109	16:40	08/04	
3345	80-3	2-100	109	17:00	08/04	
3346	80-3	2-100	109	17:20	08/04	

<u>NO.</u>	<u>SITE</u>	<u>RANGE</u>	<u>DEPTH</u>	<u>G.M.T.</u>	<u>DATE</u>	<u>REMARKS</u>
3347	80-3	2-101 m	109 m	17:40	08/04	
3348	30-3	2-100	109	18:00	08/04	
3349	80-3	2-100	109	18:20	08/04	
3350	80-3	2-100	109	18:40	08/04	
3351	80-3	2-100	109	19:00	08/04	
3352	80-3	2-100	109	19:20	08/04	
3353	80-3	2-100	109	19:40	08/04	
3354	80-3	2-100	109	20:00	08/04	
3355	80-3	2-100	109	20:20	08/04	
3356	80-3	2-100	109	20:40	08/04	
3357	80-3	2-100	109	21:00	08/04	
3358	80-3	2-100	109	21:20	08/04	
3359						Delete
3360	80-3	2-100	109	21:40	08/04	
3361	80-3	2-100	109	22:00	08/04	
3362	80-3	2-100	109	22:20	08/04	
3363	80-3	2-100	109	22:40	08/04	
3364	80-3	2-100	109	23:00	08/04	
3365	80-3	2-100	109	23:20	08/04	
3366	80-3	2-100	109	23:40	08/04	
3367	80-3	2-100	109	00:00	09/04	
3368	80-3	2-100	109	00:20	09/04	
3369	80-3	2-100	109	00:40	09/04	
3370	80-3	2-100	109	01:00	09/04	
3371	80-3	2-101	109	01:20	09/04	
3372	80-3	2-101	109	01:40	09/04	
3373	80-3	2-100	109	02:00	09/04	
3374	80-4	2-60	64	16:40	09/04	
3375	80-4	2-60	64	17:40	09/04	
3376	80-4	2-60	64	18:40	09/04	
3377	80-4	2-61	64	19:40	09/04	
3378	80-4	2-60	64	20:40	09/04	
3379	80-4	2-60	64	21:40	09/04	
3380	80-4	2-60	64	22:40	09/04	
3381	80-4	2-60	64	23:40	09/04	
3382	80-4	2-60	64	00:40	10/04	
3383	80-4	2-60	64	01:40	10/04	
3384	80-4	2-60	64	02:40	10/04	
3385	80-3	2-100	109	15:49	10/04	
3386	80-2	2-130	(137)	17:52	10/04	
3387	80-1	2-100	(120)	20:30	10/04	
3388	80-5	2-65	74	17:15	12/04	
3389	80-5	2-65	74	17:55	12/04	
3390	80-5	2-65	74	18:01	12/04	
3391	CM-4	2-58	62	17:00	22/04	
3392	CM-4	2-58	62	17:15	22/04	
3393	CM-4	2-58	62	17:30	22/04	
3394	CM-5	2-25	28	16:00	23/04	Ice in C cell
3395	CM-5	2-25	28	16:15	23/04	
3396	CM-5	2-25	28	16:30	23/04	

<u>NO.</u>	<u>SITE</u>	<u>RANGE</u>	<u>DEPTH</u>	<u>G.M.T.</u>	<u>DATE</u>	<u>REMARKS</u>
3397	CM-5	2-25 m	28 m	16:45	23/04	
3398	CM-6	2-22	26	19:00	23/04	
3399	CM-6	2-22	26	19:15	23/04	
3400	CM-6	2-22	26	19:30	23/04	
3401	CM-7	2-100	109	21:00	23/04	
3402	CM-7	2-100	109	21:15	23/04	
3403	CM-7	2-100	109	21:30	23/04	
3404	CM-7	5-63	109	21:45	23/04	Bottle Sample
3405	CM-7	2-100	109	22:30	23/04	CTD No. 2
3406	CM-7	2-100	109	22:45	23/04	CTD No. 2
3407	CM-7	2-100	109	23:15	23/04	
3408	CM-8	2-80	80	14:30	24/04	
3409	CM-8	2-80	80	14:45	24/04	
3410	CM-8	2-80	80	15:00	24/04	
3411	CM-9	2-45	50	16:00	24/04	
3412	CM-9	2-45	50	16:15	24/04	
3413	CM-9	2-45	50	16:30	24/04	
3414	CM-10	2-61	65	17:45	24/04	
3415	CM-10	2-61	65	18:00	24/04	
3416	CM-10	2-61	65	18:15	24/04	

TABLE 4

INSTRUMENT SPECIFICATIONSAANDERAA RCM-4

VARIABLE	RANGE	RESOLUTION	ACCURACY
Speed	2.2 to 45 cm s ⁻¹	0.04 cm s ⁻¹	
Direction	0 to 360°	0.35°	±7°
Temperature	-2° to +3°C	0.005°C	0.015°C
Conductivity	23 to 30.7 mmho/cm	0.007 mmho/cm (0.01 ‰)	±0.075 mmho/cm (±0.1 ‰)

Sample interval = 15 minutes

GUILDLINE CTD 8101A

Salinity	28 to 40 PPT	0.001 ‰	±0.005 ‰
Temperature	-2° to +30°C	0.001°C	±0.002°C
Pressure	0 to 1000 db	0.1 db	±1.0% of reading

AANDERAA WLR-5 WATER LEVEL RECORDER

Height of Water Column	2.7 mm	±27 mm
Time	0.5 s	±1 s d ⁻¹

Sample interval = 5 minutes

while the instruments at 50 m depth were mounted on a 3 m long horizontal spreader bar which was suspended by two lines anchored 15 m apart in the ice.

2. CTDs

CTD profiles were measured with a Guildline Model 8101A instrument. Water samples were taken frequently and salinity determined with a Hytech 6220 bench salinometer in order to monitor the performance of the conductivity cell. In addition, in-situ calibrations of the CTD temperature sensor were performed using previously calibrated thermistors. Details of the CTD calibration procedure may be found in Lewis and Sudar (1972), while salinity and density computations are discussed in Volume II.

3. Tide Gauges

Two Aanderaa WLR 5 tide gauges were deployed for a one month period at the locations shown in Figure 1 and listed in Table 2. The sampling interval was 5 minutes. No attempt was made to correct the water level data for variations in the atmospheric pressure.

4. Ultra-sonic current meter

Measurements were made with a prototype instrument developed by the Christian Mikkelsen Institute in Norway. This instrument measures the differences in travel time of an acoustic pulse between two orthogonal sets of transmitter receivers. The pulses are reflected off an acoustic mirror displaced vertically from the transmitter-receiver in order to remove the bias of a vertical flow component. The threshold of this instrument is about 1 mm s^{-1} while its accuracy varies with duration of deployment due to electronic drift. For a one hour deployment the accuracy is better than $\pm 3 \text{ mm s}^{-1}$.

In the field, the instrument was "zeroed" in the hole drilled through the sea ice with a cap covering the sensors for each profile. It was then lowered to predetermined depths and the induced turbulence permitted to dissipate. Readings were then made over about a 30 second time interval. Two profiles were measured with the instrument on a

torsionally-rigid aluminum pipe supplying directional data while an average of four profiles were measured at 8 sites with the instrument lowered on a cable. The latter profiles furnish speed versus depth data only.

II MEASURED MEAN CIRCULATION

Current meters were deployed in Bridport Inlet at the end of March 1980; their locations are shown in Figure 1 and the details of the deployment in Table 1. The meters recorded, on the average, about 30 days of data. The data were plotted as time series and de-spiked. Progressive vector diagrams were constructed in order to aid in interpretation and mean flows over the period of deployment were computed.

Examination of the records revealed that the current speeds were often below the stall speed of the Aanderaa rotors (2.2 cm s^{-1}). Rather than assign the resolvable speed to every record below stall speed, it was considered more representative to assign a value of 1.1 cm s^{-1} (halfway between zero and stall speed) to these records. The resulting current vectors are shown in Figure 6 and tabulated in Table 5.

CTD measurements were made at all the current meter sites as well as at five additional locations denoted 80-1 through 80-5. The locations of the CTD stations are shown in Figure 1 and listed in Table 2. At all the locations multiple CTD casts were taken. Time series measurements (e.g. CTD casts every twenty minutes for $9\frac{1}{2}$ hours at site 80-3) were performed at several locations over the period from the end of March to the end of April. A list of all the CTD measurements performed is presented as Table 3. The individual CTD profiles are reproduced in Volume 2 and the average CTD profiles at each location are reproduced in Appendix A.

A. GEOSTROPHIC CURRENTS

In order to describe quantitatively the circulation in Bridport Inlet, the mass field measurements were used to compute geostrophic shears. In addition an attempt was made to reference the computed shears with the measured currents.

Dynamic heights were computed at each station using an average of all the CTD casts at that location. Geostrophic shears were then computed between each station pair. There are however, important limitations on the use of the dynamic method in Bridport Inlet.

By far the most important of these is the presence of relatively weak horizontal density gradients.

The geostrophic shear is computed from the vertical derivative of the horizontal equations of motion.

$$f\hat{k} \times \bar{u} = -\frac{1}{\rho} \nabla p \quad (1)$$

are the horizontal equations of motion of a geostrophic fluid, where f is the Coriolis parameter, \hat{k} is the vertical vector, \bar{u} is the velocity vector, ρ the fluid density and ∇p the horizontal pressure gradient. The z derivative of (1) is

$$\frac{d\rho}{dz} f\hat{k} \times \bar{u} + \rho f\hat{k} \times \frac{d\bar{u}}{dz} = +g \nabla \rho \quad (2)$$

The first term on the left hand side is at most 1% of the second term in the ocean, and when it is ignored the relationship used to compute geostrophic shears results:

$$\rho f\hat{k} \times \frac{d\bar{u}}{dz} = g \nabla \rho \quad (3)$$

The precision with which (3) is evaluated is determined by the precision with which the horizontal density gradient and the station spacing can be measured. Within Bridport Inlet the station spacing is roughly 1 km, while the density can be resolved to about $\pm 2 \times 10^{-3} \text{ kg m}^{-3}$. Using typical numerical values,

$$\frac{d\bar{u}}{dz} = \frac{10 \text{ m s}^{-2} (\delta\rho \pm 2 \times 10^{-3} \text{ kg m}^{-3})}{10^3 \text{ kg m}^{-3} (1.4 \times 10^{-4} \text{ s}^{-1}) (1 \times 10^3 \text{ m})}$$

$$\frac{d\bar{u}}{dz} = 7.2 \times 10^{-2} (\delta\rho \pm 2 \times 10^{-3}) \text{ s}^{-1}$$

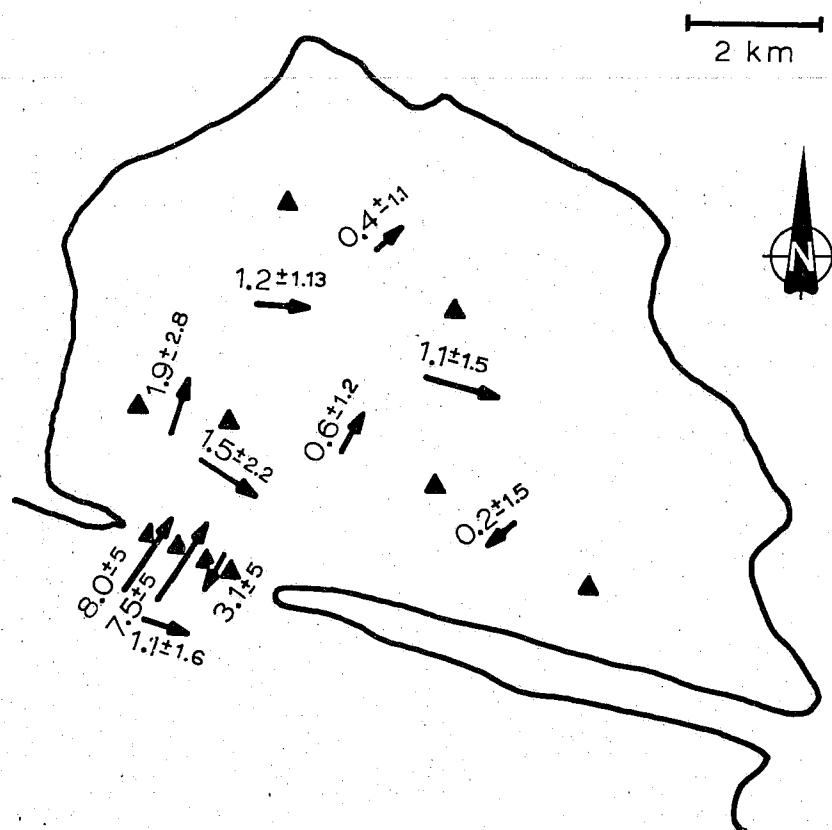


FIGURE 3. Surface geostrophic currents with precisions. The bottom is taken as the reference level where the velocity is zero.

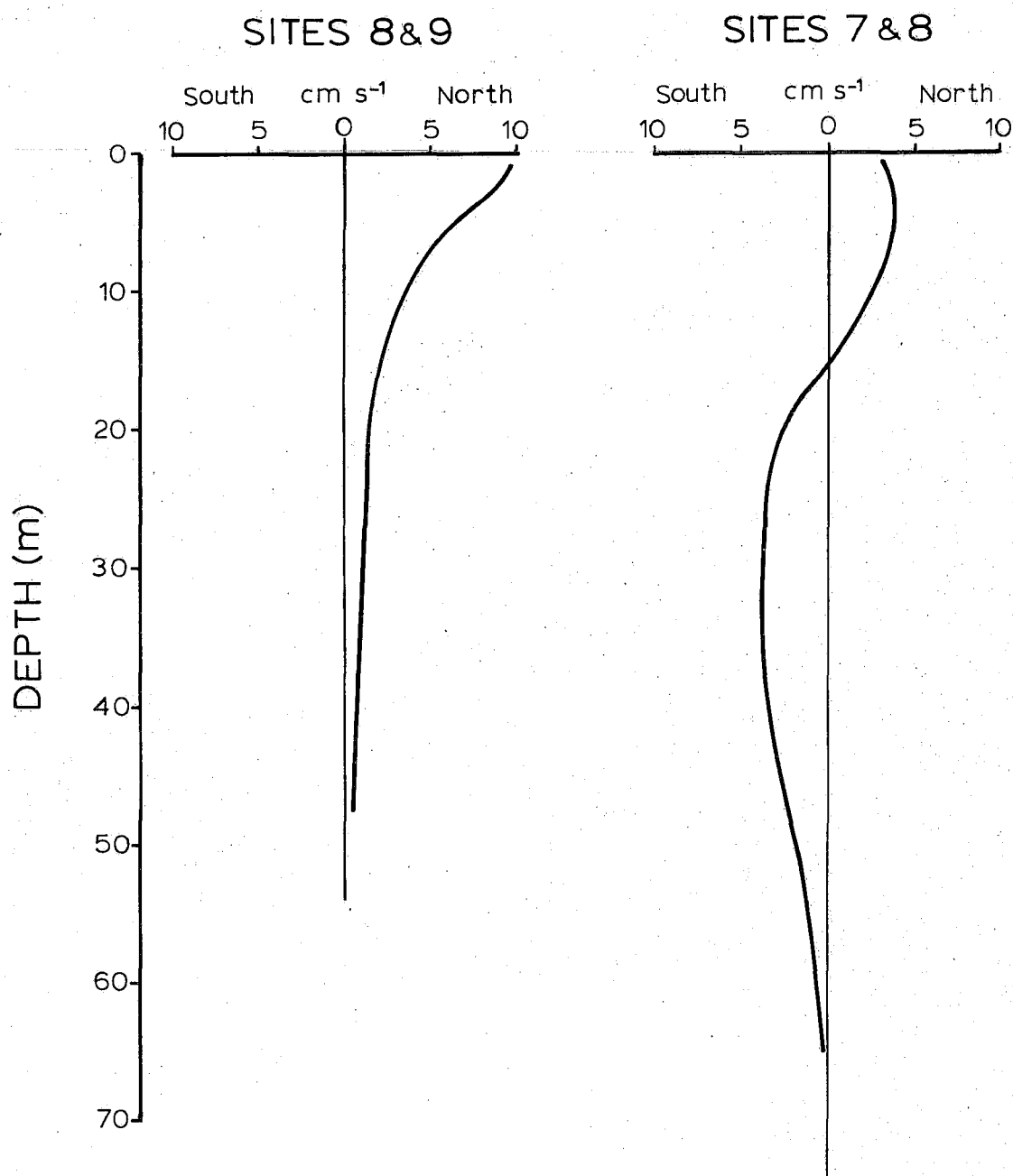


FIGURE 4. Profiles of geostrophic shear at the Inlet entrance.

The precision of the computed vertical shear is therefore $\pm 1.4 \times 10^{-4} \text{ s}^{-1}$. For a water column 100 m deep, the precision of the computed surface velocity is therefore

$$\pm 1.4 \times 10^{-2} \text{ m s}^{-1} \text{ or } \pm 1.4 \text{ cm s}^{-1}$$

The computed geostrophic surface flows using the bottom as the level of no motion are shown in Figure 3. The precisions vary due to varying station spacings. With the exception of the flows at the Inlet entrance, the computed geostrophic current magnitudes are all smaller than the associated precisions. No conclusion should be drawn therefore from the currents computed within the Inlet. Not only are the magnitudes of these flows poorly determined, but their directions too may be in error.

Significant geostrophic shears were computed at the entrance between current meter sites 7, 8 and 9 and these profiles are shown in Figure 4. The flow at the entrance is characterized by a vertical shear directed into the Inlet at the top of the water column. In order to satisfy the continuity constraint a barotropic (constant with depth) mean flow must be added. The vertical shear however, is concentrated in the interval between 10 and 25 m depth so that it is within this depth range where a reversal of the mean flow direction is expected. The total velocity difference through the water column is about 8 cm s^{-1} .

The computations suggest inward flowing surface waters with a weak outward flow at depth. Such a flow is characteristic of a "negative estuary" or a basin in which densification takes place either due to evaporation (as in the Mediterranean Sea) or to brine rejection by growing sea ice.

B. CURRENT METER MEASUREMENTS

The histograms for the 9 current meter velocity time series are shown in Figures 5a through i. The maximum speeds recorded are about 16 cm s^{-1} at the current meters at 12 m depth in the Inlet entrance. Most of the histograms show predominantly bi-directional flow suggestive of tidal oscillations. (Tidal flows are discussed in Section V.) The histogram for current meter 5 shows no currents flowing in any but the $070^\circ - 130^\circ$ sextant. This narrow range of indicated direction is almost certainly due to a malfunctioning vane. In addition, a profile measured with an ultrasonic current meter at site 5 showed the flow direction to be about 230°T , while the speeds were in agreement with the Aanderaa current meter. The data from C.M. 5 are, therefore, indicative of speed only.

Table 5 is a summary of the mean current vectors computed at each of the current meters. Included in the table is the percentage of speed records below the threshold speed of the Savonius rotor. This percentage can have a significant influence on the precision to which the average current vectors are known.

If p is the fraction of current records below stall speed, and S is the stall speed, then the maximum value of the true average current speed (\bar{V}_{max}) is

$$\bar{V}_{\text{max}} = \bar{V}_a (1 - p) + Sp$$

where \bar{V}_a is the average of the speeds above stall speed. The minimum value is

$$\bar{V}_{\text{min}} = \bar{V}_a (1 - p),$$

since the speed may lie anywhere in the interval $(0 < V \leq S)$. The mean expected speed is, therefore

$$\bar{V}_{\text{mean}} = \bar{V}_a (1 - p) + \frac{S}{2} P.$$

If it is assumed that the speeds are normally distributed on the interval $(0, S)$ then ± 3 standard deviations cover 98% of the interval. The 95% confidence interval for the speed in the range below rotor

FREQUENCY DISTRIBUTION OF DIRECTION AND RATE

BRD 12 4500270380 GMT CM-4 3123 BRIDPORT INLET 75021108413 15 3228TCTV6																											
		CMS/SEC																									
		2.3	3	4	5	6	7	8	9	10	11	12	13	14	15	16	17	18	19	20	21	22	23	24	25	26	
DIR		T0	T0	T0	T0	T0	T0	T0	T0	T0	T0	T0	T0	T0	T0	T0	T0	T0	T0	T0	T0	T0	T0	T0	T0	T0	
		2.9	4	5	6	7	8	9	10	11	12	13	14	15	16	17	18	19	20	21	22	23	24	25	26	27	
0- 9		3	17	15	2																						37
10- 19		1	15	4	2																						22
20- 29		4	1	5	1																						11
30- 39		7	3	5																							15
40- 49		3	9	14	2																						28
50- 59		3	12	5	2																						22
60- 69		5	3																								8
70- 79		2	2																								4
80- 89		3																									3
90- 99		3																									3
100-109		5																									5
110-119		2																									2
120-129		2																									2
130-139		7	11																								18
140-149		4																									4
150-159		2	7																								9
160-169		1	9	1																							11
170-179		3	3	8	27																						41
180-189		10	9	16	34																						69
190-199		5	21	3	6																						35
200-209		3	21	9	7																						40
210-219		10	38	13	3																						64
220-229		8	27																								35
230-239		7	13	1																							21
240-249		8	13	9																							30
250-259		8	6	11																							25
260-269		1	1	4																							6
270-279																											0
280-289		2																									2
290-299		1																									1
300-309																											0
310-319		3	1																								4
320-329		2	1	2																							5
330-339		4	8	12	2																						26
340-349		5	8	10	3																						26
350-359		7	25	26	4																						62
		285	95																								699
		144	175																								
NUMBER OF RECORDS AT OR BELOW STALL SPEED (2.2 CM/SEC) 2424																											

Figure 5a. Histogram for CM 4

FREQUENCY DISTRIBUTION OF DIRECTION AND RATE

BRD 12		3015270360 GMT CM-5 3070 BRIDPORT INLET										75003108423 15 1936TCTV6															
		CMS/SEC																									
		2.3	3	4	5	6	7	8	9	10	11	12	13	14	15	16	17	18	19	20	21	22	23	24	25	26	
		T0	T0	T0	T0	T0	T0	T0	T0	T0	T0	T0	T0	T0	T0	T0	T0	T0	T0	T0	T0	T0	T0	T0	T0	T0	
DIR		2.9	4	5	6	7	8	9	10	11	12	13	14	15	16	17	18	19	20	21	22	23	24	25	26	27	
0- 9																											0
10- 19																											0
20- 29																											0
30- 39																											0
40- 49			2																								2
50- 59																											0
60- 69										1																	1
70- 79		1	4	5	17	22	25	24	2																		100
80- 89		56	66	115	114	96	84	45	17	4																	597
90- 99		23	39	32	68	49	44	27	11	10	2																305
100-109		41	44	64	69	51	50	41	29	14	13	13	4	1													434
110-119		24	20	9	16	16	24	32	30	9	12	10	3	1													206
120-129		7	10	13	19	20	31	29	22	15	11	3															180
130-139																											0
140-149																											0
150-159																											0
160-169																											0
170-179																											0
180-189																											0
190-199																											0
200-209																											0
210-219																											0
220-229																											0
230-239																											0
240-249																											0
250-259																											0
260-269																											0
270-279																											0
280-289																											0
290-299																											0
300-309																											0
310-319																											0
320-329																											0
330-339																											0
340-349																											0
350-359																											0
		185	303	258	112	38	7	0	0	0	0	0	0	0	0	0	0	0	0	0	0	0	0	0	0	0	1825
		152	238	254	198	52	26	2	0	0	0	0	0	0	0	0	0	0	0	0	0	0	0	0	0	0	0
NUMBER OF RECORDS AT OR BELOW STALL SPEED (2.2 CM/SEC)		1245																									

Figure 5b. Histogram for CM 5

FREQUENCY DISTRIBUTION OF DIRECTION AND RATE

BRD 12		1619270380 GMT CM-6										3046 BRIDPORT INLET										74596109493 15 3223TCTV6									
		CMS/SEC																													
		2.3	3	4	5	6	7	8	9	10	11	12	13	14	15	16	17	18	19	20	21	22	23	24	25	26					
DIR		TO 2.9	TO 4	TO 5	TO 6	TO 7	TO 8	TO 9	TO 10	TO 11	TO 12	TO 13	TO 14	TO 15	TO 16	TO 17	TO 18	TO 19	TO 20	TO 21	TO 22	TO 23	TO 24	TO 25	TO 26	TO 27					
0- 9		5	15	16	38	51	40	45	46	33	11	4																304			
10- 19		9	16	30	31	45	37	48	42	16	8	6																288			
20- 29		9	19	21	37	45	38	33	28	18	6	4	2	1														261			
30- 39		4	14	28	25	25	27	24	28	21	4		1															201			
40- 49		4	3	3	5	8	10	9	15	6	1	1																65			
50- 59		4	2	4	4	5	3	2	6	4	3	1																38			
60- 69		4	1		1		1	2	4			1																14			
70- 79		2			1			1																				4			
80- 89		1																										1			
90- 99		1	1	1					1																			4			
100-109		1					1																					2			
110-119		1																										1			
120-129																												0			
130-139		1																										1			
140-149		1	1		1																							3			
150-159					1																							1			
160-169																												0			
170-179			5																									5			
180-189		4		3		1																						8			
190-199		3	2	2	2		1																					10			
200-209		6	7	6	1	1		4	1																			26			
210-219		4	7	9	3	7	2	2	3	1	1																	39			
220-229		7	10	9	25	34	15	20	12	4	1	1	1															139			
230-239		11	12	21	30	51	33	27	26	9	2	2																224			
240-249		14	24	34	52	38	25	26	18	10	2																	243			
250-259		9	27	25	42	22	15	9	10	12	3																	174			
260-269		11	23	17	16	13	8	4	2	2																		96			
270-279		6	12	10	8	4	2	2																				44			
280-289		5	11	4	3	1																						24			
290-299		6	5	11	3		1																					26			
300-309		8	4	10	6	1	2																					31			
310-319		2	4	3	6	3																						18			
320-329		7	13	16	7	5	1	2	1																			52			
330-339		4	6	16	16	11	9	6	7	3																		78			
340-349		8	11	12	23	27	28	24	19	14		1		1														168			
350-359		10	8	20	20	36	37	47	38	19	8	2	1															246			
		263		408		336		307		50		5		0	0	0	0	0	0	0	0	0	0	0	0	0	0	2842			
		172	331	434		338		173		23		2		0	0	0	0	0	0	0	0	0	0	0	0	0	0				
NUMBER OF RECORDS AT OR BELOW STALL SPEED (2.2 CM/SEC)																												204			

Figure 5c. Histogram for CM 6.

FREQUENCY DISTRIBUTION OF DIRECTION AND RATE

BRU 50		0023270380 GMT CM-7 3056 BRIDPORT INLET										74597108501 15 1930TCTV6															
		CMS/SEC																									
		2.3	3	4	5	6	7	8	9	10	11	12	13	14	15	16	17	18	19	20	21	22	23	24	25	26	
		T0	T0	T0	T0	T0	T0	T0	T0	T0	T0	T0	T0	T0	T0	T0	T0	T0	T0	T0	T0	T0	T0	T0	T0	T0	
DIR		2.9	4	5	6	7	8	9	10	11	12	13	14	15	16	17	18	19	20	21	22	23	24	25	26	27	
0- 9	1	1																								2	
10- 19																										0	
20- 29	3																									3	
30- 39																										0	
40- 49																										0	
50- 59	1																									1	
60- 69																										0	
70- 79																										0	
80- 89	1																									1	
90- 99	1																									1	
100-109	2																									2	
110-119	1																									1	
120-129	1	2	1																							4	
130-139	4	1	2	1																						8	
140-149	8		2	2	1																					13	
150-159	2	4	4	1																						11	
160-169	7	9	5	2	1																					24	
170-179	5	4	2	3	2																					16	
180-189	6	4	5	3	2																					20	
190-199	10	13	10	3	3	1																				40	
200-209	7	11	6	2	2																					28	
210-219	7	5	6	1	2																					21	
220-229	10	6	6	1																						23	
230-239	7	8	1	1																						17	
240-249	2	6	2																							10	
250-259	14	13	7																							34	
260-269	24	12	3	1	2																					42	
270-279	15	12	6																							33	
280-289	14	14	11	2	3																					44	
290-299	28	30	24	15	3																					100	
300-309	29	52	53	30	7																					171	
310-319	90	132	128	81	35	4	1																			471	
320-329	89	176	149	98	46	13	3																			574	
330-339	40	82	64	21	10	2	4																			223	
340-349	11	21	10	2																						44	
350-359	11	3	3																							17	
		621	270	20	8	0	0	0	0	0	0	0	0	0	0	0	0	0	0	0	0	0	0	0	0	1999	
		451	510	119	8	0	0	0	0	0	0	0	0	0	0	0	0	0	0	0	0	0	0	0	0	0	
NUMBER OF RECORDS AT OR BELOW STALL SPEED (2.2 CM/SEC)		1057																									

Figure 5d. Histogram for CM 7 at 12 m depth.

FREQUENCY DISTRIBUTION OF DIRECTION AND RATE

BRD 12		4502280380 GMT CM-7 3040 BRIDPORT INLET										74597108501 15 1932TCTV6															
		CMS/SEC																									
		2.3	3	4	5	6	7	8	9	10	11	12	13	14	15	16	17	18	19	20	21	22	23	24	25	26	
DIR		TO	TO	TO	TO	TO	TO	TO	TO	TO	TO	TO	TO	TO	TO	TO	TO	TO	TO	TO	TO	TO	TO	TO	TO	TO	
		2.9	4	5	6	7	8	9	10	11	12	13	14	15	16	17	18	19	20	21	22	23	24	25	26	27	
0- 9	13	24	34	41	45	40	28	52	32	22	20	16	7	2	4											380	
10- 19	12	25	43	65	82	70	68	121	68	69	55	33	19	16	3	2										751	
20- 29	6	16	30	59	44	70	66	83	39	51	36	16	9	3	1											529	
30- 39	3	9	11	16	18	22	36	20	23	16	7	2														183	
40- 49	3	3	5	4	1	2	1	5	2	1		1														28	
50- 59	1	1	3	4																						9	
60- 69		2	1	1	1																					5	
70- 79			1	1																						2	
80- 89																										0	
90- 99		1																								1	
100-109																										0	
110-119																										0	
120-129																										0	
130-139																										0	
140-149																										0	
150-159																										0	
160-169																										0	
170-179																										0	
180-189																										0	
190-199			1	1																						2	
200-209	1			1	2																					4	
210-219	1	2	4	5	1																					13	
220-229	6	6	2	6	4																					24	
230-239	4	5	10	8	2	1																				30	
240-249	4	3	11	11	7	2	2				1															41	
250-259	2	6	14	10	11	8	8	4	4	1																68	
260-269	6	12	10	11	9	12	12	8	6	1																87	
270-279	5	6	10	2	6	11	9	5	5	2																61	
280-289	2	7	13	8	6	2		3	2	1																44	
290-299	9	8	11	2	9	3	2	6	4																	54	
300-309	6	17	9	8	9	2	5	4	1																	61	
310-319	6	6	5	3	3	2	1		2	2																30	
320-329	8	16	13	8	2	3	1	2	3																	56	
330-339	10	17	18	11	2	5	2	2																		67	
340-349	8	15	17	8	8	4	2	3	1																	66	
350-359	9	26	32	27	11	9	5	15	18	3	5															160	
		240	312	322	281	268	248	333	213	170	123	68	35	21	8	2	0	0	0	0	0	0	0	0	0	2769	
		125																								0	
NUMBER OF RECORDS AT OR BELOW STALL SPEED (2.2 CM/SEC)		271																									

Figure 5e. Histogram for CM 7 at 50 m depth.

FREQUENCY DISTRIBUTION OF DIRECTION AND RATE

BRG 50		1520280380 GMT CM-8										2976 BRIDPORT INLET															74597108509 15 2466TCTV6														
		CMS/SEC																																							
		2.3	3	4	5	6	7	8	9	10	11	12	13	14	15	16	17	18	19	20	21	22	23	24	25	26															
		T0	T0	T0	T0	T0	T0	T0	T0	T0	T0	T0	T0	T0	T0	T0	T0	T0	T0	T0	T0	T0	T0	T0	T0	T0															
DIR		2.9	4	5	6	7	8	9	10	11	12	13	14	15	16	17	18	19	20	21	22	23	24	25	26	27															
0- 9	2	2	1																							5															
10- 19	2	2	2	1																						7															
20- 29	2	1	1																							4															
30- 39		5	1	1																						7															
40- 49	1		5	1																						7															
50- 59	3	4	10	1																						18															
60- 69	4	11	10	2																						27															
70- 79	3	9	7	1																						20															
80- 89	14	7	4	4																						29															
90- 99	4	10	9	1																						24															
100-109	4	7	5	1																						17															
110-119	9	7	1	1																						18															
120-129	1	7	3																							11															
130-139	5	7	3	1																						16															
140-149	3	5		1																						9															
150-159	6	1																								7															
160-169	7	4	2																							13															
170-179	7	6				1																				14															
180-189	9	3	1	1																						14															
190-199	8	3	1			1																				13															
200-209	8	6	2	1																						17															
210-219	17	19	13	7	3																					59															
220-229	18	17	21	20	7	2	2																			87															
230-239	28	45	53	47	21	8																				202															
240-249	18	25	46	42	28	14																				173															
250-259	18	38	55	62	33	28	7	1																		242															
260-269	20	25	33	49	42	13	1																			183															
270-279	9	10	11	17	6	2																				55															
280-289	3	12	13	11																						39															
290-299	2	5	4	2																						13															
300-309	3	3	5																							11															
310-319	4	2	2																							8															
320-329	1	2	3																							6															
330-339	2	2	2																							6															
340-349	1	1	2																							4															
350-359	2	2																								4															
		315	275	67	1	0	0	0	0	0	0	0	0	0	0	0	0	0	0	0	0	0	0	0	0	1389															
	248	331	142	10	0	0	0	0	0	0	0	0	0	0	0	0	0	0	0	0	0	0	0	0	0	0															
NUMBER OF RECORDS AT OR BELOW STALL SPEED (2.2 CM/SEC)		1587																																							

Figure 5f. Histogram for CM 8 at 12 m depth.

FREQUENCY DISTRIBUTION OF DIRECTION AND RATE

BP0 12		4518280380 GMT CM-8 2983 BP10PORT INLET										74597108509 15 3387TCTV6																
		CMS/SEC																										
		2.3	3	4	5	6	7	8	9	10	11	12	13	14	15	16	17	18	19	20	21	22	23	24	25	26		
DIR		10	10	10	10	10	10	10	10	10	10	10	10	10	10	10	10	10	10	10	10	10	10	10	10	10	10	
		2.9	4	5	6	7	8	9	10	11	12	13	14	15	16	17	18	19	20	21	22	23	24	25	26	27		
0-	9	4	10	18	18	20	6	7	1	1																	85	
10-	19	10	16	25	22	25	12	16	12	12	8	4	6	1													169	
20-	29	9	12	35	57	63	51	27	34	23	22	15		2	3												353	
30-	39	15	38	63	69	94	66	47	36	27	20	15	9	3	2												504	
40-	49	9	23	48	43	59	54	35	25	17	6	2															321	
50-	59	3	22	24	19	24	16	16	8	4																	136	
60-	69	14	22	22	25	9	6	9	3	1																	111	
70-	79	8	16	16	13	8	4	2	1																		68	
80-	89	10	14	9	8	3	1																				45	
90-	99	11	10	12	12	1	3																				49	
100-	109	4	9	11	1	1		1																			27	
110-	119	6	1	3	2																						12	
120-	129	2		5	2																						9	
130-	139	1	4	3	1																						9	
140-	149	2	2	5	1																						10	
150-	159	3	1	7																							11	
160-	169	3	4	1																							8	
170-	179	3	9	3																							15	
180-	189	4	9	2																							15	
190-	199	4	6	1		1																					12	
200-	209	3	4	3	1																						11	
210-	219	10	4		2																						16	
220-	229	6	4	4	2																						16	
230-	239	7	10	6		1																					24	
240-	249	6	6	5		1																					18	
250-	259	4	6	3	1																						14	
260-	269	3	4	2	3																						12	
270-	279	6	5	5	1																						17	
280-	289	3	3	1	2																						9	
290-	299	6		4	8	1																					19	
300-	309	2	7	2	6	4																					21	
310-	319	6	2	1	3	6																					18	
320-	329	7	5	7	3	3	5																				30	
330-	339	5	10	9	7	10	2	2																			45	
340-	349	7	9	9	4	9	3	1																			42	
350-	359	7	7	16	14	11	5	3																			63	
		213	314	390	351	356	234	166	85	36	15	56	15	6	5	0	0	0	0	0	0	0	0	0	0	0	2347	
NUMBER OF RECORDS AT OR BELOW STALL SPEED (2.2 CM/SEC)		636																										

Figure 5g. Histogram for CM 8 at 50 m depth.

FREQUENCY DISTRIBUTION OF DIRECTION AND RATE

BRD 12		1521280380 GMT CM-9 2978 BRIDPORT INLET										74598108517 15 1931TCTV6																
		CMS/SEC																										
		2.3	3	4	5	6	7	8	9	10	11	12	13	14	15	16	17	18	19	20	21	22	23	24	25	26		
DIR		10	10	10	10	10	10	10	10	10	10	10	10	10	10	10	10	10	10	10	10	10	10	10	10	10	10	
		2.9	4	5	6	7	8	9	10	11	12	13	14	15	16	17	18	19	20	21	22	23	24	25	26	27		
0- 9		15	21	29	28	20	21	16	16	5	2	1															179	
10- 19		11	26	44	43	37	37	29	24	13	6	1															271	
20- 29		16	31	75	57	51	27	28	10	3	2																300	
30- 39		22	32	57	55	29	24	8	7	2		1															237	
40- 49		5	20	31	24	11	1	5																			97	
50- 59		13	24	23	15	4	1																				80	
60- 69		12	14	16	8	1																					51	
70- 79		9	13	9	1	1																					33	
80- 89		5	12	4	2																						23	
90- 99		13	16	1	1																						31	
100-109		6	8	3	1																						18	
110-119		13	12	3																							28	
120-129		18	9	1																							28	
130-139		12	8																								20	
140-149		15	10	4	1																						30	
150-159		21	6	5	2																						34	
160-169		27	8	4																							39	
170-179		24	19	9	7	3																					62	
180-189		59	30	13	11	6	2	1																			122	
190-199		15	8	6	10	6	1																				46	
200-209		15	23	23	20	7	1																				89	
210-219		11	17	17	15	10	2																				72	
220-229		4	6	4	3			1																			18	
230-239		6	8	4	1																						19	
240-249		6	5	2																							13	
250-259		1	4																								5	
260-269		4	4	1																							9	
270-279		3	3	1																							7	
280-289		1	4																								5	
290-299		1	3	3																							7	
300-309		5	3	3	2																						13	
310-319		3	4	2	2																						11	
320-329		7	7	5	2	1	1																				23	
330-339		13	4	8	1	3	2	1	1	2																	35	
340-349		7	11	18	5	7	4	14	14	9	2																91	
350-359		13	4	19	19	18	7	11	16	8	4																119	
		437	340	132	89	20	2	0	0	0	0	0	0	0	0	0	0	0	0	0	0	0	0	0	0	0	2269	
		431	444	215	114	42	3	0	0	0	0	0	0	0	0	0	0	0	0	0	0	0	0	0	0	0	0	
NUMBER OF RECORDS AT OR BELOW STALL SPEED (2.2 CM/SEC)		709																										

Figure 5h. Histogram for CM 9.

BPD 12 4500290380 GMT CM10 3034 BRIDPORT INLET 75011108529 15 1939TCTV6

27

Figure 5i. Histogram for CM 10.

stall speed corresponds with a range of ± 2 standard deviations, and thus the 95% confidence interval is

$$\pm \frac{2}{3} \frac{S}{2} = \pm \frac{S}{3}$$

The final expression for the average speed is therefore

$$\bar{V} = \bar{V}_a (1 - p) + \left(\frac{S}{2} \pm \frac{S}{3} \right) p.$$

For a time series with 10% of the speeds below stall speed, the 95% confidence interval for the mean speed is $\pm S/30$. If 90% of the speeds are below stall speed then the confidence interval is $\pm 9S/30$.

The 5th column in Table 5 lists the confidence intervals for the computed average speeds. The last column is the ratio of the uncertainty to the mean. It must be concluded from these calculations that the mean velocity vector from CM-4 is not significantly different from zero and that the vector at CM-10 is only barely significant.

Figure 6 shows the statistically significant mean velocity vectors measured in Bridport Inlet. It would be unwise to speculate on the circulation pattern within the Inlet from these measurements since all of the interior current meter records suffer flaws: either the data are dominated by sub-stall speed records (CM 4 and CM 10) or the vane is jammed (CM-5). At the Inlet entrance all the current meters at 12 m depth recorded mean flows into the Inlet while the flow at 50 m depth is out of the Inlet at CM-8 and appears to have a negligibly small component oriented along the entrance channel at CM-7. The principal direction of flow through the Inlet entrance is taken as $023^\circ T$ below, where the mean components for flow directed into (+) and out of (-) the Inlet are summarized.

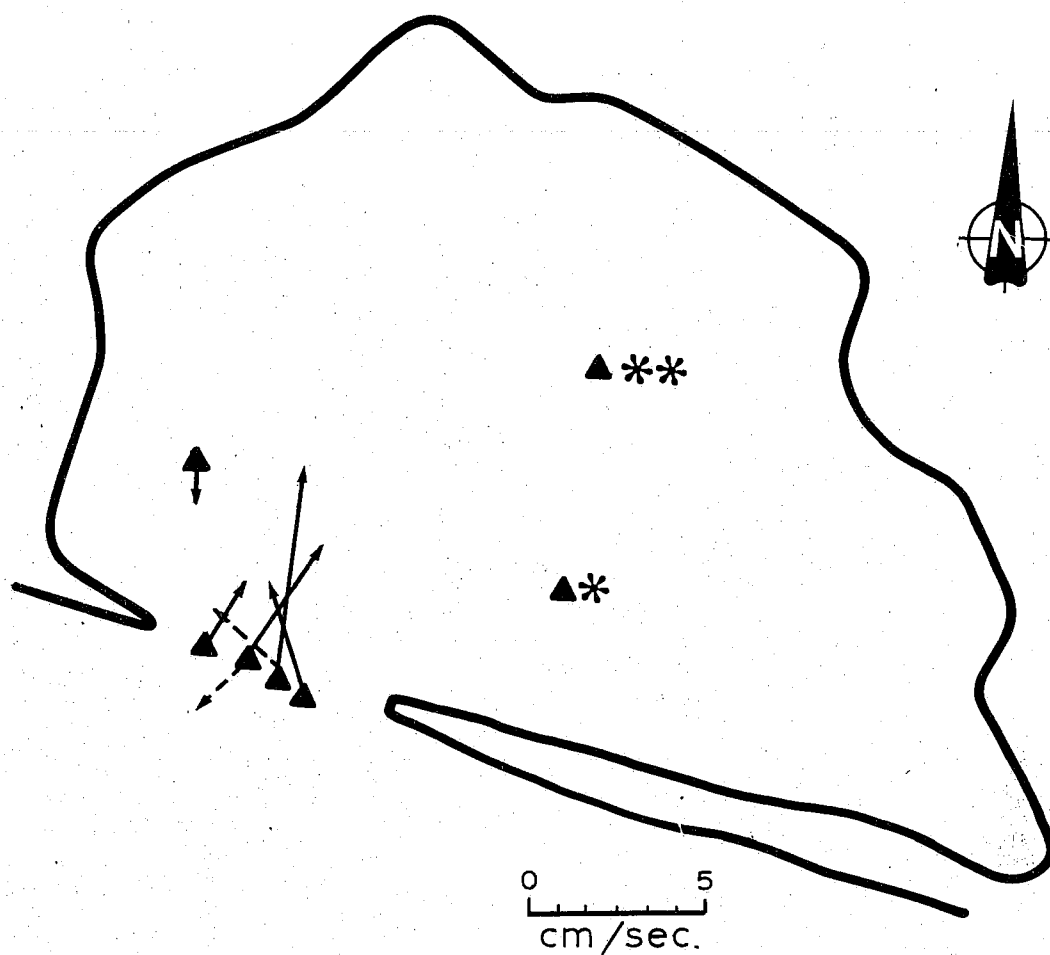


FIGURE 6. Monthly mean vectors recorded at the current meters. The dashed vectors refer to currents at 50 m depth. * = no direction information; ** = mean speed not significant.

TABLE 5

MEAN CURRENT VECTORS AND THEIR ASSOCIATED PRECISIONS

CM	Mean Speed ₁ cm s ⁻¹	Direction °T	% of records below stall speeds	Precision of av. speed (cm s ⁻¹) 95% confidence)	<u>Precision</u> Mean
4	0.5	073	77	0.57*	1.14
5	5.3	099 Φ	40	0.30	0.07
6	3.1	339	5	0.04	0.01
7 (12)	5.6	005	9	0.07	0.01
7 (50)	2.4	307	35	0.26	0.11
8 (12)	3.9	032	22	0.16	0.04
8 (50)	1.8	236	53	0.39	0.21
9	1.9	025	24	0.08	0.09
10	0.8	190	98	0.72	0.90

* The mean being smaller than the 95% confidence interval for this current meter, the mean is not significantly different from zero.

Φ direction vane jammed.

Mean Flow Component Through the Inlet Entrance (cm s^{-1})
 (+ = 023°T)

	Site	Site	Site	Site
	9	8	7	6
12 m	+1.9	+3.9	+5.3	+2.2
50 m	--	-1.7	+0.6	--

The mean shear directed along 023°T is 4.7 cm s^{-1} at site 7 and 5.6 cm s^{-1} at site 8 between 12 and 50 m depth, in good agreement with the computed geostrophic shears (see Section II.A).

The general impression from the current meter data at the Inlet entrance is of an inward near-surface flow balanced by a slow return flow at depth and thus the circulation is oppositely directed from that obtaining in estuaries where the run-off and rainfall exceed the evaporation. The process which drives this negatively directed estuarine circulation is probably brine rejection by thickening sea ice.

In order to determine if the spatial sampling at the Inlet entrance was of sufficient density, cross correlation coefficients of the velocity component along 023°T were computed among the current meter data sets. The resulting correlation coefficient matrix is shown below (the 95% significance value is 0.07):

CORRELATION COEFFICIENT MATRIX

	CM6	CM7 (12)	CM7 (50)	CM8 (12)	CM8 (50)	CM9
CM6 (12)	1.00	-0.382	+0.461	-0.310	-0.070	-0.467
CM7 (12)		1.00	-0.547	+0.751	+0.445	+0.765
CM7 (50)			1.00	-0.579	-0.342	-0.672
CM8 (12)				1.00	+0.404	+0.773
CM8 (50)					1.00	+0.473
CM9 (12)						1.00

The correlation coefficients are representative of vertical separations of 38 m and horizontal separations of 450, 900 and 1350 m (the current meters were approximately evenly spaced 450 m apart horizontally). There are six categories of coefficients in the matrix:

C(x,0)	representing 1 horizontal and no vertical separations
C(2x,0)	2 horizontal and no vertical separations
C(3x,0)	3 horizontal and no vertical separations
C(0,z)	no horizontal and 1 vertical separations
C(x,z)	1 horizontal and 1 vertical separations
C(2x,z)	2 horizontal and 1 vertical separations

The values in these categories are listed below:

C(x,0)	C(2x,0)	C(3x,0)	C(0,z)	C(x,z)	C(2x,z)
-0.38	-0.31	-0.46	-0.54	+0.44	-0.07
+0.75	+0.76		-0.40	-0.57	-0.67
+0.77				+0.46	
-0.34				+0.77	

There are no apparent significant differences among the average values of the 6 categories of correlation coefficients. Current meters 6 and 7 (50) are negatively correlated with all other current meters. In the case of current meter 6 this is probably due to the over-riding

effects of local topography (a long shallow sub-surface spit) and in the case of 7(50) the outflow from the Inlet imposes a bias in direction. Generally, however, the magnitudes of the correlation coefficients are large indicating that little spatial variation exists, particularly between the current meters at sites 7, 8 and 9, at 12 m depth. One might have expected weaker correlations since the internal Rossby radius, r_i is small, ($r_i = \frac{NH}{f}$ where N is the Väisälä frequency, H the layer depth and f the Coriolis parameter. For the Bridport Inlet entrance $r_i = 470$ m for $N = 4.4 \times 10^{-3} \text{ s}^{-1}$ and $H = 15$ m).

Cross spectra among the current meters were also computed and strong coherences were found in the semi-diurnal tidal band. Only current meter 7(50) showed a significant phase difference (53°) with respect to current meters 7(12), 8(12), 8(50) and 9(12). The other current meters were in phase ($\pm 8^\circ$) with each other in the semi-diurnal band.

C. CURRENT PROFILES

Current speed profiles were measured at 8 locations with an ultrasonic current meter. Directions as well as speeds were determined at sites 80-5 and CM-5. The ultrasonic current meter profiles were employed in two ways; to check the Aanderaa current meter operation and to obtain a detailed view of the vertical current profiles. The USCM profiles are reproduced in Appendix B.

As mentioned in Section II.B, the profiling current meter confirmed that erroneous directions were recorded by the moored Aanderaa instrument at CM-5 due to a malfunctioning vane. At the other current meter sites where intercomparisons were performed (CM-4, 9 and 10) the instantaneous speeds recorded by the two instruments were in good agreement when currents were above the Aanderaa stall speed of 2.2 cm s^{-1} .

The ultrasonic current meter profiles confirm the vertical structure of the velocity field at the Inlet entrance derived from geostrophic and mass-balance considerations. That is, a minimum current speed is measured at about 25 m depth near where a flow reversal

was computed by indirect means. In addition, the ultrasonic data show a very slight decrease of velocity near the underside of the sea ice. Such a decrease is due to the interfacial stress between the land-fast ice and the fluid motion. These boundary layer effects are not noticeable at distances of more than about 5 m below the ice.

An attempt was made to fit the observed current profiles to the log-linear boundary layer structure applicable in convective regions (such as under growing sea ice) described by Turner (1973). This profile is

$$u = \frac{u_*}{k} \left(\ln \frac{z}{z_0} + \alpha \frac{z}{L} \right) \quad (4)$$

where u is the velocity at a distance z below the ice, u_* is the friction velocity equal to $\sqrt{\tau/\rho}$ where τ is the interfacial stress, k is Von Karman's constant equal to about 0.4, z_0 is the roughness length, α is a constant with a value of about 5.0 and L is the Obukhov length, the ratio of the kinetic energy flux due to boundary shear stress to that due to convection.

$$L = \frac{\bar{\rho} u_*^3}{kg \overline{\rho'w'}} \quad (5)$$

where $\bar{\rho}$ is the mean density in the convective regime, g is the acceleration of gravity and $\overline{\rho'w'}$ is the correlation of the density and vertical velocity fluctuations equivalent to the turbulent vertical mass transport. L is negative in unstable conditions.

$\overline{\rho'w'}$ can be estimated from the ice growth rate

$$\overline{\rho'w'} \approx i \rho_i \Delta s \quad (6)$$

where i is the ice growth rate, ρ_i is the density of the ice and Δs is the difference in salinity between the ice and the sea water. u_* and z_0 can be determined with the profile data.

The results of the fit showed the Obukhov length to be between 16 and 45 metres. Convective effects are considered to be important only when the mixed layer depth is comparable to L , and since the observed depth of the truly mixed layer is only about 2 or 3 m, the velocity profile is not greatly affected by convection.

Resulting values of u_* are about 0.9 cm s^{-1} and the drag coefficient defined as

$$C_D = \frac{u_*^2}{U^2} \quad (7)$$

where U is the velocity far from the boundary, is about 3×10^{-3} . These values are in fair agreement with those of Shirasawa and Langleben (1976) who found $u_* = 0.97 \text{ cm s}^{-1}$ and $C_D = 0.97 \times 10^{-3}$.

The implication of the strong vertical gradient of horizontal velocities concentrated near the boundary is that these effects may be ignored in mass transport computations. The observed profiles show that current speeds are not appreciably decreased by the ice-water stress at distances greater than 1 or 2 metres below the ice.

III INFERRED CIRCULATION

Both dynamic computations, whereby currents are computed from the distribution of mass, and direct current measurements within Bridport Inlet are inadequate to formulate a clear picture of the circulation. In the case of dynamic computations, the horizontal density gradients are too small to accurately determine the flow velocities and in the case of the direct current measurements the speeds are often so low as to be undetectable by the Aanderaa current meter. As an alternative to these methods, plots of the distribution of properties were constructed which ultimately pointed to a mechanism for driving the mean circulation.

Horizontal plots of temperature and salinity at 5, 10, 20, 30 and 40 m were constructed from the average CTD data at each site. (Below 40 m depth the horizontal gradients were too weak to yield any details of the property fields.) These plots are shown in Figures 7a-e.

The isohalines on surfaces shallower than 20 m imply an intrusion of lower salinity water from Viscount Melville Sound into Bridport Inlet. At 30 m depth and below, the salinity plots weakly indicate that the water of Bridport Inlet have a higher salinity than those of Viscount Melville Sound but the direction of flow is not so dramatically portrayed as at shallower depths. There is an indication of a pooling of higher salinity water in the central, deep region of the Inlet from which one might infer a slow cyclonic circulation at depth. The temperature and salinity signals below 30 m depth are, however, very weak, barely exceeding the precision of the measurements. The plots therefore are only suggestive of water motions.

A vertical section of salinity, running nearly north-south through the Inlet entrance was constructed and is shown in Figure 8. Station 80-3 is coincident with CM-7 located between the two spits at the entrance. The shapes of the isohalines suggest an inflow of fresher water near the surface, and an outflow of higher salinity water at depth. The nearly horizontal 32.74 isopycnal at the entrance is located at 24 m depth indicating that this depth is, roughly, the boundary between inflow and outflow. The water column near the north shore of the inlet is homogeneous ($\pm 0.007\%$) below 20 m depth and between 20 and 60 metres it is homogeneous within $\pm 0.003\%$. This

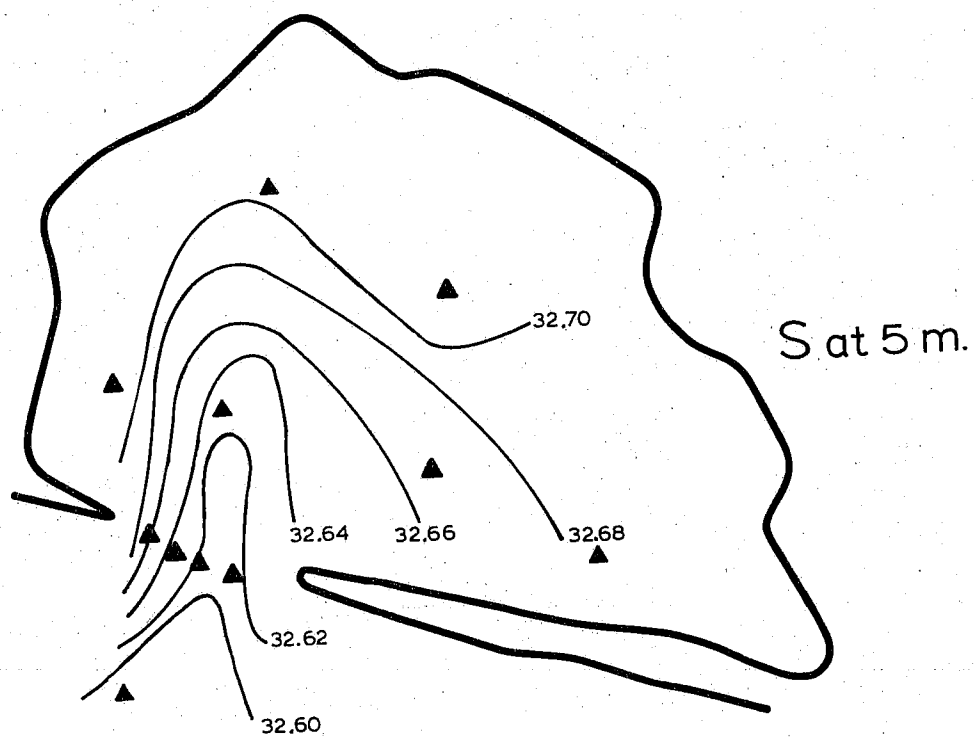
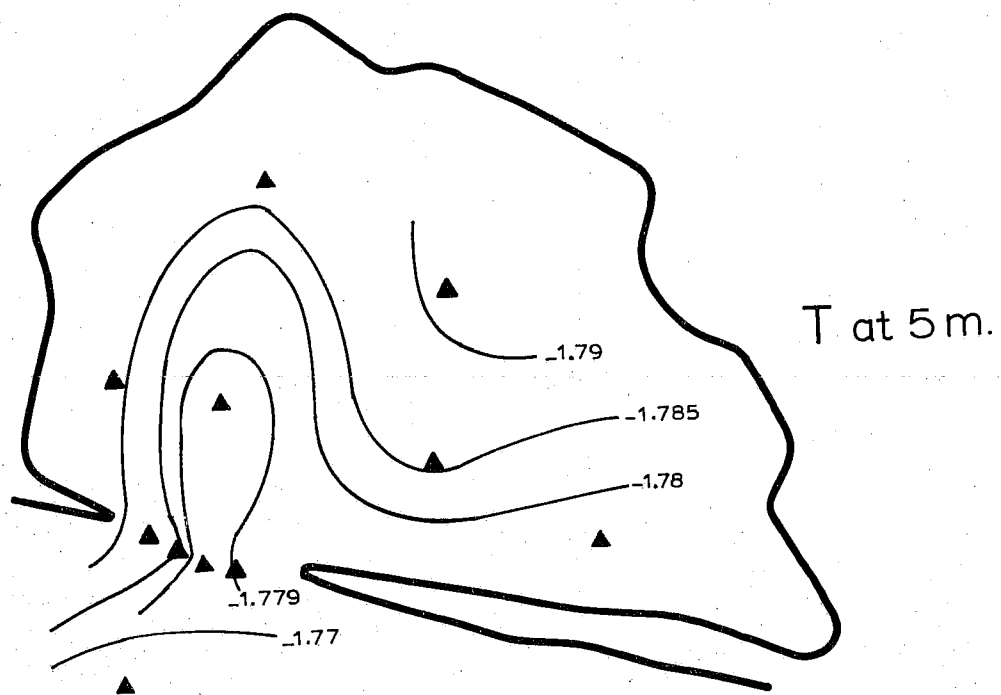


FIGURE 7a. Horizontal plots of temperature and salinity at 5 m depth.

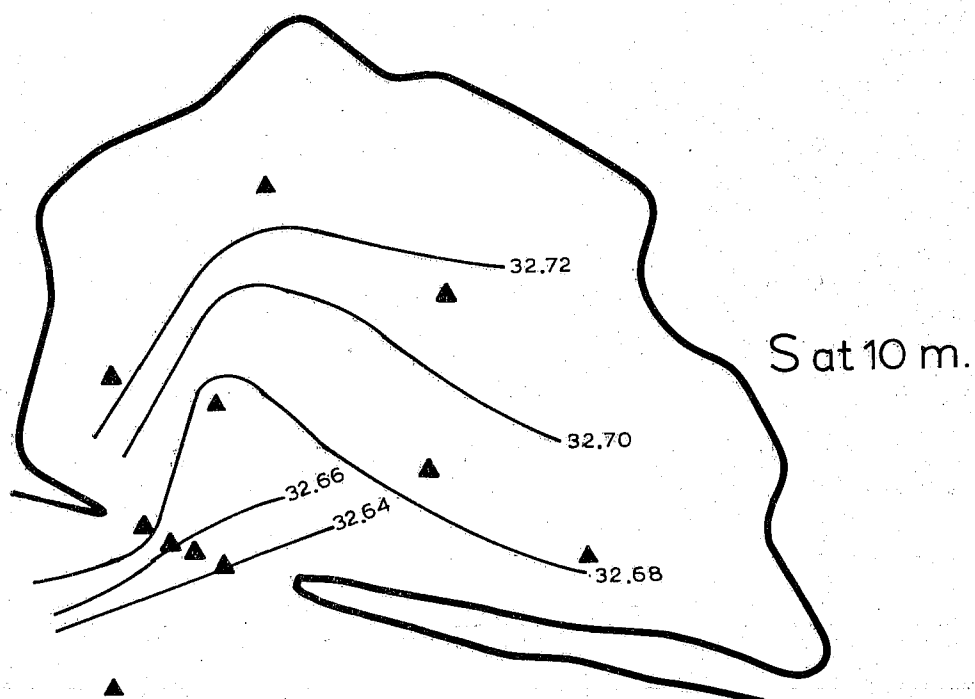
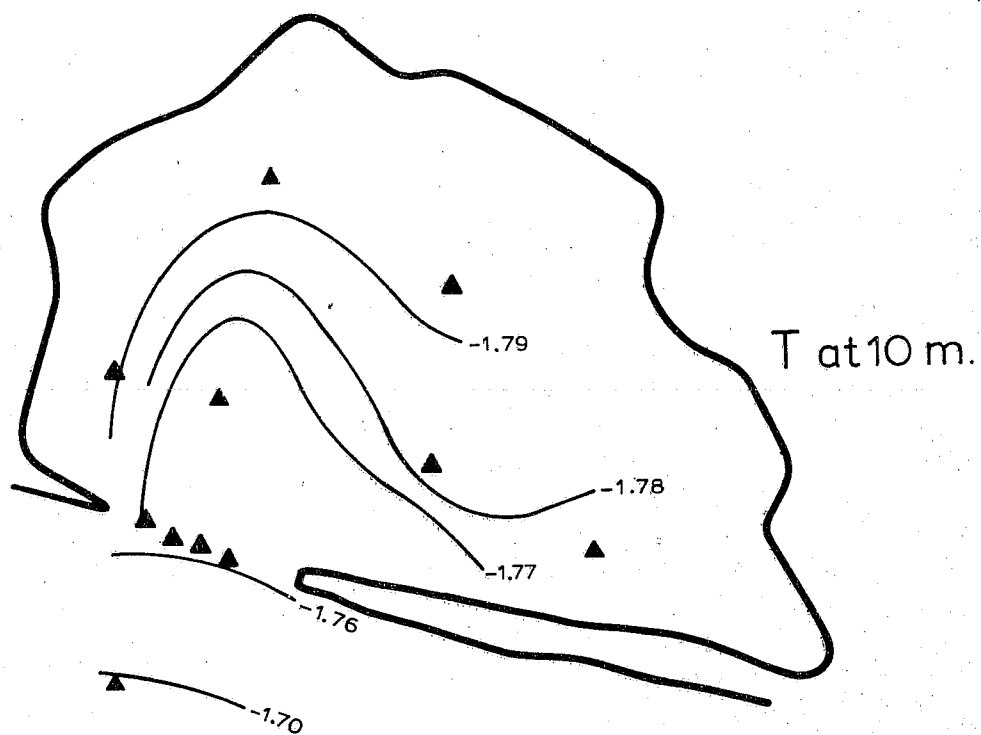


FIGURE 7b. Horizontal plots of temperature and salinity at 10 m depth.

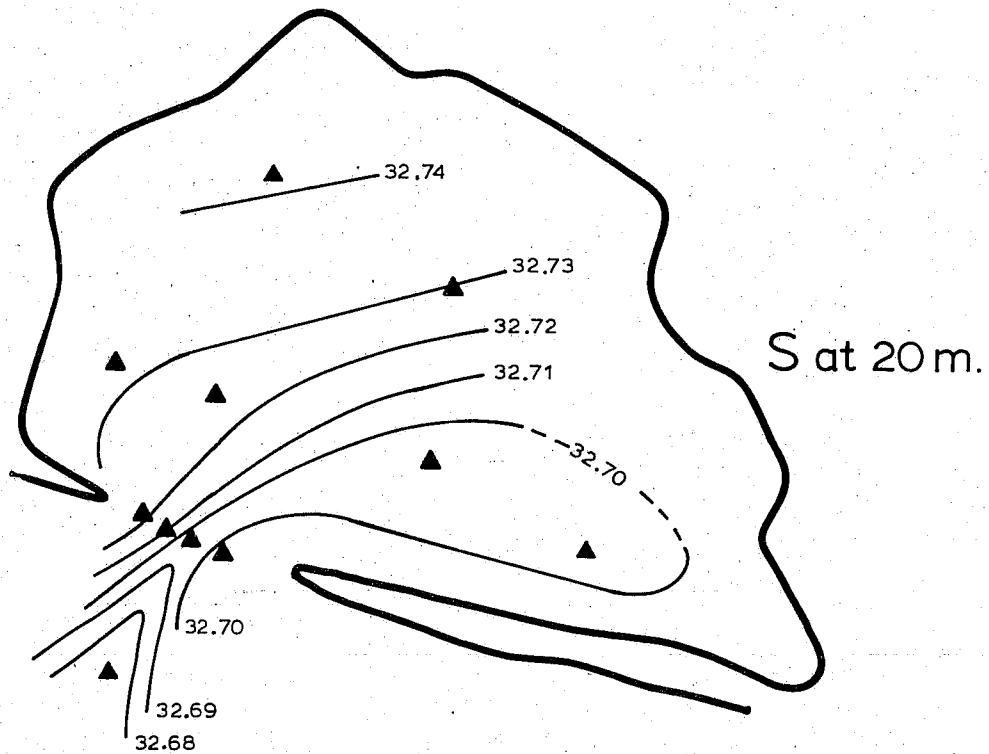
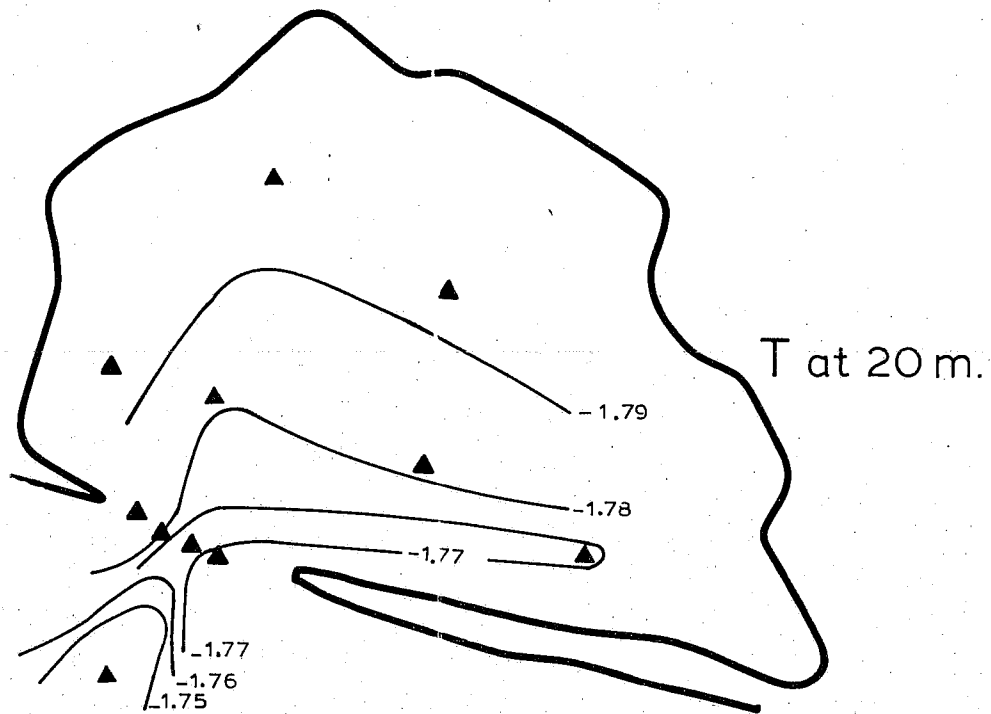


FIGURE 7c. Horizontal plots of temperature and salinity at 20 m depth.

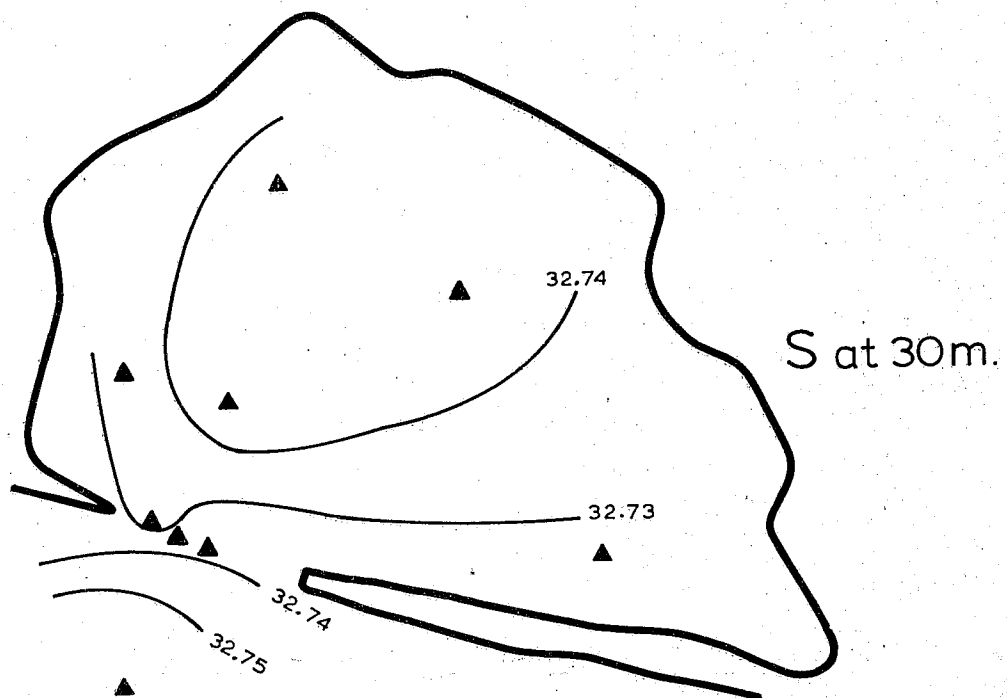
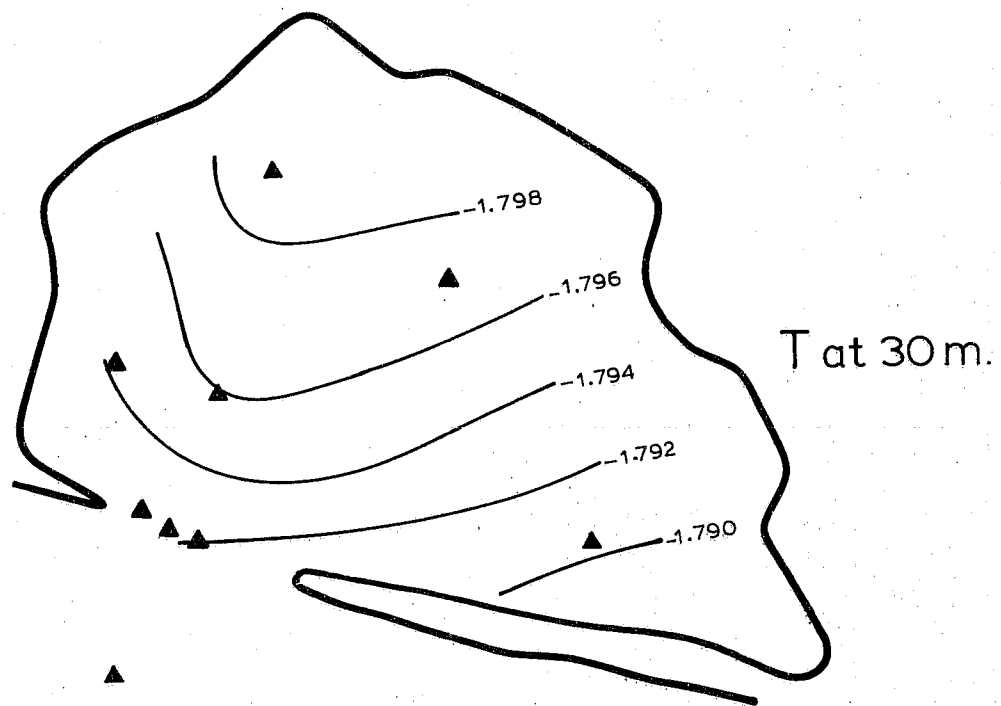


FIGURE 7d. Horizontal plots of temperature and salinity at 30 m depth.

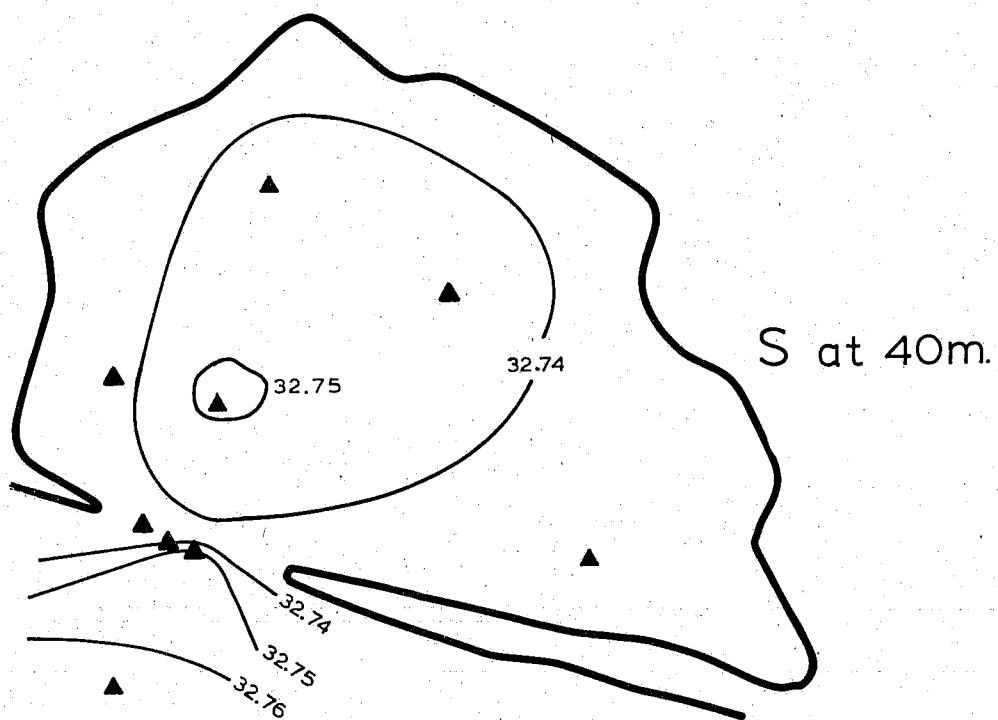


FIGURE 7e. Horizontal plots of temperature and salinity at 40 m depth.

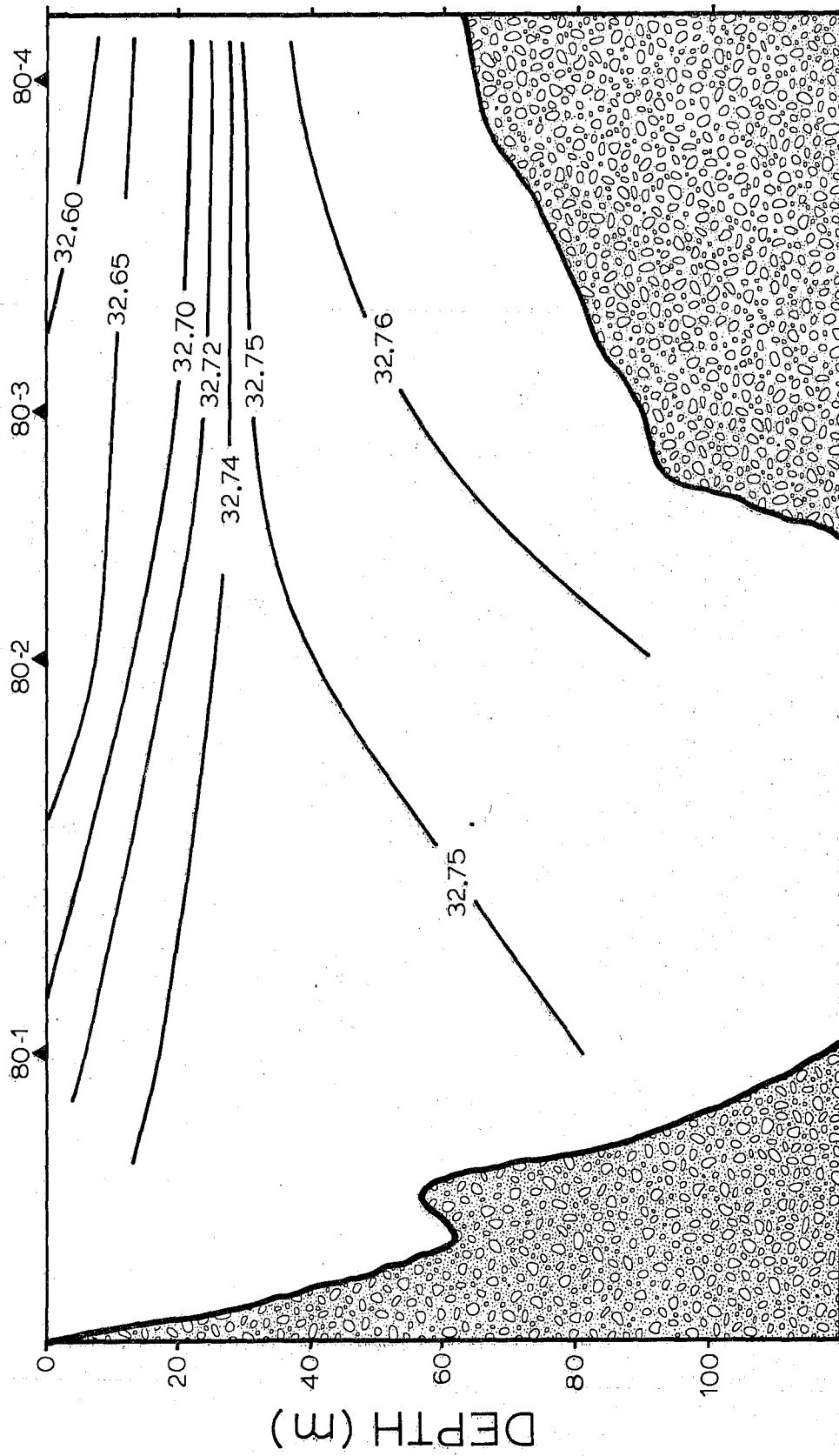


FIGURE 8. Vertical salinity section running nearly north-south through the Inlet entrance.

structure is indicative of the presence of convective processes within the inlet, probably driven by the rejection of brine from growing sea ice.

The modification of the mass field due to brine rejection can be graphically portrayed by a method conceived by Melling (personal communication). The difference between the in-situ temperature and the surface freezing point at the in-situ salinity is contoured on a vertical section. Waters cooled to or below the freezing point at the surface are indicated by values of $T - T_f \leq 0$. The formula used for computation of the freezing point at 1 bar (the ocean surface) is taken from Millero (1977):

$$T_f = -.0575 S + 1.710523 \times 10^{-3} S^{3/2} - 2.154996 \times 10^{-4} S^2 \quad (8)$$

where T_f is the freezing point and S is the salinity.

A vertical section of $T - T_f$ from Bridport Inlet in 1980 is shown in Figure 9. Except for a thin layer less than 2 metres thick below the ice, all the water at, or below its surface freezing point is found at depths greater than 10 m near the north shore, and at depths greater than 30 m at the entrance. There is however, a strong suggestion of the upper surface of the deep "cold" water mass shoaling toward the north shore and the $T - T_f = 0$ isolines connecting in shallower water, just a few hundred metres north of station 80-1.

The section indicates that water warmer than 0.06°C above its surface freezing point enters the inlet at 8 to 12 m depth. As this relatively warm water flows northward it loses heat and approaches the surface freezing point. In order to balance the intrusion of relatively warm water at shallow depths there must be an outflow of colder water below it.

The estuarine circulation described may be driven by rejection of brine and the establishment of denser waters within the Inlet than are found in Viscount Melville Sound. Such an estuarine circulation is supported by the geostrophic shear computed at the Inlet entrance.

If the salinity distribution shown in Figure 8 is due to a quasi-stationary process, then a balance between vertical diffusion and horizontal

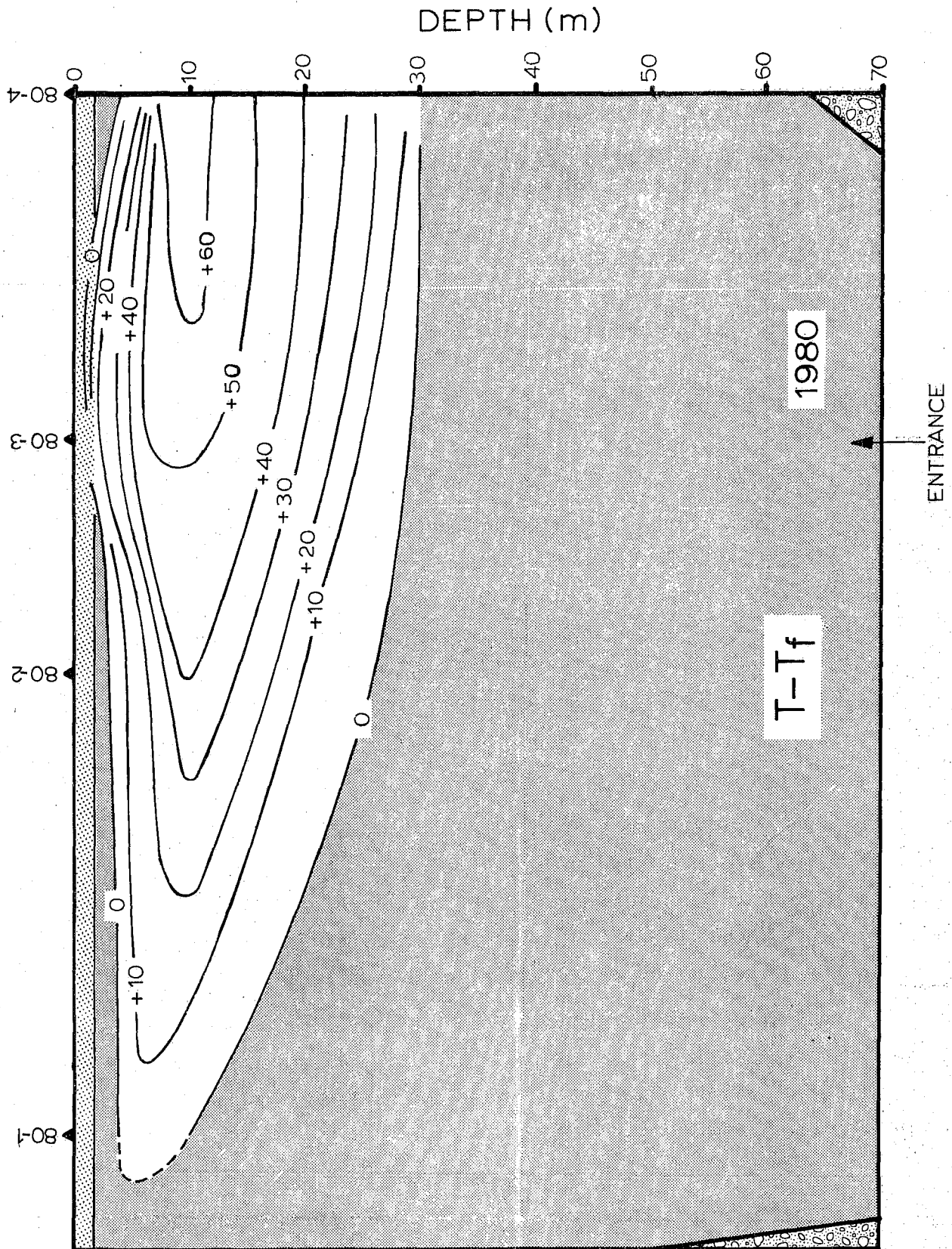


FIGURE 9. Vertical north-south section of the difference between in-situ temperature (T) and the freezing point temperature at atmospheric pressure and in-situ salinity (T_f) for 1980 (Millidegrees).

advection might be present. Such a balance can be represented as

$$u \frac{\partial s}{\partial x} = K_z \frac{\partial^2 s}{\partial z^2} \quad (9)$$

where u is the horizontal velocity in the x direction and K_z is the eddy diffusivity of salt. If a velocity of 1 cm s^{-1} is assumed, then the necessary value of K_z is approximately $10^{-3} \text{ m}^2 \text{ s}^{-1}$. This value is an order of magnitude too high for the stratification present in Bridport Inlet ($N^2 \approx 5 \times 10^{-5} \text{ s}^{-2}$) when compared with values determined in Agfardlikavså Fjord by the Danish Hydraulic Institute which was about $10^{-4} \text{ m}^2 \text{ s}^{-1}$ (Lewis and Perkin, 1982). If the rejection of brine by growing sea ice is included in the processes which maintain the salinity field, then (9) may be rewritten as

$$u \frac{\partial s}{\partial x} = K_z \frac{\partial^2 s}{\partial z^2} + i \frac{\rho_i}{\rho_w} (S_w - S_i)/h \quad (10)$$

where i is the growth rate of the ice ($= 1 \text{ cm d}^{-1}$), the subscripts i and w signify ice and water respectively, ρ is density and h is the depth of the inward moving layer. The numerical values of the terms in (10) are

$$1.5 \times 10^{-7} \text{ } \text{‰} \text{ s}^{-1} = K_z (3 \times 10^{-4}) + 1.1 \times 10^{-7}$$

which yields a value of $K_z = 1.3 \times 10^{-4}$, in better agreement with values from Agfardlikavså Fjord.

In (10), the rejection of brine by ice growth is probably very nearly in balance with the advection but is almost certainly much larger than the diffusion of salt upward from the deeper layer. The system is thus advectively controlled.

The process by which the brine increases the salinity of the inward flowing surface layer is not revealed by the data. The mixed layer depths may be as small as 1 or 2 metres, while the classical concept of the density structure under growing sea ice has a mixed layer extending below the ice over the entire depth where convective processes dominate. In Bridport Inlet it is likely that the convection is an intermittent

process. Examination of all the instantaneous CTD profiles did not, however, yield any convincing evidence of intermittent convection.

The degree of stratification can also be scrutinized by evaluating the mass of salt required to be added at the surface to mix the water column. Figure 10 shows the average temperature, salinity and density profiles at Site 80-1 near the northern shore of the Inlet. The mixed layer is entirely absent immediately below the ice while the water column is nearly completely homogeneous below a depth of about 20 m. The Väisälä frequency below 20 m depth is less than $2 \times 10^{-3} \text{ s}^{-1} + 10^{-3} \text{ s}^{-1}$ (Figure 11). The mass of salt, M_s , which must be added to the water column by sea ice growth in order to cause convection to 50 m depth (approximate sill depth) can be computed from

$$M_s = \rho w \sum_{j=0}^{50} S_{50} - S_j \Delta z \quad (11)$$

where S_{50} is the salinity at 50 m depth, S_j are the salinities at depths j and Δz is the depth interval taken to be one metre.

The required salt input from ice formation to destabilize the water column, and the time required (at an ice growth rate of 1 cm d^{-1}) to produce that amount of salt is graphed in Figure 12, versus site location. At the Inlet entrance approximately 8 days of ice growth would mix the water column while at site 80-1 just over one day's ice growth would be sufficient. If this trend of increasing vertical homogeneity is extrapolated into the shallower waters north of site 80-1, then one can conjecture that the water column is completely homogeneous about 1 km north of site 80-1 in a depth of about 50 m. The apparent stability associated with the upper water column is therefore probably not reflective of the convective process which is known to be occurring in the Inlet.

In summary, the property distributions on a vertical section running nearly north-south through the Inlet entrance imply a mean circulation characteristic of a negative estuary. Flow appears to be inward in the upper 25 m and outward below that depth. The upper layer salinity is increased as the fluid moves northward by brine rejection until the water column is completely destabilized near the north shore in depths of about

SALINITY

32.0

32.5

33.0

TEMPERATURE (DEG. C)

-2.0

-1.5

-1.0

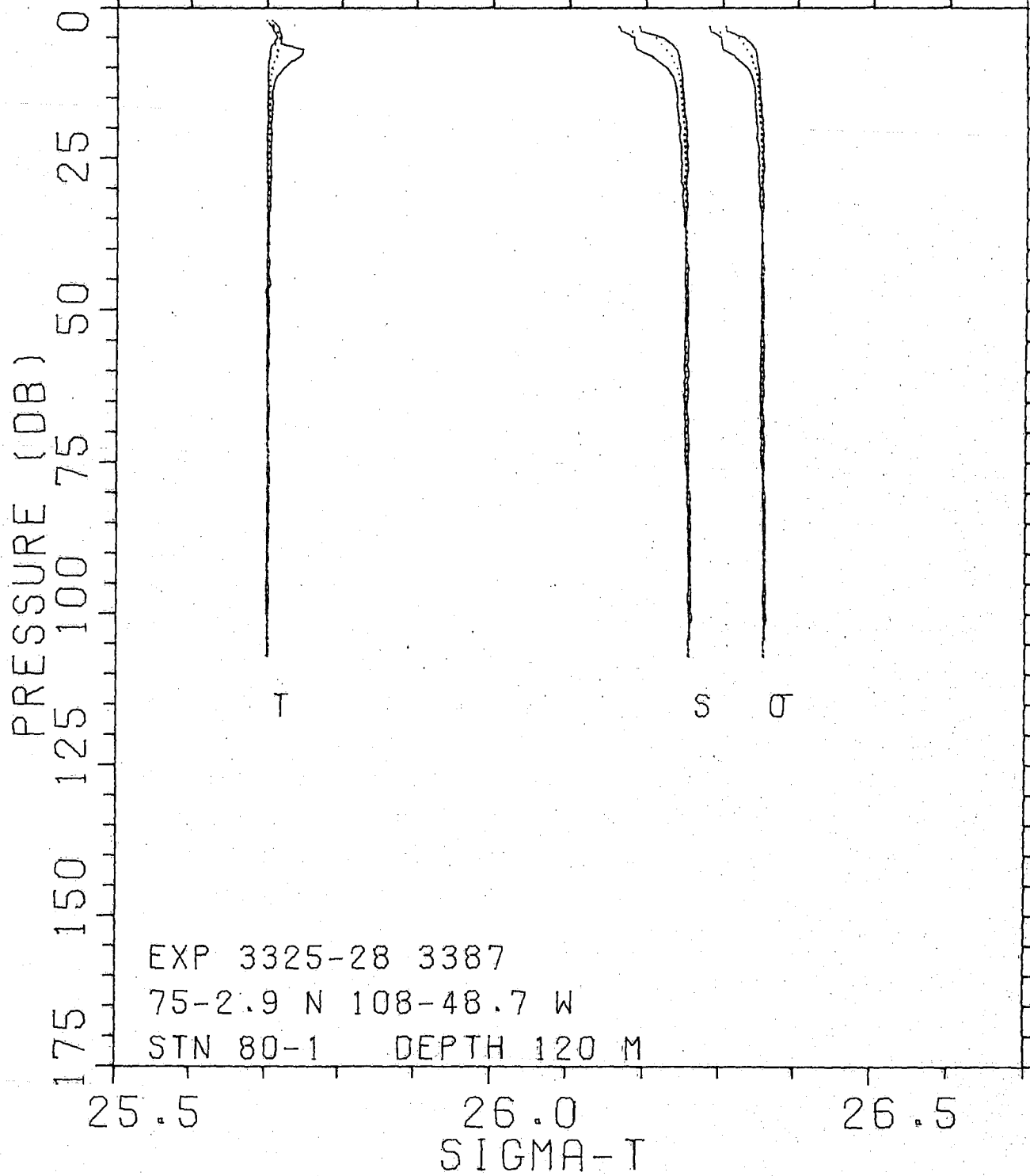


FIGURE 10. Average T, S, and σ_t profiles of 80-1. The envelopes about each dotted mean profile span all the values recorded.

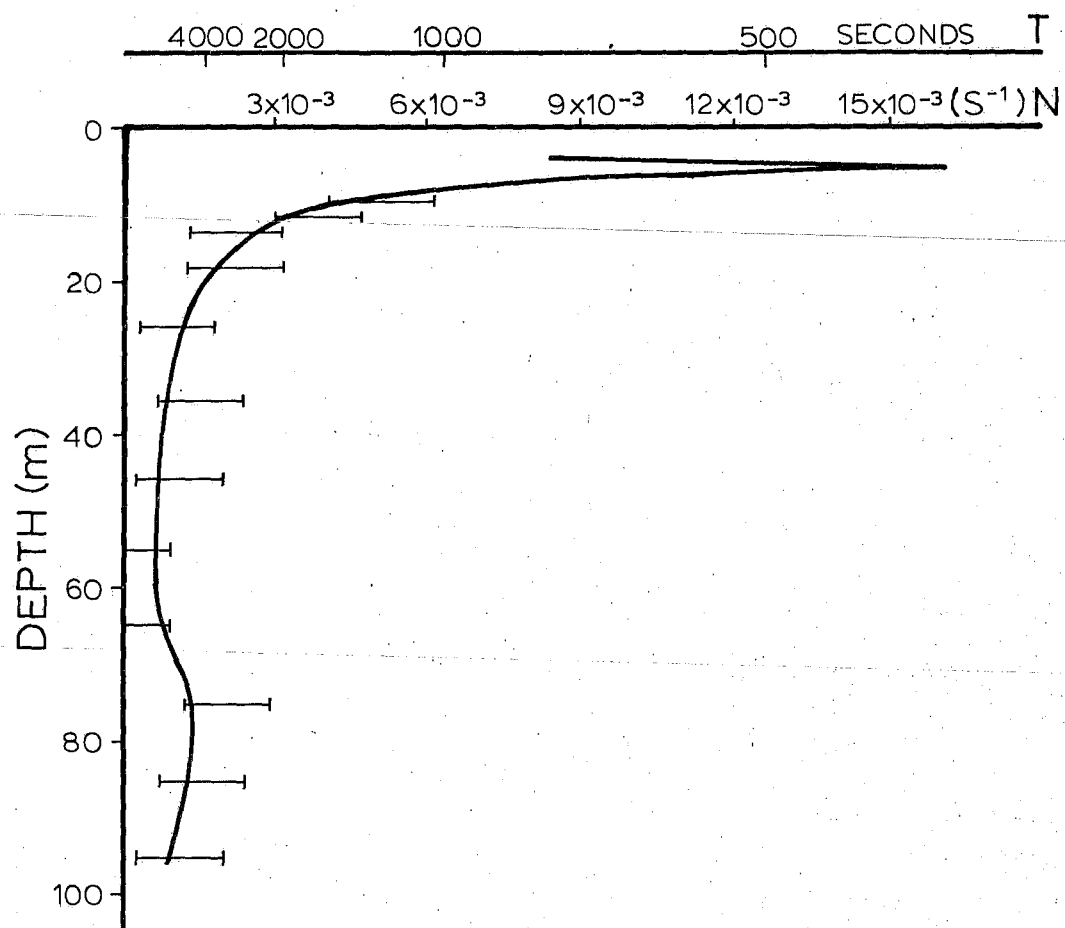


FIGURE 11. Profile of the Väisälä frequency $\left(\sqrt{\frac{g}{\rho} \frac{\partial \rho}{\partial z}} \right)$ at site 80-1. The horizontal bars indicate the pre-computed values at several depths.

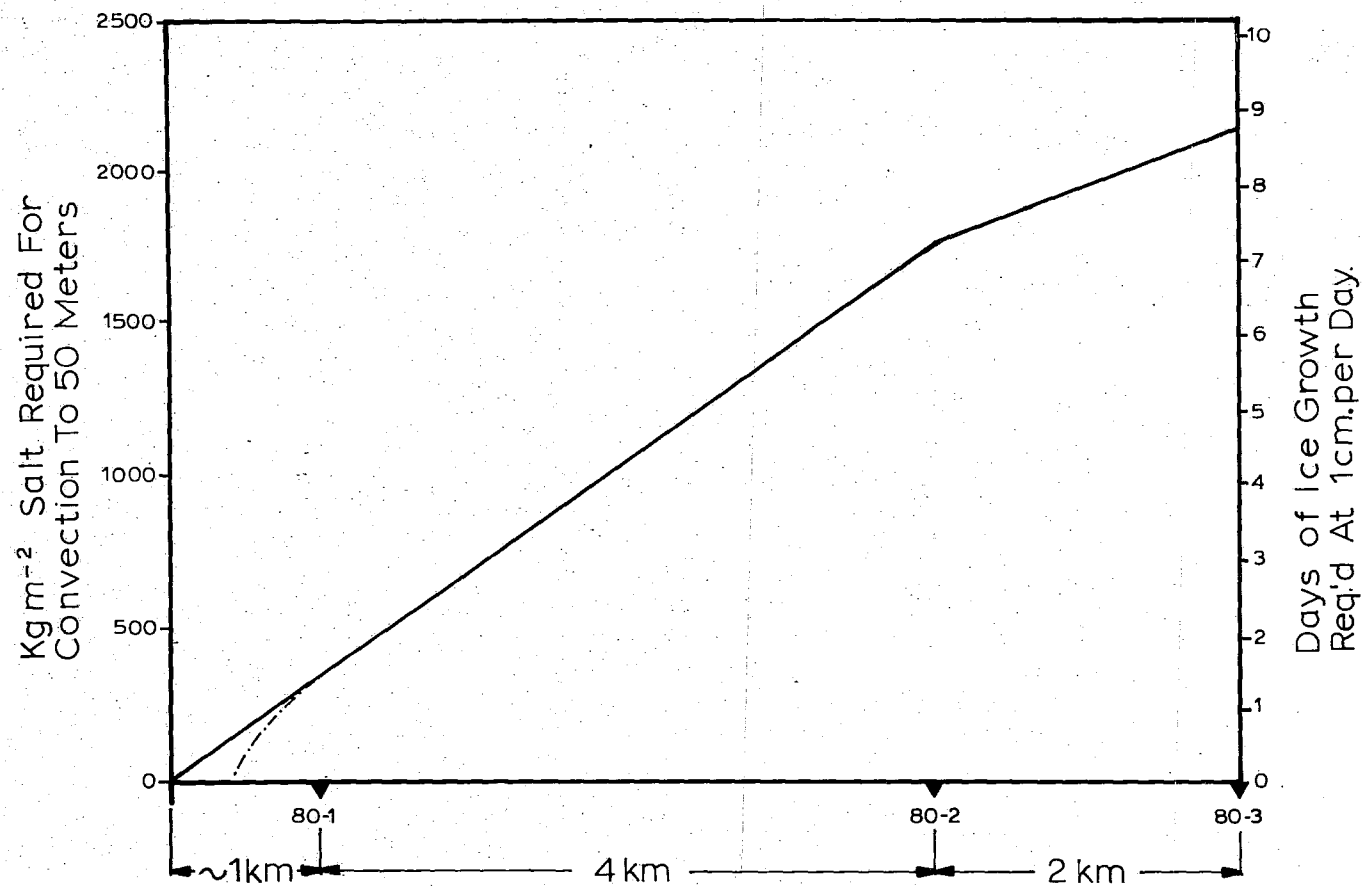


FIGURE 12. The amount of salt required for convection to 50 m depth and the time required for ice growth to reject sufficient brine for convection. Section north-south through the Inlet entrance.

50 m. At this location the relatively high salinity freezing point water is advected downward to depths below about 25 m and flows south (outward) through the Inlet entrance. The southerly flow is probably largely confined to the depths above sill depth which is approximately 50 m. The salt balance in the Inlet is advectively dominated.

Cyclonic Flow?

The north-south section cannot address the possibility which is weakly indicated by the horizontal temperature and salinity plots, i.e. the presence of a slow cyclonic flow. A plot of $T - T_f$ at stations taken in series around the periphery of the Inlet in a cyclonic sense is presented in Figure 13. The flow is taken to begin in Viscount Melville Sound, follow a course past CM6 on the east side of the entrance steered by the Coriolis force, and then proceed cyclonically around the Inlet exiting towards the west of the entrance at CM9. The concept of weak cyclonic circulation is supported by Figure 13. The isoline $T - T_f = 0$ generally shoals in the cyclonic direction, intersects the surface at CM-10 and the fluid hypothesized to leave the Inlet at CM9 is at or below its surface freezing point.

The weak cyclonic circulation is, however, most probably a response to the pressure gradient established between the Inlet entrance and its interior. The balance of forces maintaining the estuarine flow is analysed in Section IV where a vertical velocity profile and a salt balance is computed.

This page is blank.

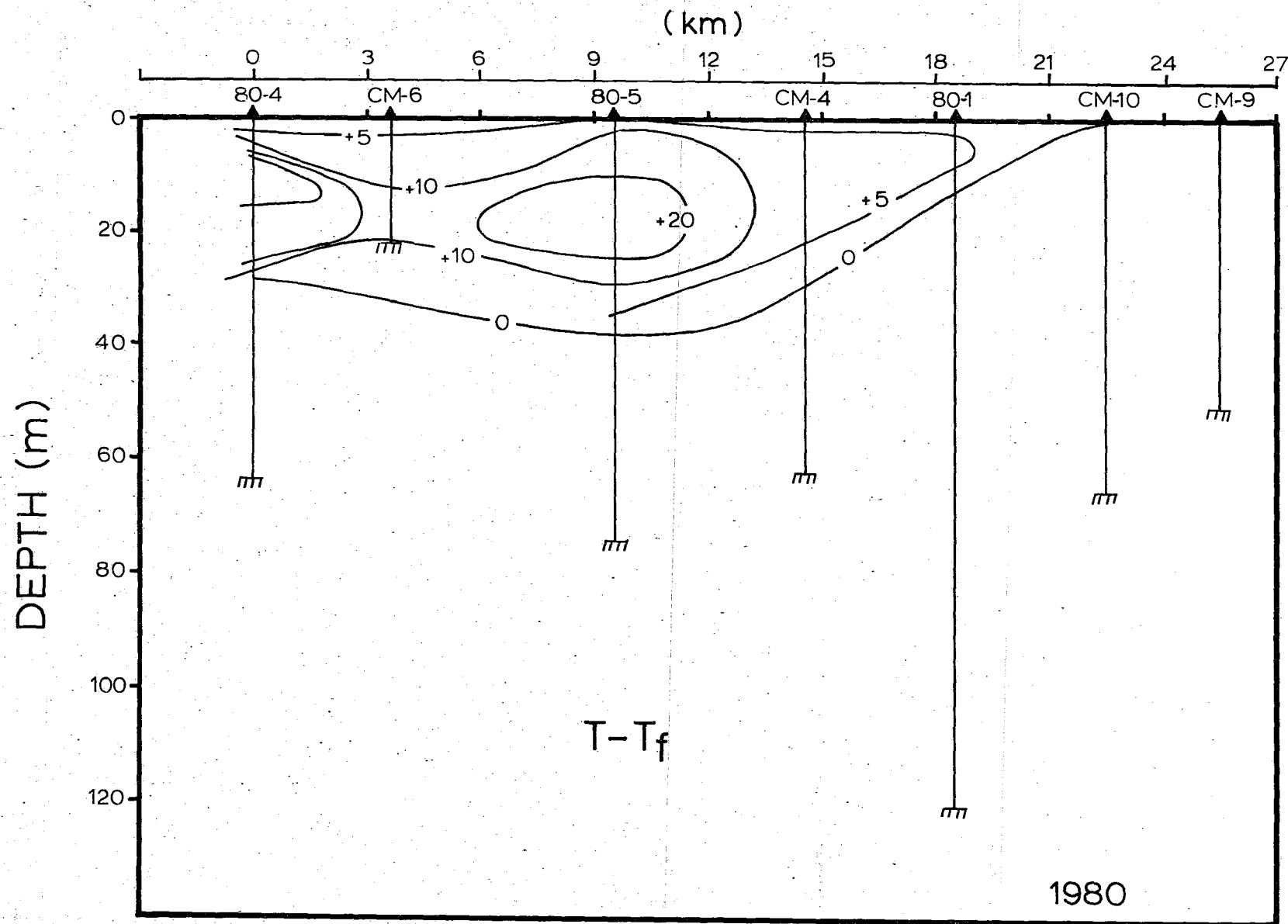


FIGURE 13. Vertical section of $T - T_f$ counter clockwise around the periphery of the Inlet (millidegrees).

IV ESTUARINE CIRCULATION

A. DYNAMICS

The current meter measurements, the computed geostrophic currents at the entrance, and the property distributions suggest that the mean flow (over the period of the measurements) is into the inlet near the surface and outward at depth. The sense of this circulation is suggestive of a "negative" estuary in which processes of densification predominate. Evaporation is the usual agent for densification in lower latitudes, but in the Arctic brine rejection from growing sea ice will increase the density of the underlying waters. If a situation occurs where there is a horizontal difference in the rate of ice growth then a horizontal density gradient can be established and a resulting horizontal pressure gradient. Flows would result near the surface from the less dense (less ice growth) region toward the more dense region, with oppositely directed return flows at depth. Depending upon the horizontal and vertical scales of the system, rotation and friction respectively, may become important.

In order to investigate the possibility of a negative estuarine circulation driven by ice growth, the density structures within Bridport Inlet and at the entrance (about 6 km away) were compared. The data from the average of 5 profiles at site 80-1 within the Inlet and the average of 31 profiles at site 80-3 at the Inlet entrance were used to compute dynamic heights at these stations. The differences between dynamic heights at each depth were used to compute the pressure difference at 1 m depth intervals between the stations.

If it is assumed for a first coarse approximation that friction can be ignored, that the estuarine circulation is non-rotational in character, and that the flow is steady, then the equation of motion for flow through the entrance reduces to

$$u \frac{\partial u}{\partial x} = - \frac{1}{\rho} \frac{\partial P}{\partial x} \quad (12)$$

The balance of forces in (12) is between the non-linear acceleration and the pressure gradient. Such a balance is more commonly seen in flows with small radii of curvature such as tornadoes, than in estuaries. However, the situation in Bridport Inlet does intuitively justify this balance. The mean currents within the inlet are very weak ($\sim 1 \text{ cm s}^{-1}$) (see Section II) while they are about 3 to 8 cm s^{-1} at the entrance. One can therefore visualize stream lines widely spread within the inlet and converging at the entrance. The most important missing terms are friction and the Coriolis force but it can be estimated that frictional terms are small because of the relatively large depth and cross stream velocities are limited by the narrow entrance.

The relative size of the frictional term can be estimated by comparing it with the acceleration term. If friction is included in (12) then

$$u \frac{\partial u}{\partial x} = -\frac{1}{\rho} \frac{\partial P}{\partial x} + \frac{1}{\rho} \frac{\partial}{\partial z} \tau_{xz} \quad (13)$$

and we seek to compare the first and last terms

$$\frac{u \frac{\partial u}{\partial x}}{\frac{1}{\rho} \frac{\partial}{\partial z} \tau_{xz}} \sim \frac{u^2 / x}{\frac{\rho C_D U^2}{\rho H}} = \frac{H}{XC_D}$$

where τ_{xz} is the stress on z planes in the x direction, u is the velocity scale, H is the depth and X the horizontal scale.

$$\frac{H}{XC_D} = \frac{100 \text{ m}}{6000 \text{ m} \cdot 2 \times 10^{-5}} = \frac{100}{12} = 8$$

The acceleration is thus approximately an order of magnitude larger than the frictional forces.

While it is probably justifiable to ignore the cross channel velocities resulting from rotation at the Inlet entrance, the interior of the Inlet presents no such topographical constraint. If x is the primary direction of flow, then the equation of motion in the cross-stream direction would be for the above assumptions

$$f_u = -\frac{1}{\rho} \frac{\partial p}{\partial y} \quad (14)$$

The two equations (12) and (14) describe a flow in the x direction, accelerated through the Inlet entrance by pressure gradients in the x direction. The Coriolis force associated with this flow is balanced by cross stream pressure gradients. Thus the geostrophic shear at the Inlet entrance is expected to be and is in fairly good agreement with the current meter data. The cross stream pressure gradients are established in response to the density driven estuarine flow. A similar balance of forces was proposed by Garrett and Petrie (1981) for the Strait of Belle Isle where both tidal oscillations and mean flows were investigated.

The right hand side of equation (12) is known at each depth and if we assume that the flow is accelerated across the Inlet through the entrance then at any level

$$\frac{u^2}{2} = \Delta X \left(-\frac{1}{\rho} \frac{\partial p}{\partial x} \right) \quad (15)$$

The velocities resulting from (15) were computed for each depth between 3 m and 95 m (3 m depth is approximately 1 m below the ice). The velocity profile resulting from this computation is shown in Figure 14.

In order to maintain a long-term constant sea level, continuity must be satisfied and the flow into the Inlet must balance the flow out of the Inlet. This condition is clearly not satisfied by the profile of Figure 14. If a constant sea surface slope is superimposed upon the internal pressure gradients due to horizontal density gradients

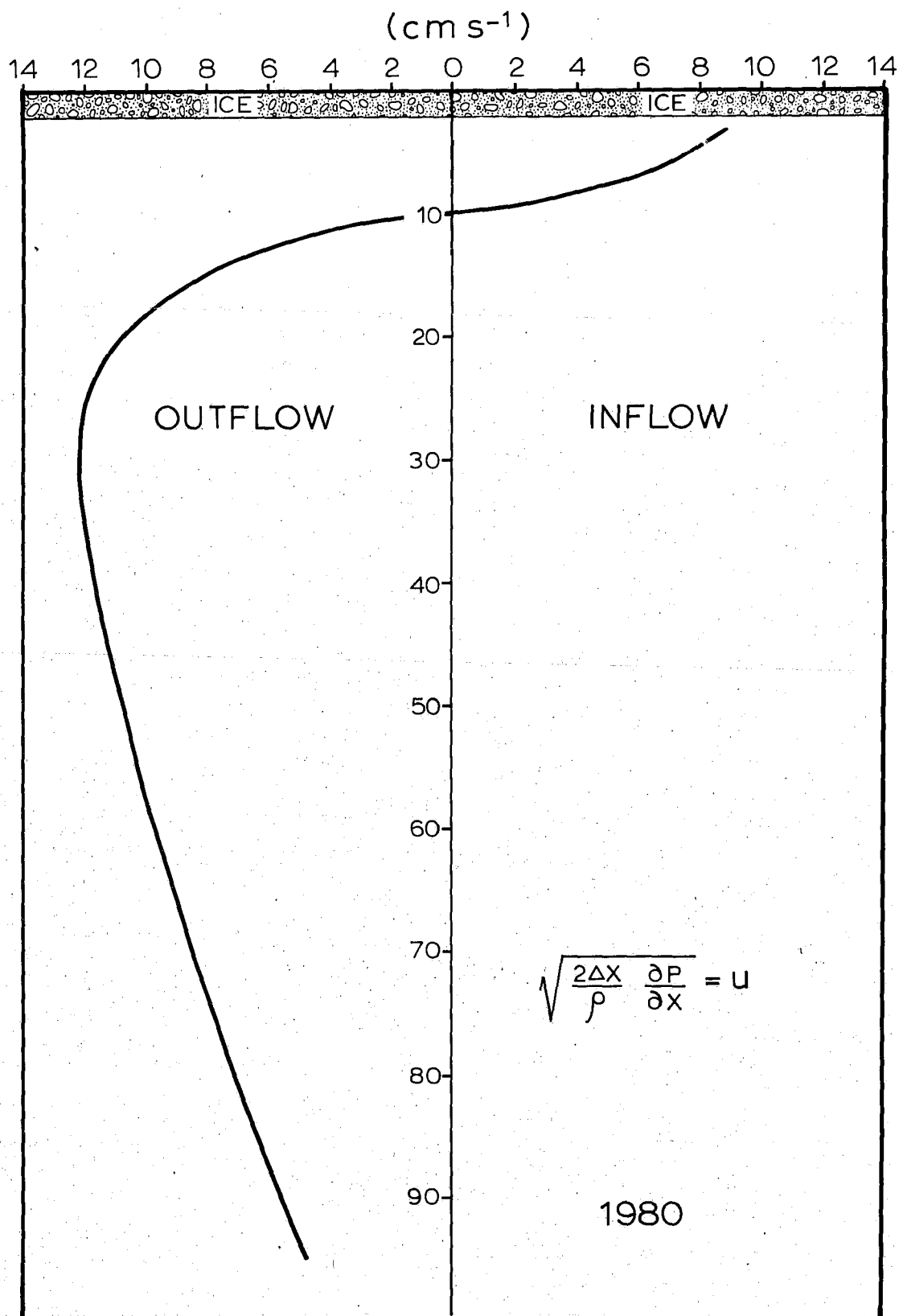


FIGURE 14. Computed thermohaline velocity profile $\left(u = \sqrt{\frac{2\Delta x}{\rho} \frac{d\rho}{dx}} \right)$ unbalanced for continuity.

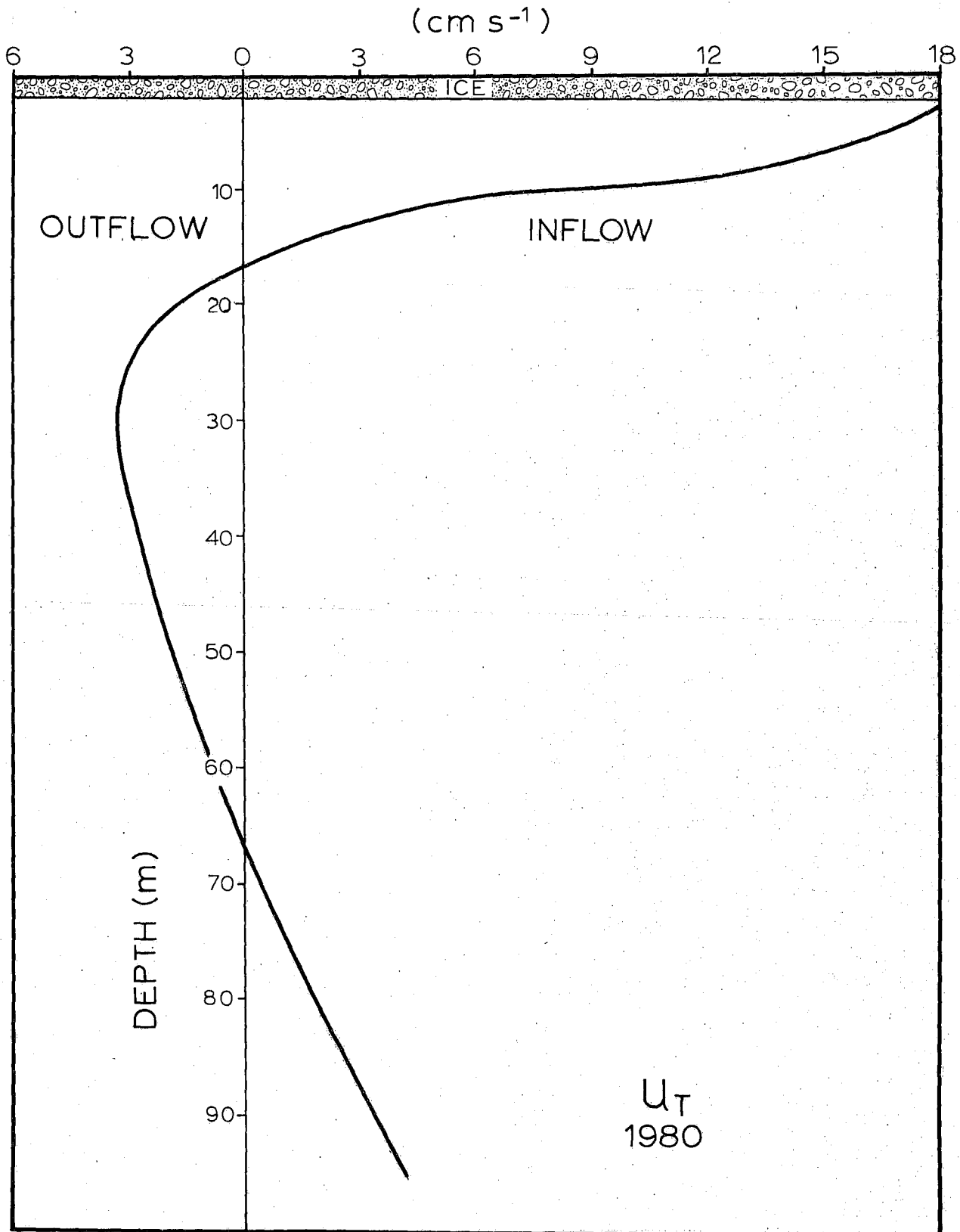


FIGURE 15. Continuity balanced thermohaline flow, u_T .

then a velocity constant with depth will be added to the thermohaline flow. This constant flow u_0 was computed by integrating the thermohaline velocity u with depth:

$$\sum_{j=3}^{95} u_j \Delta Z + u_0 H = 0 \quad (16)$$

In (16) H is the total depth, the u_j are the thermohaline velocities computed at depth intervals (ΔZ) of 1 metre. u_0 resulting from (4) is 8.90 cm s^{-1} into the inlet.

The total velocity profile $u + u_0 = u_T$ is plotted versus depth in Figure 15.

The velocity profile of Figure 15 is in rough quantitative agreement with the mean currents measured at current meter stations 7 and 8 as well as with the geostrophic current shear computed from stations across the Inlet entrance. The validity of (15) is therefore relatively well supported. The concept of the process driving the mean circulation through the Inlet entrance presented in Section III is supported by these computations: Horizontal density differences between the Inlet and the Viscount Melville Sound accelerate the flow through the entrance. In response to this flow, geostrophic balance is established in the Inlet entrance with the vertical shear obeying the thermal wind relations.

The ratio of equation (14) to (12) yields

$$\frac{f}{\frac{\partial u}{\partial x}} = - \frac{\frac{\partial p}{\partial y}}{\frac{\partial p}{\partial x}} \approx 5$$

This comparison implies that in the absence of cross-channel flow, the cross-stream pressure gradient at the entrance is approximately 5 times as large as the along-stream pressure gradient.

B. SALT FLUX

Further confirmation of the concept of estuarine flow driven by brine rejection as well as information on the mechanisms of salt balance were obtained by computing the salt flux directed through the Inlet entrance. The velocity computed from (15) was multiplied by the difference in salinity between stations 80-1 and 80-3 at each depth. A profile of the salinity difference is shown in Figure 16 while a profile of the salt flux is shown in Figure 17.

In the upper 28 m of the water column the salinity is greater within the Inlet than at the entrance. Below 29 m the salinity is greater at the entrance than within. The salt flux profile of Figure 18, however, is more complicated; there are four flux conditions which apply in 4 depth intervals:

1. Positive salt flux (out of the Inlet) due to inward flow and higher salinity within the Inlet $3 < d < 17$ m
2. Negative salt flux due to outward flow and higher salinity within the Inlet $17 < d < 29$ m
3. Positive salt flux due to outward flow and lower salinity within the Inlet $29 < d < 67$ m
4. Negative salt flux due to inward flow and lower salinity within the Inlet $67 < d < 95$ m

It is clear, however, that the contribution to the salt flux from the flow below 30 or 40 metres depth is negligible.

The salt flux at each depth was multiplied by the entrance width at that depth to compute the total salt flux.

$$\text{Salt flux} = \frac{\rho}{1000} \sum_3^{95} (u_j + u_o) \Delta S_j W_j \Delta Z \quad (17)$$

In (17) ρ is the mean density of sea water, ΔS_j are the salinity difference at each depth between station 80-3 and 80-1, and W_j are the entrance widths at each depth.

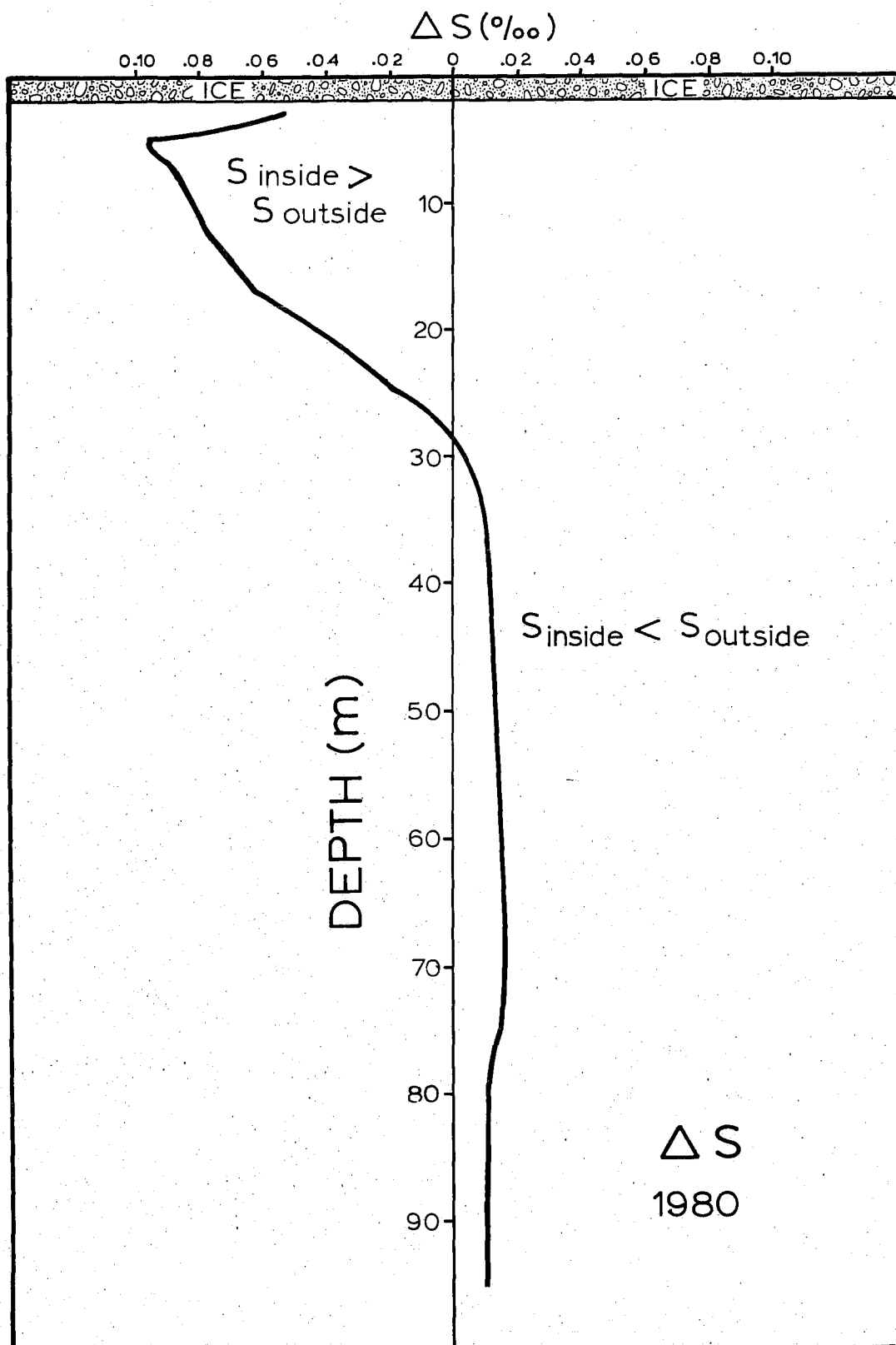


FIGURE 16. Salinity difference, ΔS , between station 80-1 and 80-3 versus depth.

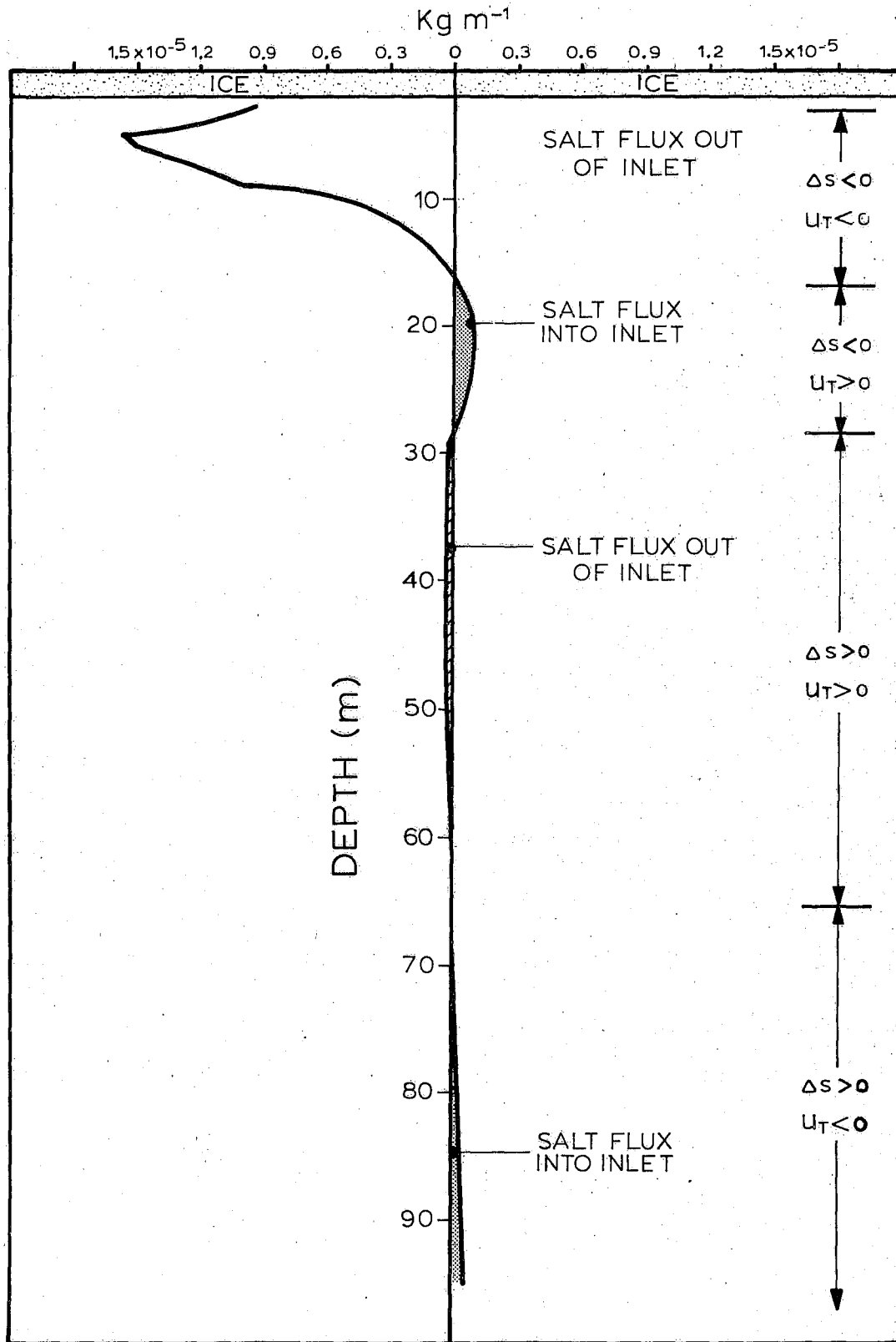


FIGURE 17. Profile of computed salt flux, $u_T \Delta S$, versus depth.

The computed salt flux is 200 Kg s^{-1} out of Bridport Inlet. The sign of this result is expected since relatively shallow areas in the Arctic are thought to be sources of higher salinity water for the rest of the Arctic Basin (Melling & Lewis, 1982). The source of the high salinity water is brine rejection by growing sea ice during the winter months. The amount of salt rejected by the growing sea ice can also be estimated:

$$\text{Salt rejection} = d A \rho_i (S_w - S_i) \quad (18)$$

where d is the thickness of the ice, A is the surface area of the Inlet, ρ_i is the density of ice, S_w is the salinity of the water from which the ice congeals, and S_i is the salinity of the sea ice. (18) yields a figure of $4.52 \times 10^9 \text{ Kg}$ of salt rejected by growing ice if the ice salinity is 5% (Greisman, 1978). If we assume that ice formation began in Bridport Inlet on 1 September, then the time elapsed from the beginning of the ice formation to the time of the measurements was 222 days or $1.92 \times 10^7 \text{ s}$. The average rate of salt rejected as brine is therefore

$$\text{Average salt rejection rate} = \frac{4.52 \times 10^9 \text{ Kg}}{1.92 \times 10^7 \text{ s}} = 236 \text{ Kg s}^{-1}$$

This figure agrees with the computed salt balance to within 7%! The very close agreement is somewhat fortuitous, however, it lends credence to the dynamical assumption of the advective acceleration balancing the pressure gradient force.

C. COMPARISON WITH 1979

Data collected in 1979 (Lake 1979 b,c) were examined to determine if the ice growth driven circulation was present in that year. The situation in 1979 was, however, very different from 1980. Figure 18 is a vertical section of $T - T_f$ for the 1979 data. There is little resemblance to Figure 9 from the 1980 data. The layer which is below the surface freezing point is 10 to 20 m deep in 1979 compared with

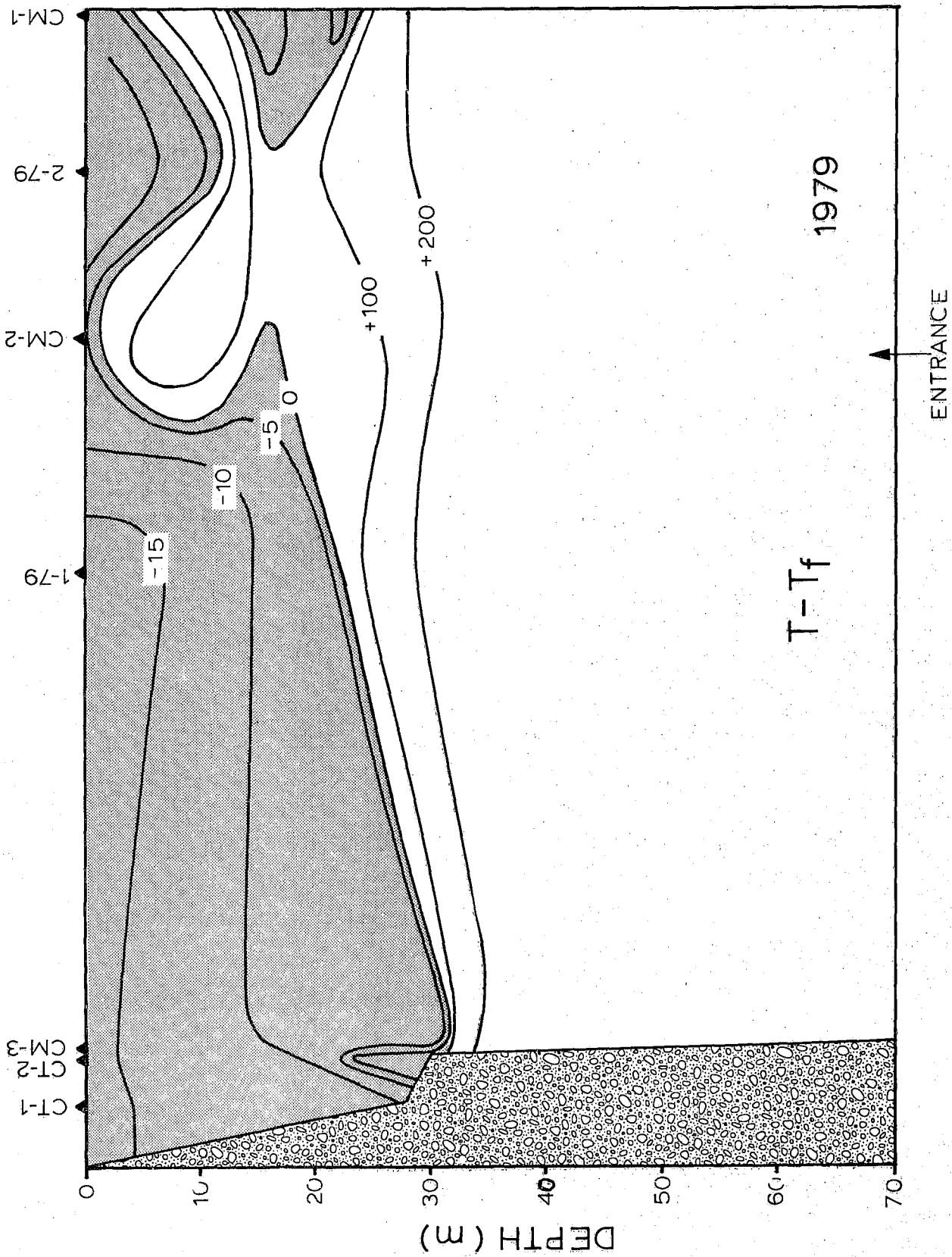


FIGURE 18. Vertical north-south section of $T - T_f$, 1979 (Millidegrees).

less than 4 m deep in 1980. In 1979 the deep water of the Inlet (below 30 m) was about 0.2°C above the surface freezing point while in 1980 the deep water was about 0.005° below the surface freezing point. Apparently convective processes had penetrated to the bottom in 1980 but not in 1979. This supposition is confirmed by comparing the CTD profiles from site 80-2 (1980) with that from site 1-79 (1979) in Figure 19. These casts were both made at the centre of the Inlet. The mixed layer depth was clearly 25 m in 1979, while in 1980, if strong intermittent convection is assumed, the mixed layer extends to the bottom and if the assumption is not made, the mixed layer depth is about 4 m. The salinity at 130 m depth in 1979 is 32.616 which is lower than the salinity found at the surface in 1980. Finally, the overall stability (in terms of the Väisälä frequency, N) of the water column between 3 m and 130 m depth is

$$N^2 = -\frac{g}{\rho} \frac{\rho_{130} - \rho_3}{127 \text{ m}}$$

and was $2.1 \times 10^{-6} \text{ s}^{-2}$ in 1979 and $0.9 \times 10^{-6} \text{ s}^{-2}$ in 1980.

The salt flux computation described in the previous section was performed with the 1979 data and yielded a figure of 130 Kg s^{-1} of outward transport of salt; roughly half the value computed with the 1980 data.

The difference in the year-to-year pictures is due to processes in Viscount Melville Sound which ultimately determine the mass structure of Bridport Inlet. At stations outside the Inlet the surface salinity was $0.35 \text{ }^{\circ}/\text{oo}$ higher in 1980 than in 1979 and the vertical density gradient was about half as large in 1980 as in 1979.

It would seem that inter-annual differences are so large as to eclipse the variations over a several month interval. The important point here is that a single year's data would not have been representative of the system. This last point is gradually being accepted as pertinent to most areas of the Archipelago and, indeed the Arctic Ocean.

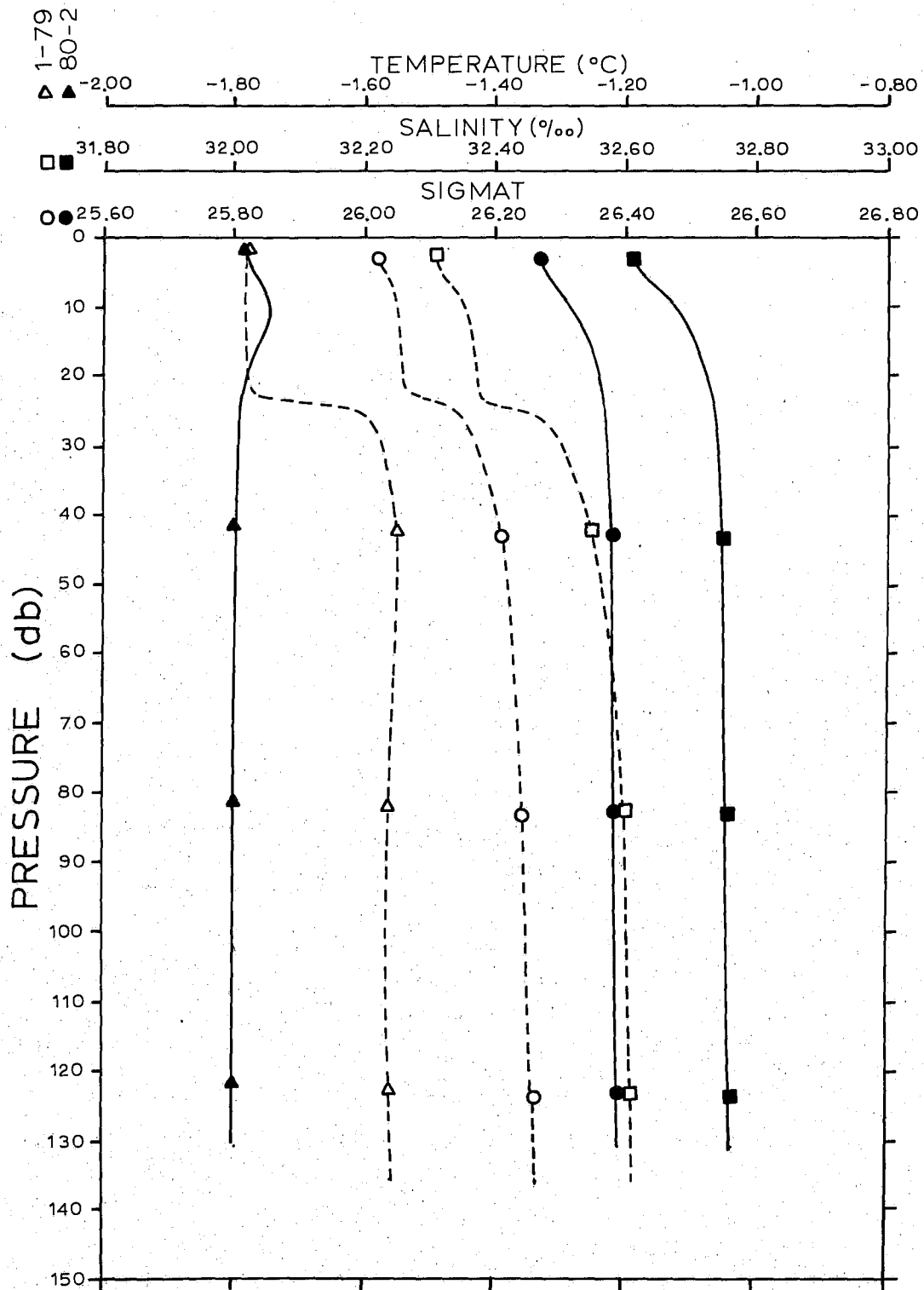


FIGURE 19. Mean CTD profiles from sites 80-2 and 1-79.

V TIDAL OSCILLATIONS

The tidal heights in Bridport Inlet had been observed in 1978 (Greisman, 1978) and in 1979 (Lake, 1979 c).

During the 1980 field program two tide gauges were installed: one near the inlet entrance and the other near the eastern shore of the inlet (see Figure 1 for tide gauge locations). The two tide gauge records are in good agreement with each other as well as with the record from 1978. There is an indication of a phase lag between the two gauges which indicates that the tide wave has a progressive component and that some tidal energy is transported into and dissipated within the inlet. Table 6 lists the major tidal constituents, their amplitude and Greenwich phase as measured in 1980.

The current meter data were subjected to tidal stream analyses, and the results for the major constituents are shown in Table 7. The larger tidal signal at the Inlet entrance makes these data sets more attractive than the interior current data for scrutiny and comparison with tidal height oscillations.

At current meter sites 7 and 8 there is significant difference in the amplitude of the tidal currents measured at depths of 10 and 50 metres. In addition, there is a nearly 180° phase difference between the 10 m and 50 m currents at site 7 while the currents at site 8 are nearly in phase. Foreman (1978) explains that the tidal stream analysis routine can be biased by 180° when the computed phases are near 0° or 180° . Since a 180° phase difference between shallow and deep currents might be ascribed to the presence of internal waves, this possibility was investigated.

It was first assumed that there was a 180° error in the phase of the semi-diurnal components at the 50 m depth current meter at site 8. Applying this correction to the analysis resulted in a coherent picture of the tidal oscillation at the entrance: stronger shallow currents in phase across the entrance with weaker deep currents also roughly in phase with each other and out of phase with the shallow flow.

Tidal current profiles may be regarded as the sum of barotropic and baroclinic components, the former being uniform through the water column and the latter being determined by the vertical stratification, the latitude and

TABLE 6a
TIDAL HEIGHT ANALYSIS

TIDE GAUGE WEST OF ENTRANCE SPIT

Name	Speed	Amp	G
ZO	0.0000000000	36.1816	.00
MSF	0.0028219327	0.0170	212.98
2Q1	0.0367063506	0.0029	164.10
Q1	0.0372185027	0.0138	196.98
O1	0.0387306544	0.0383	266.59
N01	0.0402685944	0.0013	241.17
K1	0.0417807461	0.0586	359.94
J1	0.0432928982	0.0088	60.85
001	0.0448308382	0.0058	170.65
UPS1	0.0463429899	0.0048	228.46
N2	0.9789992493	0.0683	207.74
M2	0.0805114005	0.3673	251.25
S2	0.0833333330	0.2084	304.36
ETA2	0.0850736443	0.0094	315.38
MO3	0.1192420553	0.0040	83.14
Mc	0.1207671007	0.0023	308.42
MK3	0.1222921470	0.0004	245.53
SK3	0.1251140796	0.0009	160.81
MN4	0.1595106497	0.0010	270.10
M4	0.1610228010	0.0003	53.06
MS4	0.1638447344	0.0005	326.20
S4	0.1666666660	0.0004	315.35
2MK5	0.2028035484	0.0003	230.97
2SK5	0.2084474135	0.0014	30.61
2MN6	0.2400220502	0.0006	157.01
M6	0.2415342014	0.0007	216.07
2MS6	0.2443561349	0.0013	294.40
2SM6	0.2471780665	0.0005	300.53
3MK7	0.2833149470	0.0008	97.68
M8	0.3220456019	0.0003	299.29

TABLE 6b

TIDAL HEIGHT ANALYSIS

INTERIOR TIDE GAUGE

Name	Speed	Amp	G
ZO	0.0000000000	49.7912	.00
MM	0.0015121518	0.0331	225.91
MSF	0.0028219327	0.0159	205.71
ALP1	0.0343965697	0.0039	131.05
2Q1	0.0357063506	0.0041	161.03
Q1	0.0372185027	0.0139	202.02
O1	0.0387306544	0.0373	268.53
NO1	0.0402685944	0.0024	273.44
K1	0.0417807461	0.0571	1.38
J1	0.0432928982	0.0059	38.79
001	0.0448308382	0.0058	160.76
UPS1	0.0463429899	0.0050	225.35
EPS2	0.0761773158	0.0012	193.85
MU2	0.0776894679	0.0159	201.2]
N2	0.0789992493	0.0684	211.63
M2	0.0805114005	0.3638	251.66
L2	0.0820235526	0.0202	322.95
S2	0.0833333330	0.2111	305.84
ETA2	0.0850736443	0.0092	299.45
MO3	0.1192420553	0.0038	81.95
M3	0.1207671007	0.0017	290.29
MK3	0.1222921470	0.0007	249.33
SK3	0.1251140796	0.0012	169.02
MN4	0.1595106497	0.0007	357.06
M4	0.1610228010	0.0011	53.30
SN4	0.1623325814	0.0010	222.27
MS4	0.1638447344	0.0006	348.83
S4	0.1666666660	0.0012	108.10
2MK5	0.2028035484	0.0007	357.41

continued...

TABLE 6b continued

Name	Speed	Amp	G
2SK5	0.2084474135	0.0013	155.58
2MN6	0.2400220502	0.0007	176.91
M6	0.2415342014	0.0009	192.63
2MS6	0.2443561349	0.0012	277.82
2SM6	0.2471780665	0.0007	282.82
3MK7	0.2833149470	0.0006	251.86
M8	0.3220456019	0.0001	102.88

TABLE 7

TIDAL STREAM ANALYSES FOR COMPONENTS $> 1 \text{ cm s}^{-1}$

Current Meter	Depth	Constituent	Speed (cyc/hr)	Major Axis cm s^{-1}	Minor Axis cm s^{-1}	Inclin- ation *	Greenwich Phase
CM4	12	No tidal constituents $> 0.5 \text{ cm s}^{-1}$					
CM5	12	Direction vane malfunctioned					
CM6	12	MSF	.002822	1.6	-0.3	44°	196°
		N2	.078999	2.2	0.1	57°	359°
		M2	.080511	4.2	0.6	62°	17°
		S2	.083333	2.3	0.4	58°	96°
		ETA2	.085074	2.1	-0.2	54°	359°
		M4	.161023	1.0	0.0	25°	278°
CM7	12	MSF		1.2	-0.3	16°	214°
		M2		5.4	-0.4	56°	165°
		S2		3.2	-0.4	56°	225°
		M4		1.0	-0.0	13°	201°
		MS4	.163845	1.0	-0.2	12°	270°
CM7	50	M2		2.3	-0.2	116°	356°
		SZ		1.3	-0.2	111°	51°
CM*	12	MSF		1.5	-0.3	108°	39°
		M2		3.9	-1.1	45°	162°
		S2		2.2	-0.7	58°	229°
CM8	50	M2		2.5	-0.6	10°	168°
		S2		1.9	-0.5	16°	215°
CM9	12	MSF		1.1	0.3	117°	47°
		M2		4.2	-0.6	75°	164°
		S2		2.4	-0.1	83°	221°
CM10	12	No tidal constituents $> 0.2 \text{ cm s}^{-1}$					

* Inclination in degrees measured counter-clockwise from east (mathematical convention)

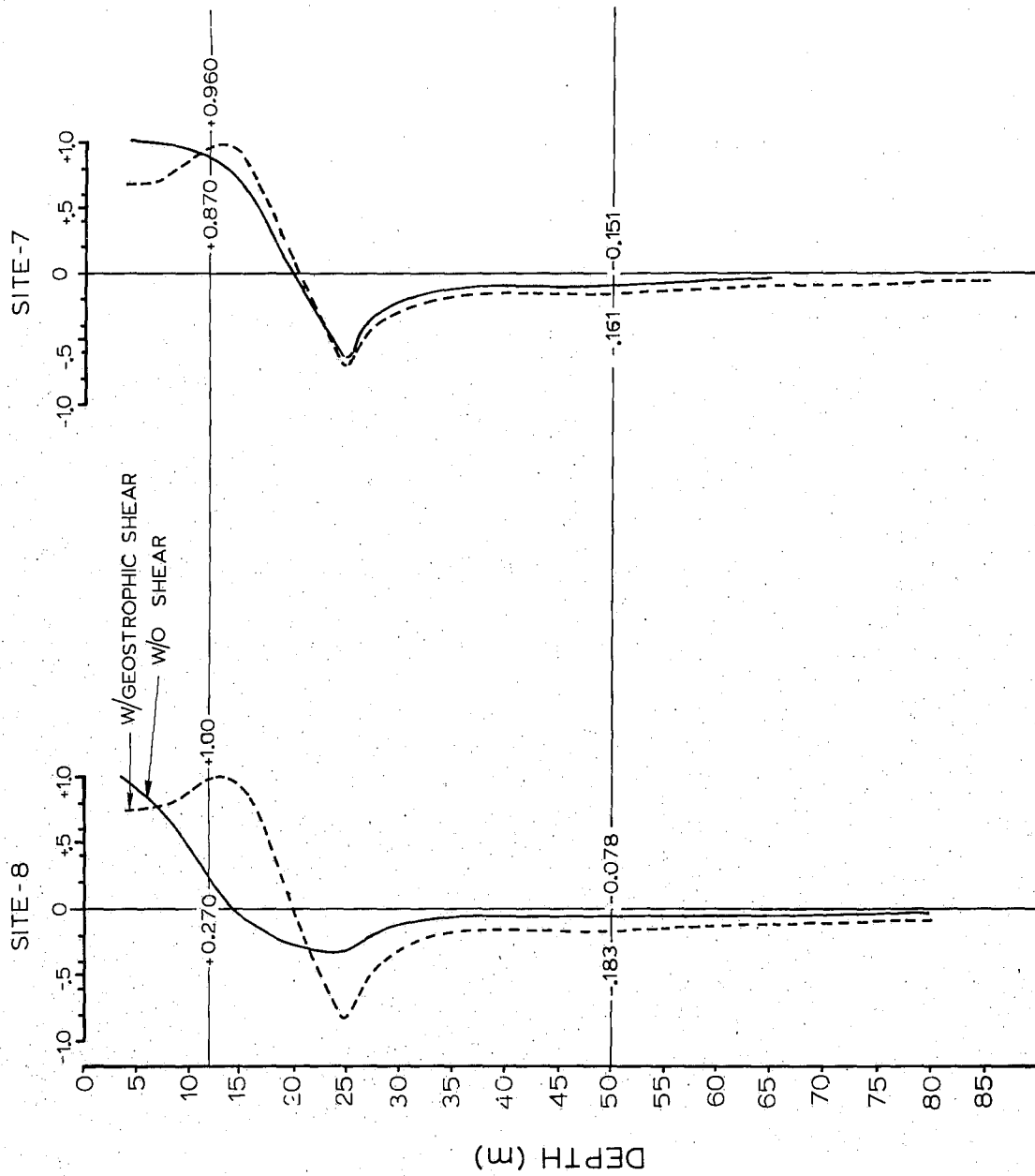


FIGURE 20. Profiles of the first internal mode at tidal frequency at the Inlet entrance.

the frequency of oscillation. In order to separate the two components, current measurements are required at several depths along with the mass structure which is obtainable from CTD casts.

Internal wave mode profiles were computed for several conditions with the Coriolis parameter set to zero. This limitation is justified in narrow channels where rotational effects are negligible but is questionable in the entrance to Bridport Inlet where, although only 2 km wide, the weak stratification yields an internal Rossby radius of deformation of only about 500 m. However, no internal waves of tidal period on a rotating earth can theoretically exist at this latitude so rotational effects cannot be included in any case in mode profile computations.

Several mode structure computations were performed using the averages of all the CTD casts made at sites 7 and 8. It was found that the computations were extremely insensitive to varying the tidal frequency from semi-diurnal to diurnal. On the other hand the computations were extremely sensitive to the magnitude of the mean shear. Two mean shear profiles were used: the first reflecting the average currents recorded at 10 and 50 m depth and the second, more detailed profile, was the geostrophic shear computed by the dynamic method.

The resulting mode structures for sites 7 and 8 in the absence of shear and with geostrophic shear are shown in Figure 20. These profiles represent the normalized amplitude of the first mode velocity oscillations.

The magnitude of the first mode baroclinic and barotropic oscillations can be computed at each tidal frequency by solving a pair of simultaneous equations:

$$X \sin (\omega t - \phi_0) + \alpha_1 Y \sin (\omega t - \phi_1) = R_1 \sin (\omega t - \phi_{R_1}) \quad (19a)$$

$$X \sin (\omega t - \phi_0) + \alpha_2 Y \sin (\omega t - \phi_1) = R_2 \sin (\omega t - \phi_{R_2}) \quad (19b)$$

where X = the amplitude of the barotropic tidal velocity oscillation
(uniform with depth)

Y = the amplitude of the first mode baroclinic velocity oscillation

$R_{1,2}$ = the measured tidal oscillation at the current meters

$\alpha_{1,2}$ = the magnitude of the mode structure at the depth of the current meters

ω = the frequency of the tidal oscillation

ϕ_0 = the Greenwich phase of the barotropic component

ϕ_1 = the Greenwich phase of the baroclinic component

$\phi_{R_{1,2}}$ = the Greenwich phase of the measured tidal oscillations at the current meters

The results of the modal decomposition for the semi-diurnal components at site 7 are presented below:

	1st baroclinic		Barotropic		Tidal Height	
	AMP (cm s ⁻¹)	Phase	AMP (cm s ⁻¹)	Phase	AMP (cm)	Phase
M_2	6.4	174°	1.1	012°	36.7	251°
S_2	4.1	227°	1.0	040°	20.8	304

It is immediately apparent that the baroclinic component as computed is substantially larger than the barotropic. The amplitude of the barotropic component however, can be independently checked. Since the internal waves at no time are responsible for the horizontal transport of fluid, it is the barotropic mode which must drive the oscillating water level in the Inlet. The transport at any instant is equal to the barotropic tidal current integrated over the cross-sectional area of the Inlet entrance. This mass transport must be equal to the rate of change of the water level integrated over the surface area of Bridport Inlet and the mass transport over half a tidal cycle must be equal to the volume change of the Inlet, or

$$CS_0 \int_0^\pi X \sin \omega t = 2H_0 A \quad (20)$$

where CS = the cross-sectional area of the Inlet entrance = $1.2 \times 10^5 \text{ m}^2$

H_0 = the tidal amplitude so that $2H_0$ = tidal range

A = the surface area of the inlet = $9.2 \times 10^7 \text{ m}^2$

The above computation reveals that a barotropic tidal current amplitude of 4.1 cm s^{-1} would be required to force the observed tidal range for the M_2 component.

The barotropic currents computed from the modal decomposition are therefore too small to explain the observed tidal range. In addition the phase difference between the barotropic currents and height should be approximately $\pi/2$ close to that for a standing wave. The computed phase difference for the baroclinic components relative to the tidal heights are about $\pi/2$ but the computed barotropic currents lead the tidal heights by about $3\pi/2$.

The conclusion must be that the modal decomposition is in some way inadequate to unify the observations. Phillips (1969) develops the theory of internal waves in the presence of a weak mean shear. In order for his development (and the methods of mode structure computation available) to apply, the shear must be much smaller than the Väisälä frequency or

$$\frac{\partial u}{\partial z} \ll N$$

where $\partial u/\partial z$ is the mean shear and N is the Väisälä frequency $= \left(-\frac{g}{\rho} \frac{\partial \rho}{\partial z} \right)^{1/2}$.
at the entrance to Bridport Inlet, the following approximate values apply

$$N = 4 \times 10^{-3} \text{ s}^{-1}$$

$$\partial u/\partial z = 6 \times 10^{-3} \text{ s}^{-1}$$

Since $\partial u/\partial z$ is not much smaller than N , the observed oscillatory flow may be a manifestation of internal waves in a strong mean shear. This phenomenon may be of interest to fluid dynamicists working in this field, but the problem is not pursued further here.

The presence of a relatively strong mean shear can be represented in terms of an overall Richardson number, which is

$$Ri_o = \frac{N^2 H^2}{U^2}$$

where Ri_o is the overall Richardson number, N is the Väisälä frequency, H is the field depth and U is the maximum velocity (such that $UH \approx \partial u / \partial z$).

For the entrance to Bridport Inlet, the overall Richardson number is 20. According to Turner (1973) the oscillating flow becomes critical when the overall Richardson number is less than π^2 . This flow is therefore stable, but barely.

Maximum tidal currents at the entrance reach about 10 cm s^{-1} at spring tide while they are less than 2 cm s^{-1} within the Inlet. The energy contained in the tidal oscillations is therefore relatively small in Bridport Inlet and it is not surprising that no events of instability such as lee waves of internal hydraulic jumps were apparent from the data set.

SOME COMMENTS ON THE EFFECTS OF AN LNG TERMINAL

From three years' of oceanographic data collection in Bridport Inlet the picture has emerged of an area characterized by relatively slow flows and dominated by convective processes due to brine rejection from growing sea ice. Currents rarely exceed 10 cm s^{-1} at the entrance and are not discernable in the interior of the Inlet. The stratification is extremely weak, so much so that convection to the bottom could be triggered by just a few days' ice growth.

In the advent of the development of a natural gas liquifaction plant and an LNG tanker terminal at Bridport Inlet, both ship operations and the discharge of heated cooling water would contribute discernably to the energy balance of the Inlet. The heated cooling water is to be discharged in a confined region to minimize the ice thickness in the berthing area. Most of the heat derived from the liquifaction of the natural gas will therefore melt ice in a confined area and eventually be lost to the atmosphere. The motion of the ships themselves, however, will probably affect the density structure within the Inlet.

By computing the potential energy difference between a fully mixed water column and that observed in 1980 and multiplying this difference by the Inlet surface area and it was found that 1.5×10^{12} joules would have been required to completely mix the Inlet. This amount of energy could be added to the system by dissipating about 17 Mega Watts continuously over a one day period.

The LNG carriers proposed are to have approximately 100 MW power plants. It is not unreasonable to assume that at least 20 MW would be required for maneuvering within the Inlet. 24 hours of such maneuvering would provide enough kinetic energy (through dissipation of the propellor wash) to fully mix Bridport Inlet.

It is the combination of an extremely weak stratification of the Inlet with the very large ship power plants which make this situation possible. Induced mixing would increase the apparent diffusive exchange of salt and decrease the advective exchange. However, the impact (if any) of the

altered mass structure on the biological community is out of the realm of expertise of this writer.

REFERENCES

1. Foreman, M.G.G. 1978. Manual for Tidal Currents Analysis and Prediction. Unpublished manuscript. Pacific Marine Science Report 78-6, Institute of Ocean Sciences, Patricia Bay, 70 p.
2. Millero, F.J. 1977. Freezing Point of Seawater. Eighth report of the joint panel on oceanographic tables and standards. 29-31.
3. Greisman, P. 1978. Bridport Inlet, Melville Island: Physical Oceanographic and Ice Surveys, February - June 1978. Arctic Sciences Ltd., report for Phoenix Ventures, Calgary, 118 p.
4. Lake, R.A. 1979a. An Oceanographic Study of Bridport Inlet, Melville Island, NWT, Part I, August 1979. Unpublished manuscript. Frozen Sea Research Group, Institute of Ocean Sciences, Patricia Bay, 12 p.
5. _____. 1979b. An Oceanographic Study of Bridport Inlet, Melville Island, NWT, Part II, March 1979. Unpublished manuscript. Frozen Sea Research Group, Institute of Ocean Sciences, Patricia Bay, 288 p.
6. _____. 1979c. An Oceanographic Study of Bridport Inlet, Melville Island, NWT, Part III, March - August 1979. Unpublished manuscript. Frozen Sea Research Group, Institute of Ocean Sciences, Patricia Bay. 59 p.
7. Lewis, E.L. and R.G. Perkin. 1982. Seasonal Mixing Process in an Arctic Fjord System. J. Phys. Ocean. 12: No. 1, 74-83.
8. Lewis, E.L. and R.B. Sudar. 1972. Measurement of Conductivity and Temperature in the Sea for Salinity Determination. J. of Geophys. Res., 77: No. 33, 6611-6617.
9. Melling, H. Personal communication.
10. Melling, H. and E.L. Lewis. 1982. Shelf Drainage Flows in the Beaufort Sea and Their Effect on the Arctic Ocean Pycnocline. Dee Sea Res., 29: No. 84, 967-985.
11. Phillips, O.M. 1969. The Dynamics of the Upper Ocean. Cambridge University Press, Cambridge, 261 p.

12. Shirasawa, K. and M.P. Langleben. 1976. Water Drag on Arctic Sea Ice. J. Geophys. Res. 81: no. 36, 6451-6454.
13. Turner, J.S. 1973. Buoyancy Effects in Fluids. Cambridge University Press, Cambridge, 367 p.

This page is blank.

APPENDIX A
MEAN CTD PROFILES

SALINITY

32.0

32.5

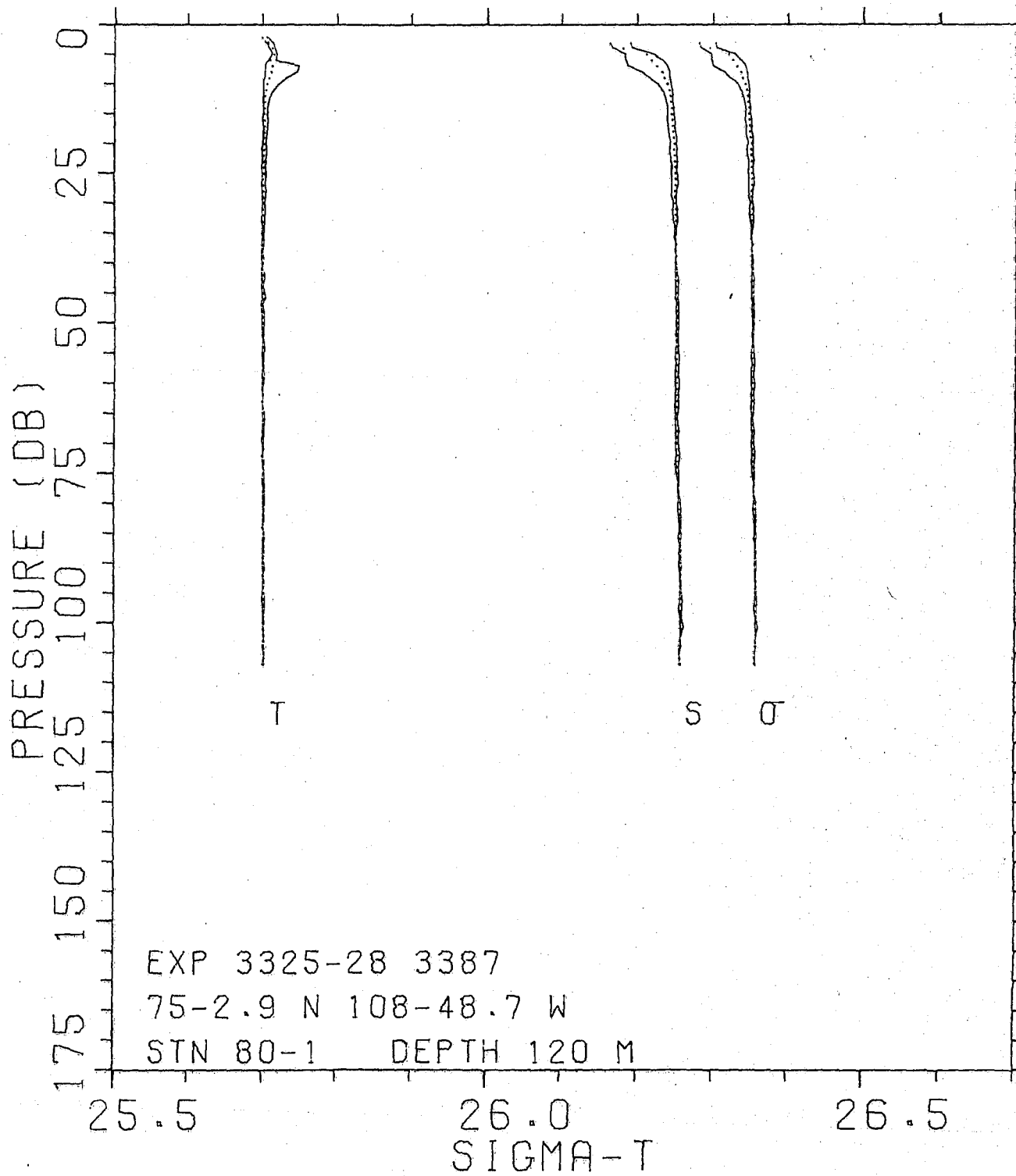
33.0

TEMPERATURE (DEG. C)

-2.0

-1.5

-1.0



CRUISE 15-80-020 BRIDPORT INLET-80
 STATION 80-1 EXPERIMENT NO.S 3325-28,3387
 LAT. 75-02.9 N LONG. 108-48.7 W
 WATER DEPTH 120.0 M

PRESSURE (DBARS)	T MEAN (DEG.C)	T RANGE (DEG.C)	S MEAN	S RANGE	SIGMAT MEAN	SIGMAT RANGE
2.0	-1.800	.007				
3.0	-1.793	.009	32.673	.027	26.289	.022
4.0	-1.786	.008	32.682	.026	26.296	.021
5.0	-1.784	.005	32.712	.038	26.321	.031
6.0	-1.790	.010	32.719	.048	26.326	.039
7.0	-1.787	.047	32.726	.053	26.332	.044
8.0	-1.788	.043	32.733	.036	26.337	.030
9.0	-1.791	.029	32.736	.027	26.340	.022
10.0	-1.794	.021	32.740	.017	26.343	.014
11.0	-1.795	.014	32.742	.013	26.345	.011
12.0	-1.797	.009	32.744	.010	26.346	.008
13.0	-1.797	.007	32.744	.008	26.346	.007
14.0	-1.798	.005	32.745	.008	26.348	.007
15.0	-1.797	.005	32.745	.007	26.347	.006
16.0	-1.798	.007	32.746	.011	26.348	.009
17.0	-1.798	.005	32.747	.009	26.349	.007
18.0	-1.798	.005	32.747	.009	26.349	.007
19.0	-1.798	.004	32.748	.010	26.350	.009
20.0	-1.798	.004	32.749	.007	26.351	.006
21.0	-1.798	.007	32.749	.011	26.351	.009
22.0	-1.799	.005	32.749	.009	26.351	.007
23.0	-1.799	.004	32.750	.009	26.351	.007
24.0	-1.799	.005	32.750	.006	26.352	.005
25.0	-1.798	.005	32.750	.008	26.351	.007
26.0	-1.799	.005	32.751	.007	26.352	.006
27.0	-1.799	.005	32.751	.009	26.352	.007
28.0	-1.798	.005	32.749	.006	26.351	.005
29.0	-1.799	.004	32.750	.006	26.351	.005
30.0	-1.799	.002	32.750	.002	26.352	.002
31.0	-1.799	.005	32.751	.007	26.353	.006
32.0	-1.799	.003	32.751	.005	26.352	.004
33.0	-1.799	.005	32.751	.006	26.352	.005
34.0	-1.799	.001	32.751	.001	26.352	.001
35.0	-1.799	.003	32.751	.003	26.353	.002
36.0	-1.799	.001	32.750	.001	26.352	.001
37.0	-1.800	.003	32.752	.001	26.353	.001
38.0	-1.799	.001	32.751	.001	26.353	.001
39.0	-1.799	.003	32.752	.002	26.353	.002
40.0	-1.799	.002	32.752	.002	26.353	.001
41.0	-1.800	.000	32.752	.001	26.354	.001
42.0	-1.799	.005	32.752	.002	26.353	.002
43.0	-1.800	.003	32.753	.005	26.354	.004
44.0	-1.800	.002	32.753	.003	26.354	.002

PRESSURE (DBARS)	T MEAN (DEG.C)	T RANGE (DEG.C)	S MEAN	S RANGE	SIGMAT MEAN	SIGMAT RANGE
45.0	-1.799	.004	32.753	.003	26.354	.002
46.0	-1.799	.004	32.753	.003	26.354	.002
47.0	-1.801	.002	32.754	.002	26.355	.002
48.0	-1.800	.003	32.753	.004	26.354	.003
49.0	-1.800	.003	32.754	.003	26.355	.002
50.0	-1.799	.003	32.754	.003	26.355	.003
51.0	-1.800	.002	32.754	.002	26.354	.002
52.0	-1.799	.002	32.753	.003	26.354	.002
53.0	-1.799	.001	32.753	.002	26.354	.001
54.0	-1.799	.003	32.753	.003	26.354	.002
55.0	-1.799	.002	32.753	.005	26.354	.004
56.0	-1.799	.002	32.753	.006	26.354	.005
57.0	-1.800	.001	32.754	.003	26.355	.002
58.0	-1.799	.002	32.752	.005	26.353	.004
59.0	-1.799	.003	32.753	.004	26.354	.003
60.0	-1.799	.001	32.753	.006	26.354	.005
61.0	-1.799	.001	32.753	.004	26.354	.003
62.0	-1.799	.001	32.752	.004	26.353	.003
63.0	-1.800	.000	32.754	.004	26.354	.003
64.0	-1.799	.001	32.753	.006	26.354	.005
65.0	-1.798	.003	32.753	.003	26.354	.002
66.0	-1.798	.002	32.753	.002	26.354	.002
67.0	-1.798	.002	32.753	.004	26.354	.003
68.0	-1.799	.002	32.754	.005	26.354	.004
69.0	-1.799	.002	32.754	.003	26.355	.002
70.0	-1.799	.002	32.753	.004	26.354	.003
71.0	-1.798	.001	32.753	.005	26.354	.004
72.0	-1.799	.001	32.755	.004	26.356	.004
73.0	-1.798	.002	32.754	.005	26.355	.004
74.0	-1.799	.001	32.754	.003	26.355	.002
75.0	-1.798	.001	32.755	.004	26.356	.003
76.0	-1.798	.003	32.756	.002	26.356	.002
77.0	-1.798	.002	32.757	.001	26.357	.001
78.0	-1.797	.002	32.756	.001	26.356	.001
79.0	-1.798	.002	32.757	.002	26.357	.001
80.0	-1.798	.002	32.758	.003	26.358	.003
81.0	-1.798	.001	32.757	.004	26.357	.003
82.0	-1.798	.002	32.758	.003	26.358	.002
83.0	-1.798	.002	32.759	.003	26.359	.002
84.0	-1.799	.001	32.758	.001	26.358	.001
85.0	-1.798	.001	32.758	.003	26.358	.002
86.0	-1.798	.002	32.758	.004	26.358	.003
87.0	-1.798	.002	32.759	.000	26.358	.000
88.0	-1.798	.002	32.759	.003	26.359	.003
89.0	-1.798	.001	32.759	.001	26.359	.001
90.0	-1.798	.002	32.758	.003	26.358	.002
91.0	-1.798	.002	32.759	.002	26.359	.002
92.0	-1.798	.001	32.759	.001	26.359	.001

PRESSURE (DBARS)	T MEAN (DEG.C)	T RANGE (DEG.C)	S MEAN	S RANGE	SIGMAT MEAN	SIGMAT RANGE
93.0	-1.798	.002	32.759	.002	26.359	.002
94.0	-1.798	.001	32.759	.002	26.359	.001
95.0	-1.798	.002	32.760	.002	26.359	.002
96.0	-1.798	.004	32.759	.003	26.359	.003
97.0	-1.798	.002	32.760	.004	26.359	.003
98.0	-1.798	.003	32.759	.004	26.359	.003
99.0	-1.798	.001	32.759	.002	26.359	.001
100.0	-1.798	.002	32.759	.004	26.359	.003
101.0	-1.798	.000	32.760	.004	26.360	.003
102.0	-1.798	.001	32.759	.000	26.359	.000
103.0	-1.798	.000	32.759	.000	26.358	.000
104.0	-1.798	.002	32.759	.002	26.359	.002
105.0	-1.797	.001	32.757	.001	26.357	.001
106.0	-1.798	.001	32.758	.000	26.358	.000
107.0	-1.798	.002	32.758	.002	26.358	.002

SALINITY

32.0

32.5

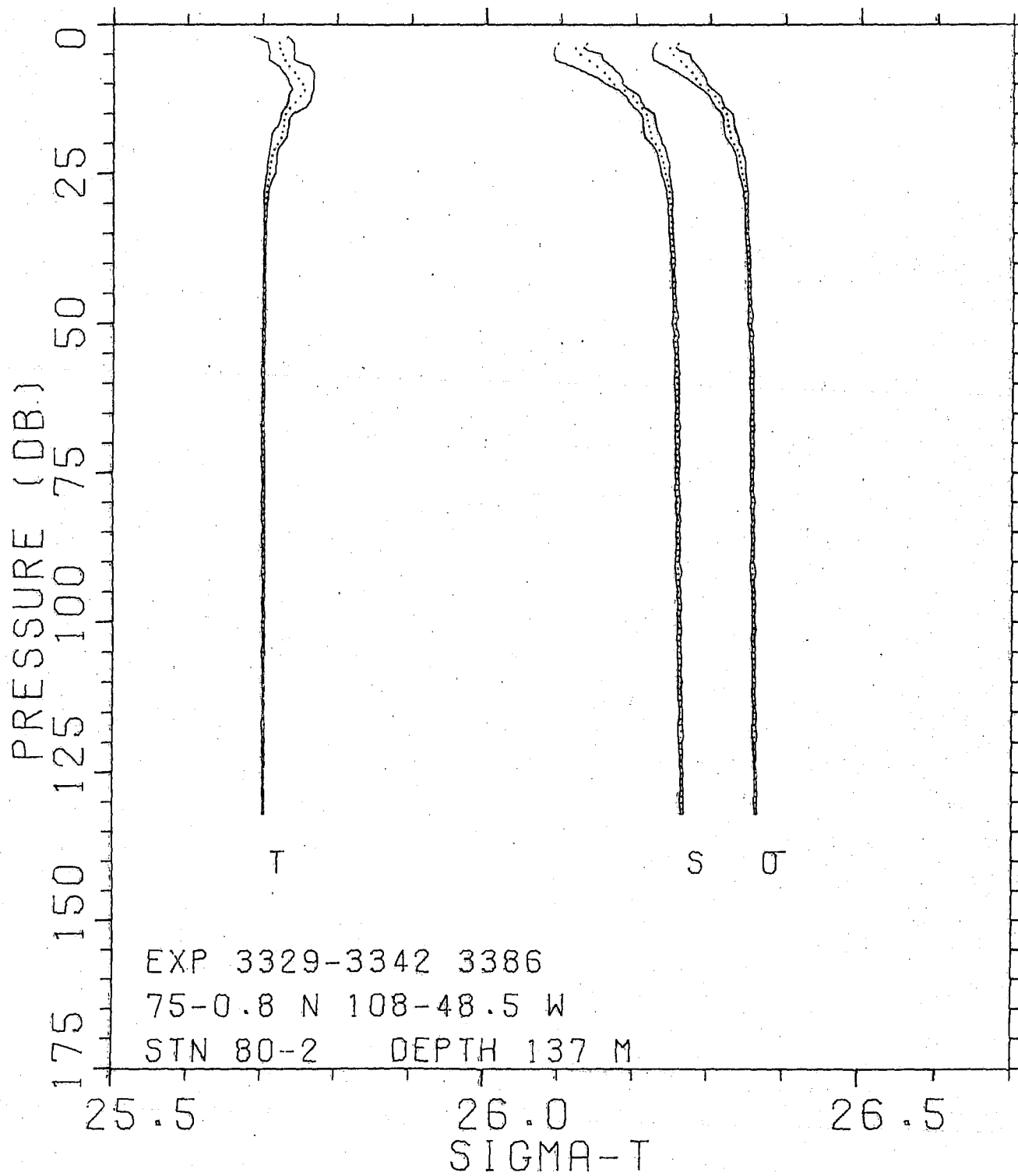
33.0

TEMPERATURE (DEG. C)

-2.0

-1.5

-1.0



CRUISE 15-80-020 BRIDPORT INLET-80
 STATION 80-2 EXPERIMENT NO.S 3329-42,3386
 LAT. 75-00.8 N LONG. 108-48.5 W
 WATER DEPTH 137.0 M

PRESSURE (DBARS)	T MEAN (DEG.C)	T RANGE (DEG.C)	S MEAN	S RANGE	SIGMAT MEAN	SIGMAT RANGE
2.0	-1.789	.045				
3.0	-1.778	.035	32.622	.037	26.247	.030
4.0	-1.777	.034	32.620	.038	26.245	.031
5.0	-1.773	.033	32.626	.064	26.250	.052
6.0	-1.770	.034	32.637	.064	26.259	.052
7.0	-1.765	.041	32.648	.051	26.268	.041
8.0	-1.757	.042	32.657	.044	26.275	.035
9.0	-1.752	.035	32.664	.032	26.280	.026
10.0	-1.747	.033	32.671	.021	26.286	.017
11.0	-1.744	.028	32.684	.016	26.297	.014
12.0	-1.750	.031	32.696	.018	26.306	.015
13.0	-1.757	.030	32.702	.016	26.311	.014
14.0	-1.765	.027	32.708	.014	26.317	.012
15.0	-1.770	.016	32.714	.018	26.322	.015
16.0	-1.772	.011	32.716	.016	26.323	.013
17.0	-1.773	.014	32.717	.017	26.324	.014
18.0	-1.774	.020	32.720	.019	26.326	.016
19.0	-1.776	.021	32.721	.021	26.328	.017
20.0	-1.781	.015	32.727	.015	26.332	.012
21.0	-1.785	.011	32.732	.014	26.336	.012
22.0	-1.788	.010	32.735	.012	26.339	.010
23.0	-1.790	.012	32.737	.014	26.341	.012
24.0	-1.791	.011	32.738	.012	26.342	.010
25.0	-1.791	.012	32.740	.011	26.343	.009
26.0	-1.793	.009	32.742	.009	26.345	.008
27.0	-1.794	.007	32.744	.007	26.347	.006
28.0	-1.795	.006	32.745	.007	26.348	.006
29.0	-1.795	.006	32.746	.007	26.348	.006
30.0	-1.796	.004	32.747	.005	26.349	.004
31.0	-1.796	.003	32.747	.006	26.349	.004
32.0	-1.796	.003	32.748	.004	26.350	.003
33.0	-1.797	.003	32.748	.006	26.350	.005
34.0	-1.797	.002	32.748	.005	26.350	.004
35.0	-1.796	.003	32.748	.005	26.350	.004
36.0	-1.797	.003	32.749	.005	26.351	.004
37.0	-1.797	.003	32.750	.005	26.351	.004
38.0	-1.797	.002	32.750	.005	26.351	.004
39.0	-1.797	.003	32.751	.005	26.352	.004
40.0	-1.797	.002	32.750	.005	26.352	.004
41.0	-1.797	.003	32.751	.003	26.352	.002
42.0	-1.798	.002	32.752	.003	26.353	.002
43.0	-1.798	.002	32.752	.005	26.353	.004
44.0	-1.798	.004	32.752	.005	26.353	.004

PRESSURE (DBARS)	T MEAN (DEG.C)	T RANGE (DEG.C)	S MEAN	S RANGE	SIGMAT MEAN	SIGMAT RANGE
45.0	-1.798	.002	32.752	.003	26.353	.002
46.0	-1.798	.003	32.753	.005	26.354	.004
47.0	-1.798	.002	32.753	.003	26.354	.002
48.0	-1.798	.003	32.753	.006	26.354	.005
49.0	-1.798	.003	32.754	.007	26.355	.006
50.0	-1.798	.003	32.753	.006	26.354	.005
51.0	-1.799	.003	32.755	.004	26.355	.003
52.0	-1.799	.003	32.755	.006	26.355	.005
53.0	-1.798	.003	32.754	.005	26.355	.004
54.0	-1.799	.003	32.755	.006	26.356	.005
55.0	-1.799	.002	32.756	.003	26.356	.002
56.0	-1.799	.002	32.756	.005	26.356	.004
57.0	-1.799	.002	32.756	.004	26.357	.004
58.0	-1.799	.005	32.756	.006	26.356	.005
59.0	-1.799	.002	32.756	.006	26.357	.005
60.0	-1.799	.003	32.757	.006	26.357	.005
61.0	-1.798	.002	32.756	.005	26.357	.004
62.0	-1.799	.003	32.757	.004	26.358	.003
63.0	-1.799	.003	32.757	.005	26.357	.004
64.0	-1.798	.003	32.757	.003	26.357	.003
65.0	-1.799	.002	32.758	.005	26.358	.004
66.0	-1.799	.001	32.757	.004	26.358	.003
67.0	-1.799	.005	32.758	.007	26.358	.006
68.0	-1.798	.003	32.758	.005	26.358	.004
69.0	-1.799	.003	32.759	.005	26.359	.004
70.0	-1.798	.004	32.758	.006	26.358	.005
71.0	-1.798	.003	32.758	.003	26.358	.003
72.0	-1.798	.003	32.758	.005	26.358	.004
73.0	-1.798	.005	32.758	.005	26.358	.004
74.0	-1.798	.003	32.758	.005	26.358	.004
75.0	-1.798	.002	32.758	.005	26.358	.004
76.0	-1.798	.003	32.758	.003	26.358	.003
77.0	-1.798	.002	32.759	.005	26.359	.004
78.0	-1.798	.004	32.758	.005	26.358	.004
79.0	-1.798	.003	32.759	.005	26.359	.004
80.0	-1.798	.004	32.759	.006	26.359	.005
81.0	-1.798	.003	32.758	.005	26.358	.004
82.0	-1.798	.003	32.759	.003	26.359	.003
83.0	-1.798	.004	32.759	.005	26.359	.004
84.0	-1.798	.002	32.759	.004	26.359	.004
85.0	-1.798	.002	32.759	.004	26.359	.004
86.0	-1.798	.004	32.759	.005	26.359	.004
87.0	-1.799	.003	32.760	.004	26.359	.003
88.0	-1.798	.002	32.759	.005	26.359	.004
89.0	-1.798	.003	32.760	.005	26.359	.004
90.0	-1.798	.002	32.759	.004	26.359	.003
91.0	-1.798	.004	32.760	.009	26.359	.008
92.0	-1.798	.005	32.760	.007	26.360	.006

PRESSURE (DBARS)	T MEAN (DEG.C)	T RANGE (DEG.C)	S MEAN	S RANGE	SIGMAT MEAN	SIGMAT RANGE
93.0	-1.798	.002	32.760	.005	26.360	.004
94.0	-1.798	.002	32.760	.004	26.360	.003
95.0	-1.798	.002	32.760	.005	26.360	.004
96.0	-1.798	.003	32.761	.004	26.360	.003
97.0	-1.799	.002	32.761	.005	26.361	.004
98.0	-1.798	.003	32.761	.005	26.361	.004
99.0	-1.798	.003	32.761	.003	26.360	.003
100.0	-1.798	.003	32.761	.004	26.361	.004
101.0	-1.798	.003	32.761	.005	26.361	.004
102.0	-1.798	.002	32.762	.005	26.361	.004
103.0	-1.798	.003	32.761	.005	26.360	.004
104.0	-1.798	.002	32.762	.004	26.361	.003
105.0	-1.798	.005	32.762	.005	26.361	.005
106.0	-1.798	.003	32.762	.005	26.361	.004
107.0	-1.798	.002	32.762	.004	26.362	.003
108.0	-1.798	.002	32.762	.004	26.361	.003
109.0	-1.798	.002	32.763	.004	26.362	.003
110.0	-1.798	.002	32.763	.005	26.362	.004
111.0	-1.798	.003	32.762	.004	26.362	.003
112.0	-1.798	.001	32.763	.004	26.362	.004
113.0	-1.798	.003	32.763	.005	26.362	.004
114.0	-1.798	.002	32.764	.003	26.362	.002
115.0	-1.798	.002	32.763	.005	26.362	.004
116.0	-1.798	.002	32.763	.005	26.362	.004
117.0	-1.797	.005	32.763	.005	26.362	.004
118.0	-1.798	.002	32.764	.007	26.363	.005
119.0	-1.798	.003	32.763	.008	26.362	.006
120.0	-1.798	.003	32.764	.003	26.363	.003
121.0	-1.798	.002	32.764	.005	26.363	.004
122.0	-1.797	.003	32.764	.004	26.363	.003
123.0	-1.798	.003	32.765	.002	26.363	.002
124.0	-1.797	.002	32.764	.003	26.363	.002
125.0	-1.798	.002	32.765	.003	26.364	.003
126.0	-1.798	.002	32.765	.003	26.364	.003
127.0	-1.797	.001	32.765	.003	26.364	.003
128.0	-1.798	.003	32.766	.003	26.364	.002
129.0	-1.797	.003	32.765	.005	26.364	.004
130.0	-1.797	.002	32.765	.005	26.364	.004
131.0	-1.797	.002	32.765	.004	26.364	.003
132.0	-1.797	.003	32.766	.004	26.364	.003

SALINITY

32.0

32.5

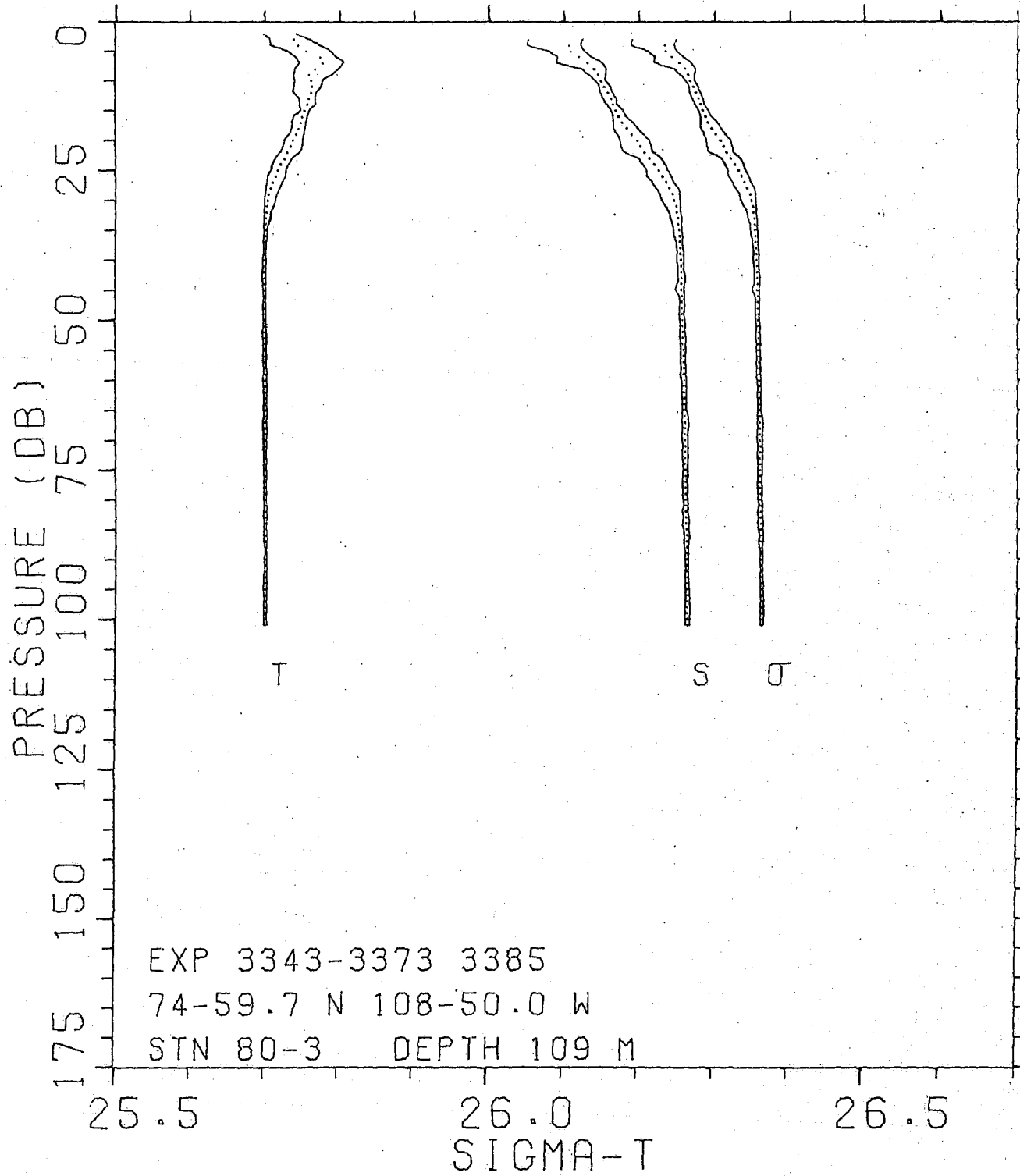
33.0

TEMPERATURE (DEG. C)

-2.0

-1.5

-1.0



CRUISE 15-80-020 BRIDPORT INLET-80
 STATION 80-3 EXPERIMENT NO.S 3343-73,3385
 LAT. 74-59.7 N LONG. 108-50.0 W
 WATER DEPTH 109.0 M

PRESSURE (DBARS)	T MEAN (DEG.C)	T RANGE (DEG.C)	S MEAN	S RANGE	SIGMAT MEAN	SIGMAT RANGE
2.0	-1.784	.043				
3.0	-1.762	.051	32.609	.072	26.236	.058
4.0	-1.756	.066	32.606	.071	26.234	.057
5.0	-1.745	.058	32.609	.047	26.236	.037
6.0	-1.727	.055	32.620	.044	26.244	.036
7.0	-1.723	.060	32.631	.061	26.253	.050
8.0	-1.733	.059	32.640	.032	26.260	.028
9.0	-1.741	.051	32.645	.022	26.265	.018
10.0	-1.738	.036	32.649	.013	26.268	.011
11.0	-1.737	.037	32.653	.014	26.272	.012
12.0	-1.738	.031	32.658	.017	26.275	.014
13.0	-1.742	.020	32.662	.018	26.279	.015
14.0	-1.744	.022	32.665	.013	26.282	.011
15.0	-1.747	.010	32.669	.016	26.284	.013
16.0	-1.750	.019	32.673	.017	26.288	.014
17.0	-1.752	.019	32.678	.026	26.292	.022
18.0	-1.755	.017	32.684	.034	26.297	.028
19.0	-1.759	.020	32.691	.034	26.302	.028
20.0	-1.763	.025	32.698	.039	26.309	.032
21.0	-1.766	.026	32.703	.041	26.312	.034
22.0	-1.770	.026	32.708	.038	26.317	.032
23.0	-1.775	.023	32.714	.030	26.322	.025
24.0	-1.779	.022	32.721	.030	26.327	.025
25.0	-1.783	.019	32.727	.027	26.332	.022
26.0	-1.786	.024	32.731	.033	26.336	.027
27.0	-1.790	.019	32.737	.028	26.340	.023
28.0	-1.792	.018	32.740	.031	26.344	.025
29.0	-1.794	.015	32.745	.026	26.348	.021
30.0	-1.796	.014	32.747	.025	26.349	.020
31.0	-1.797	.011	32.750	.020	26.351	.016
32.0	-1.797	.008	32.751	.015	26.352	.012
33.0	-1.798	.008	32.752	.015	26.353	.013
34.0	-1.798	.006	32.753	.011	26.354	.009
35.0	-1.799	.004	32.754	.011	26.355	.009
36.0	-1.799	.005	32.754	.011	26.355	.009
37.0	-1.799	.004	32.755	.008	26.356	.007
38.0	-1.799	.003	32.756	.008	26.356	.007
39.0	-1.799	.003	32.756	.009	26.356	.007
40.0	-1.800	.005	32.757	.010	26.357	.008
41.0	-1.800	.004	32.756	.007	26.357	.006
42.0	-1.800	.004	32.757	.008	26.357	.007
43.0	-1.800	.005	32.757	.010	26.358	.008
44.0	-1.800	.004	32.758	.009	26.358	.008

PRESSURE (DBARS)	T MEAN (DEG.C)	T RANGE (DEG.C)	S MEAN	S RANGE	SIGMAT MEAN	SIGMAT RANGE
45.0	-1.799	.003	32.757	.012	26.357	.010
46.0	-1.800	.003	32.758	.006	26.358	.005
47.0	-1.800	.003	32.758	.005	26.358	.004
48.0	-1.799	.004	32.758	.007	26.358	.006
49.0	-1.799	.003	32.759	.006	26.359	.005
50.0	-1.799	.003	32.759	.007	26.359	.005
51.0	-1.800	.003	32.759	.006	26.359	.005
52.0	-1.800	.004	32.759	.006	26.359	.005
53.0	-1.799	.005	32.759	.009	26.359	.007
54.0	-1.799	.003	32.759	.006	26.359	.005
55.0	-1.799	.003	32.760	.006	26.360	.005
56.0	-1.799	.004	32.760	.006	26.360	.005
57.0	-1.799	.003	32.760	.006	26.360	.005
58.0	-1.799	.003	32.760	.006	26.360	.005
59.0	-1.799	.004	32.760	.007	26.360	.006
60.0	-1.799	.004	32.761	.007	26.360	.006
61.0	-1.799	.004	32.760	.005	26.360	.004
62.0	-1.799	.004	32.761	.006	26.361	.005
63.0	-1.799	.002	32.761	.005	26.360	.004
64.0	-1.799	.003	32.762	.005	26.361	.004
65.0	-1.799	.004	32.761	.005	26.361	.004
66.0	-1.799	.004	32.762	.008	26.361	.007
67.0	-1.799	.004	32.762	.009	26.362	.007
68.0	-1.799	.005	32.762	.008	26.361	.006
69.0	-1.799	.004	32.762	.007	26.361	.006
70.0	-1.799	.003	32.762	.008	26.362	.006
71.0	-1.799	.004	32.763	.006	26.362	.005
72.0	-1.799	.003	32.763	.008	26.362	.006
73.0	-1.799	.003	32.763	.007	26.362	.006
74.0	-1.799	.004	32.763	.006	26.362	.005
75.0	-1.799	.003	32.763	.006	26.362	.005
76.0	-1.799	.004	32.763	.006	26.362	.005
77.0	-1.799	.002	32.763	.005	26.362	.004
78.0	-1.799	.003	32.763	.007	26.362	.006
79.0	-1.799	.004	32.763	.006	26.362	.005
80.0	-1.799	.003	32.763	.006	26.362	.005
81.0	-1.799	.004	32.764	.006	26.363	.005
82.0	-1.799	.004	32.764	.007	26.363	.006
83.0	-1.799	.005	32.764	.007	26.363	.006
84.0	-1.799	.003	32.764	.009	26.363	.007
85.0	-1.799	.003	32.764	.006	26.363	.005
86.0	-1.799	.004	32.765	.007	26.363	.005
87.0	-1.799	.004	32.765	.007	26.363	.006
88.0	-1.799	.002	32.765	.005	26.363	.004
89.0	-1.799	.002	32.765	.004	26.364	.003
90.0	-1.799	.004	32.765	.005	26.364	.004
91.0	-1.799	.003	32.765	.003	26.363	.003
92.0	-1.799	.003	32.765	.003	26.364	.003

PRESSURE (DBARS)	T MEAN (DEG.C)	T RANGE (DEG.C)	S MEAN	S RANGE	SIGMAT MEAN	SIGMAT RANGE
93.0	-1.799	.004	32.765	.005	26.364	.004
94.0	-1.800	.005	32.765	.005	26.364	.004
95.0	-1.799	.005	32.765	.005	26.364	.004
96.0	-1.799	.004	32.765	.005	26.364	.004
97.0	-1.799	.003	32.765	.005	26.364	.004
98.0	-1.800	.005	32.765	.006	26.364	.005
99.0	-1.800	.004	32.766	.006	26.364	.005
100.0	-1.799	.003	32.766	.006	26.364	.005
101.0	-1.799	.004	32.766	.005	26.364	.004

SALINITY

32.0

32.5

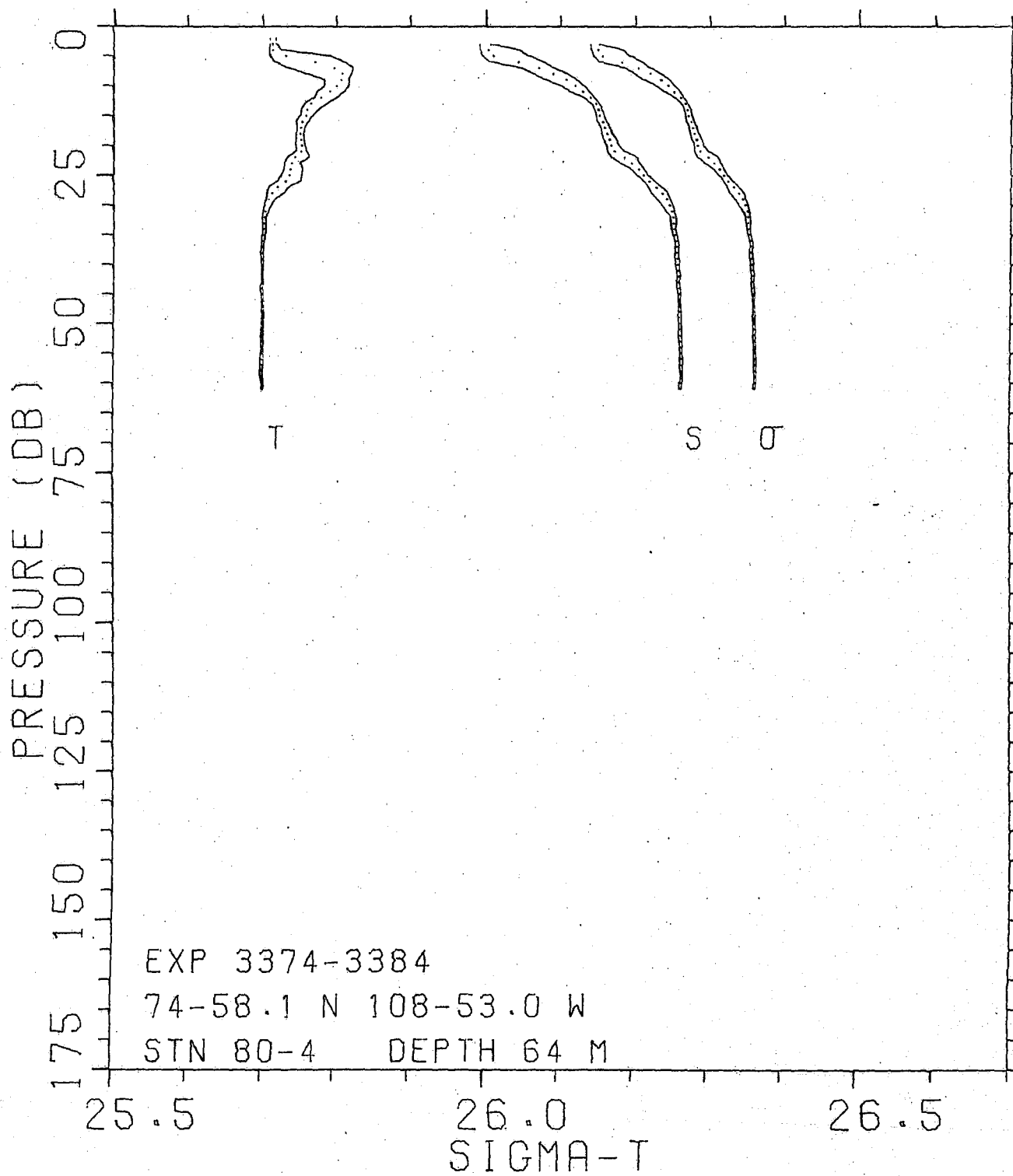
33.0

TEMPERATURE (DEG. C)

-2.0

-1.5

-1.0



CRUISE 15-80-020 BRIDPORT INLET-80
 STATION 80-4 EXPERIMENT NO.S 3374-3384
 LAT. 74-58.1 N LONG. 108-53.0 W
 WATER DEPTH 64.0 M

PRESSURE (DBARS)	T MEAN (DEG.C)	T RANGE (DEG.C)	S MEAN	S RANGE	SIGMAT MEAN	SIGMAT RANGE
2.0	-1.787	.007				
3.0	-1.787	.007	32.500	.015	26.148	.012
4.0	-1.786	.016	32.503	.054	26.151	.044
5.0	-1.769	.083	32.511	.062	26.157	.049
6.0	-1.729	.095	32.544	.073	26.183	.057
7.0	-1.702	.091	32.571	.042	26.204	.032
8.0	-1.691	.063	32.591	.045	26.220	.035
9.0	-1.693	.032	32.609	.043	26.234	.035
10.0	-1.699	.033	32.621	.030	26.244	.025
11.0	-1.708	.038	32.631	.026	26.253	.022
12.0	-1.721	.031	32.641	.014	26.262	.012
13.0	-1.734	.032	32.648	.010	26.268	.009
14.0	-1.739	.024	32.652	.010	26.270	.008
15.0	-1.741	.017	32.654	.011	26.272	.009
16.0	-1.746	.018	32.658	.012	26.276	.010
17.0	-1.748	.010	32.661	.012	26.278	.010
18.0	-1.748	.010	32.664	.014	26.280	.011
19.0	-1.747	.011	32.667	.017	26.283	.014
20.0	-1.746	.013	32.670	.015	26.285	.012
21.0	-1.747	.014	32.674	.023	26.289	.019
22.0	-1.755	.031	32.687	.034	26.299	.028
23.0	-1.760	.021	32.697	.025	26.307	.021
24.0	-1.762	.026	32.706	.017	26.315	.014
25.0	-1.763	.028	32.712	.014	26.320	.012
26.0	-1.769	.032	32.720	.014	26.326	.012
27.0	-1.780	.027	32.729	.018	26.334	.015
28.0	-1.787	.023	32.737	.023	26.340	.019
29.0	-1.792	.012	32.743	.017	26.346	.014
30.0	-1.794	.009	32.747	.015	26.349	.012
31.0	-1.796	.007	32.750	.012	26.351	.010
32.0	-1.797	.005	32.752	.007	26.353	.006
33.0	-1.797	.004	32.752	.008	26.353	.007
34.0	-1.798	.004	32.753	.005	26.354	.004
35.0	-1.798	.004	32.754	.006	26.355	.005
36.0	-1.799	.004	32.756	.004	26.356	.004
37.0	-1.799	.003	32.756	.005	26.357	.004
38.0	-1.799	.004	32.756	.005	26.357	.004
39.0	-1.799	.003	32.758	.005	26.358	.005
40.0	-1.800	.003	32.758	.006	26.358	.005
41.0	-1.799	.002	32.758	.004	26.358	.003
42.0	-1.800	.002	32.760	.005	26.359	.004
43.0	-1.799	.002	32.759	.003	26.359	.003
44.0	-1.800	.004	32.760	.005	26.360	.004

PRESSURE (DBARS)	T MEAN (DEG.C)	T RANGE (DEG.C)	S MEAN	S RANGE	SIGMAT MEAN	SIGMAT RANGE
45.0	-1.800	.003	32.760	.004	26.360	.003
46.0	-1.800	.002	32.761	.003	26.360	.003
47.0	-1.800	.002	32.761	.002	26.361	.002
48.0	-1.800	.003	32.761	.003	26.361	.003
49.0	-1.799	.002	32.761	.005	26.360	.004
50.0	-1.800	.003	32.762	.003	26.361	.003
51.0	-1.800	.002	32.762	.004	26.361	.003
52.0	-1.800	.003	32.763	.005	26.362	.004
53.0	-1.800	.003	32.762	.004	26.362	.003
54.0	-1.800	.002	32.763	.003	26.362	.003
55.0	-1.800	.002	32.763	.003	26.362	.002
56.0	-1.800	.004	32.764	.005	26.363	.004
57.0	-1.800	.003	32.764	.004	26.363	.003
58.0	-1.800	.003	32.764	.004	26.363	.003
59.0	-1.800	.003	32.764	.002	26.363	.002
60.0	-1.799	.002	32.763	.004	26.362	.003
61.0	-1.799	.002	32.763	.003	26.362	.002

This page is blank.

102

SALINITY

32.0

32.5

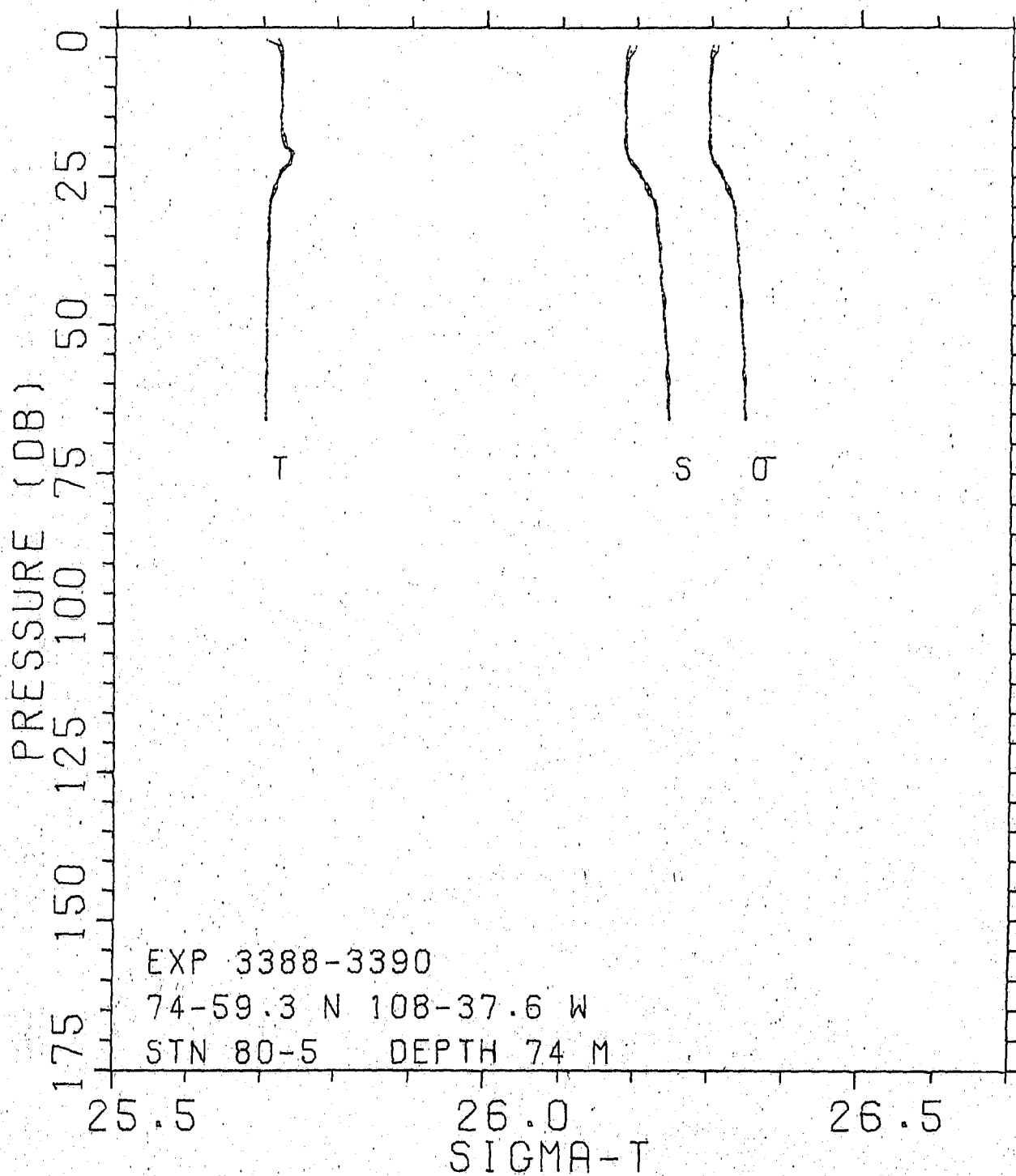
33.0

TEMPERATURE (DEG. C)

-2.0

-1.5

-1.0



CRUISE 15-80-020 BRIDPORT INLET-80
 STATION 80-5 EXPERIMENT NO.S 3388-3390
 LAT. 74-59.3 N LONG. 108-37.6 W
 WATER DEPTH 74.0 M

PRESSURE (DBARS)	T MEAN (DEG.C)	T RANGE (DEG.C)	S MEAN	S RANGE	SIGMAT MEAN	SIGMAT RANGE
2.0	-1.786	.016				
3.0	-1.778	.005	32.694	.009	26.306	.007
4.0	-1.775	.004	32.690	.010	26.303	.009
5.0	-1.774	.002	32.686	.004	26.299	.003
6.0	-1.775	.001	32.687	.002	26.300	.002
7.0	-1.775	.003	32.686	.003	26.299	.003
8.0	-1.774	.002	32.686	.002	26.299	.002
9.0	-1.774	.001	32.685	.002	26.298	.002
10.0	-1.775	.001	32.686	.001	26.299	.001
11.0	-1.774	.001	32.685	.002	26.298	.002
12.0	-1.775	.001	32.685	.001	26.298	.001
13.0	-1.774	.001	32.685	.001	26.298	.001
14.0	-1.774	.001	32.685	.001	26.298	.001
15.0	-1.775	.001	32.687	.000	26.299	.000
16.0	-1.775	.001	32.686	.001	26.299	.001
17.0	-1.774	.002	32.685	.001	26.298	.001
18.0	-1.773	.005	32.687	.002	26.299	.002
19.0	-1.770	.005	32.686	.003	26.299	.002
20.0	-1.769	.003	32.687	.003	26.300	.003
21.0	-1.758	.004	32.688	.001	26.300	.001
22.0	-1.762	.001	32.691	.002	26.303	.001
23.0	-1.765	.005	32.697	.005	26.308	.004
24.0	-1.774	.003	32.704	.003	26.314	.003
25.0	-1.777	.001	32.707	.002	26.316	.001
26.0	-1.781	.000	32.713	.000	26.321	.000
27.0	-1.784	.006	32.717	.008	26.324	.007
28.0	-1.786	.002	32.720	.002	26.326	.002
29.0	-1.790	.001	32.726	.001	26.331	.001
30.0	-1.790	.001	32.727	.003	26.332	.002
31.0	-1.790	.001	32.728	.001	26.333	.001
32.0	-1.792	.001	32.729	.001	26.334	.001
33.0	-1.791	.002	32.728	.003	26.334	.002
34.0	-1.791	.001	32.730	.003	26.335	.002
35.0	-1.791	.001	32.729	.000	26.335	.000
36.0	-1.793	.003	32.732	.003	26.336	.002
37.0	-1.792	.002	32.733	.003	26.337	.003
38.0	-1.793	.001	32.733	.000	26.337	.000
39.0	-1.792	.001	32.732	.002	26.337	.001
40.0	-1.794	.001	32.734	.001	26.338	.001
41.0	-1.794	.000	32.736	.001	26.340	.001
42.0	-1.793	.002	32.735	.003	26.339	.002
43.0	-1.792	.002	32.734	.002	26.339	.001
44.0	-1.793	.002	32.736	.002	26.340	.002

PRESSURE (DBARS)	T MEAN (DEG.C)	T RANGE (DEG.C)	S MEAN	S RANGE	SIGMAT MEAN	SIGMAT RANGE
45.0	-1.794	.001	32.737	.003	26.341	.002
46.0	-1.794	.001	32.738	.004	26.342	.003
47.0	-1.794	.001	32.738	.001	26.342	.001
48.0	-1.794	.001	32.738	.001	26.342	.001
49.0	-1.794	.000	32.739	.002	26.342	.002
50.0	-1.794	.000	32.740	.000	26.343	.000
51.0	-1.794	.002	32.740	.003	26.344	.002
52.0	-1.794	.001	32.741	.001	26.344	.001
53.0	-1.794	.001	32.741	.001	26.344	.000
54.0	-1.794	.002	32.743	.001	26.346	.001
55.0	-1.794	.000	32.744	.000	26.347	.000
56.0	-1.794	.002	32.743	.002	26.346	.002
57.0	-1.793	.000	32.743	.000	26.346	.000
58.0	-1.794	.003	32.743	.003	26.346	.003
59.0	-1.794	.002	32.744	.004	26.347	.003
60.0	-1.794	.001	32.745	.002	26.348	.002
61.0	-1.794	.000	32.745	.000	26.347	.000
62.0	-1.795	.000	32.746	.002	26.348	.001
63.0	-1.794	.001	32.744	.002	26.347	.002
64.0	-1.794	.001	32.745	.002	26.347	.002
65.0	-1.794	.001	32.747	.001	26.349	.001
66.0	-1.794	.002	32.746	.002	26.349	.002

This page is blank.

SALINITY

32.0

32.5

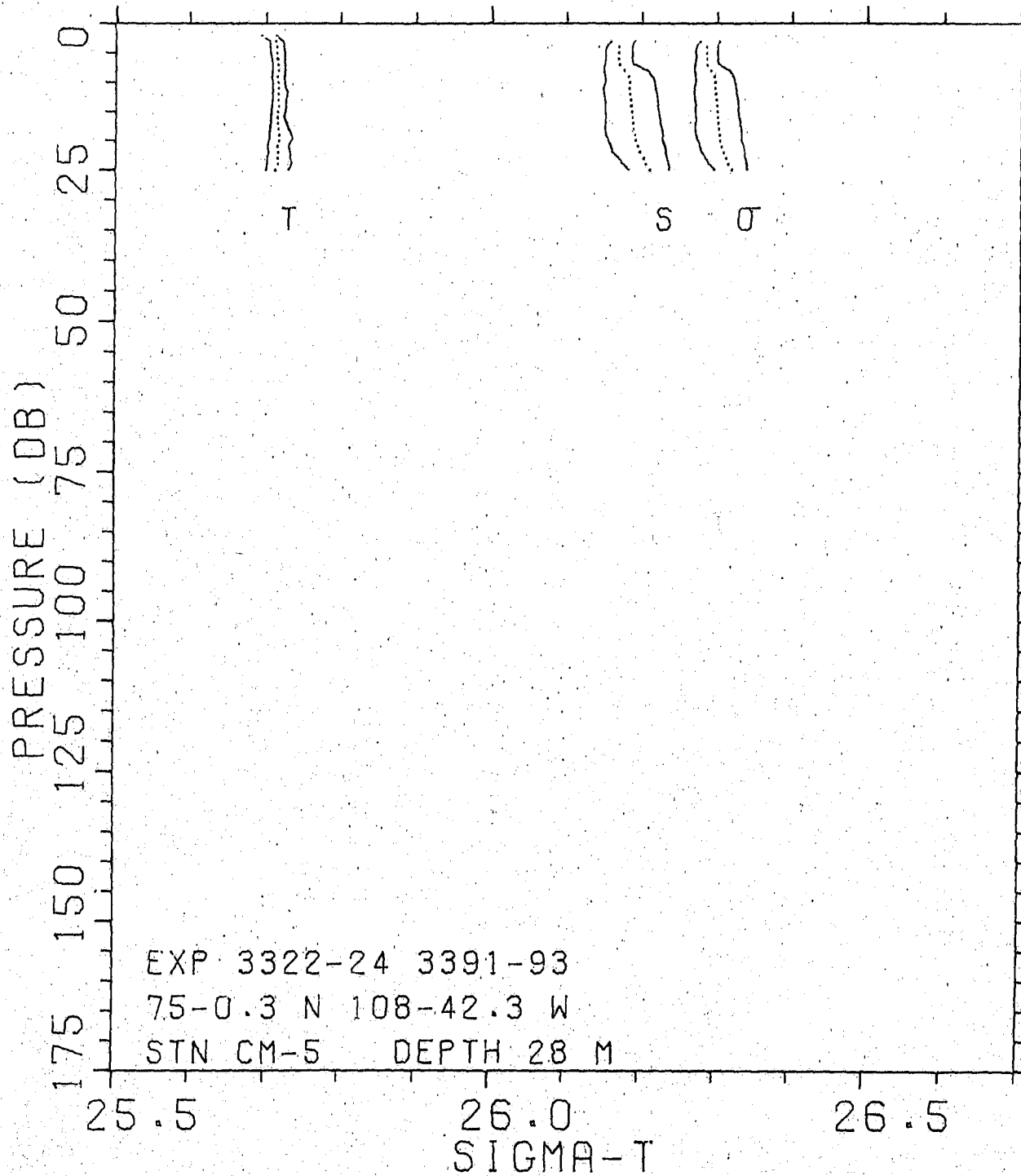
33.0

TEMPERATURE (DEG. C)

-2.0

-1.5

-1.0



CRUISE 15-80-020 BRIDPORT INLET-80
 STATION CM-4 EXPERIMENT NO.S 3322-24,3391-93
 LAT. 75-02.1 N LONG. 108-41.3 W
 WATER DEPTH 62.0 M

PRESSURE (DBARS)	T MEAN (DEG.C)	T RANGE (DEG.C)	S MEAN	S RANGE	SIGMAT MEAN	SIGMAT RANGE
2.0	-1.813	.017				
3.0	-1.794	.023				
4.0	-1.792	.018	32.704	.097	26.314	.080
5.0	-1.792	.019	32.703	.097	26.313	.080
6.0	-1.793	.017	32.706	.089	26.316	.072
7.0	-1.793	.014	32.710	.072	26.319	.059
8.0	-1.793	.017	32.713	.067	26.321	.055
9.0	-1.793	.018	32.715	.067	26.323	.055
10.0	-1.792	.019	32.717	.061	26.325	.050
11.0	-1.791	.021	32.718	.059	26.326	.048
12.0	-1.789	.027	32.719	.055	26.326	.045
13.0	-1.789	.024	32.719	.053	26.326	.044
14.0	-1.789	.026	32.720	.055	26.327	.045
15.0	-1.788	.024	32.720	.050	26.327	.042
16.0	-1.788	.024	32.721	.048	26.328	.040
17.0	-1.791	.019	32.724	.043	26.330	.035
18.0	-1.792	.017	32.726	.040	26.332	.033
19.0	-1.792	.017	32.728	.036	26.334	.030
20.0	-1.793	.016	32.730	.033	26.335	.027
21.0	-1.792	.014	32.728	.034	26.334	.028
22.0	-1.794	.014	32.733	.033	26.338	.027
23.0	-1.793	.014	32.731	.031	26.336	.026
24.0	-1.793	.013	32.733	.028	26.338	.023
25.0	-1.794	.013	32.735	.023	26.340	.019
26.0	-1.793	.013	32.736	.022	26.340	.018
27.0	-1.794	.011	32.739	.017	26.342	.014
28.0	-1.795	.011	32.740	.015	26.343	.013
29.0	-1.796	.007	32.742	.011	26.345	.009
30.0	-1.796	.007	32.743	.007	26.346	.005
31.0	-1.796	.006	32.743	.007	26.346	.006
32.0	-1.797	.007	32.745	.009	26.347	.007
33.0	-1.798	.003	32.745	.003	26.348	.002
34.0	-1.799	.003	32.746	.006	26.348	.005
35.0	-1.798	.003	32.746	.004	26.348	.003
36.0	-1.799	.001	32.745	.002	26.348	.001
37.0	-1.798	.003	32.745	.006	26.347	.005
38.0	-1.798	.002	32.745	.002	26.348	.002
39.0	-1.798	.001	32.746	.003	26.348	.002
40.0	-1.798	.003	32.746	.006	26.348	.005
41.0	-1.799	.003	32.747	.004	26.349	.003
42.0	-1.799	.001	32.747	.002	26.349	.001
43.0	-1.799	.002	32.747	.004	26.349	.003
44.0	-1.799	.002	32.747	.004	26.349	.003

PRESSURE (DBARS)	T MEAN (DEG.C)	T RANGE (DEG.C)	S MEAN	S RANGE	SIGMAT MEAN	SIGMAT RANGE
45.0	-1.799	.002	32.747	.001	26.349	.001
46.0	-1.799	.001	32.748	.003	26.350	.002
47.0	-1.799	.002	32.748	.005	26.350	.004
48.0	-1.799	.002	32.748	.005	26.350	.004
49.0	-1.799	.003	32.747	.004	26.349	.003
50.0	-1.799	.001	32.749	.002	26.351	.002
51.0	-1.799	.002	32.750	.005	26.351	.004
52.0	-1.799	.001	32.749	.001	26.351	.001
53.0	-1.799	.002	32.750	.005	26.351	.004
54.0	-1.799	.002	32.750	.002	26.351	.001
55.0	-1.799	.002	32.749	.006	26.351	.005
56.0	-1.799	.002	32.751	.003	26.352	.003
57.0	-1.799	.003	32.750	.003	26.352	.002
58.0	-1.798	.003	32.750	.002	26.352	.002
59.0	-1.799	.003	32.750	.002	26.352	.002

This page is blank.

SALINITY

32.0

32.5

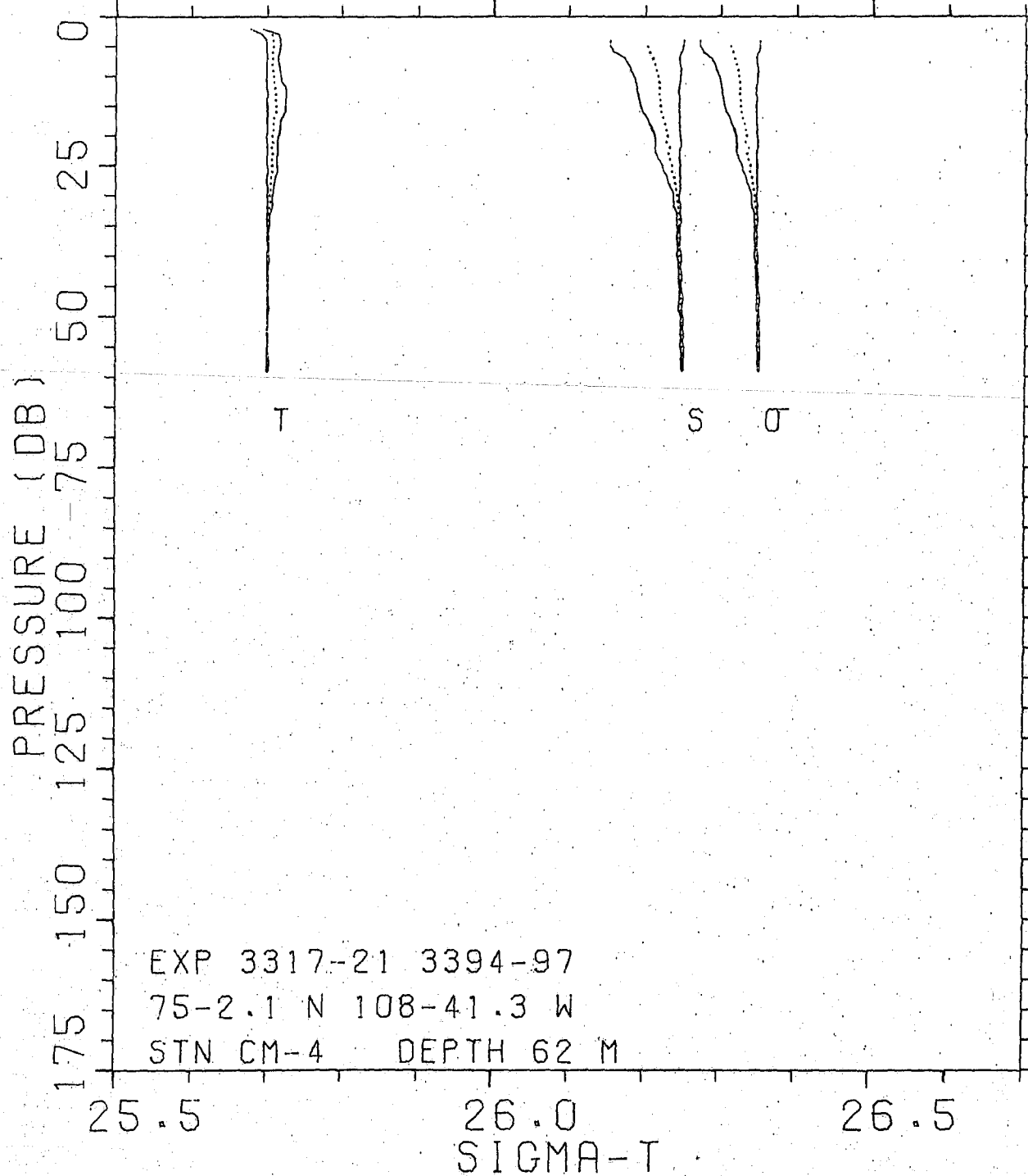
33.0

TEMPERATURE (DEG. C)

-2.0

-1.5

-1.0



CRUISE 15-80-020 BRIDPORT INLET-80
 STATION CM-5 EXPERIMENT NO.S 3317-21,3394-97
 LAT. 75-00.3 N LONG. 108-42.3 W
 WATER DEPTH 28.0 M

PRESSURE (DBARS)	T MEAN (DEG.C)	T RANGE (DEG.C)	S MEAN	S RANGE	SIGMAT MEAN	SIGMAT RANGE
2.0	-1.801	.020				
3.0	-1.787	.018	32.681	.031	26.295	.026
4.0	-1.785	.018	32.670	.034	26.286	.028
5.0	-1.786	.019	32.670	.037	26.286	.030
6.0	-1.785	.017	32.670	.035	26.286	.028
7.0	-1.784	.017	32.671	.040	26.287	.032
8.0	-1.784	.017	32.677	.058	26.292	.048
9.0	-1.785	.017	32.683	.063	26.297	.051
10.0	-1.784	.016	32.684	.065	26.298	.053
11.0	-1.784	.018	32.684	.069	26.297	.056
12.0	-1.783	.020	32.685	.070	26.298	.057
13.0	-1.784	.018	32.686	.070	26.299	.057
14.0	-1.783	.019	32.686	.070	26.299	.057
15.0	-1.785	.019	32.687	.071	26.300	.058
16.0	-1.785	.017	32.688	.071	26.301	.058
17.0	-1.785	.021	32.689	.073	26.302	.060
18.0	-1.784	.025	32.690	.076	26.302	.062
19.0	-1.783	.031	32.691	.075	26.303	.062
20.0	-1.783	.031	32.692	.071	26.304	.058
21.0	-1.785	.028	32.695	.071	26.306	.058
22.0	-1.784	.029	32.698	.070	26.309	.058
23.0	-1.784	.031	32.703	.064	26.313	.052
24.0	-1.784	.034	32.706	.061	26.315	.050
25.0	-1.788	.030	32.712	.053	26.320	.043

SALINITY

32.0

32.5

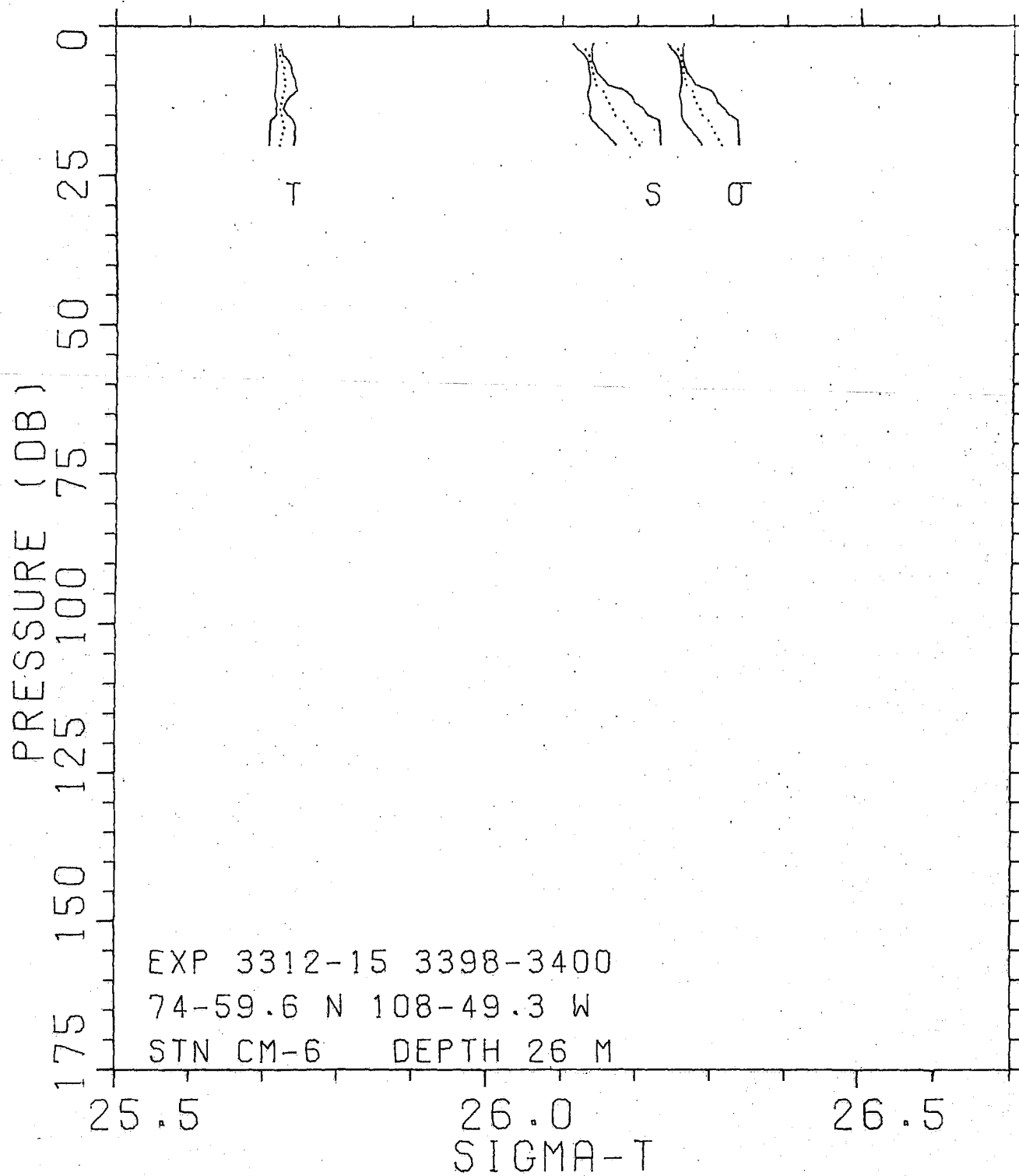
33.0

TEMPERATURE (DEG. C)

-2.0

-1.5

-1.0



CRUISE 15-80-020 BRIDPORT INLET-80
 STATION CM-6 EXPERIMENT NO.S 3312-15,3398-3400
 LAT. 74-59.6 N LONG. 108-49.3 W
 WATER DEPTH 26.0 M

PRESSURE (DBARS)	T MEAN (DEG.C)	T RANGE (DEG.C)	S MEAN	S RANGE	SIGMAT MEAN	SIGMAT RANGE
3.0	-1.782	.008	32.627	.026	26.251	.021
4.0	-1.779	.008	32.630	.017	26.254	.014
5.0	-1.779	.009	32.635	.010	26.258	.008
6.0	-1.776	.017	32.636	.005	26.258	.004
7.0	-1.773	.019	32.637	.009	26.260	.007
8.0	-1.774	.021	32.640	.009	26.261	.007
9.0	-1.772	.025	32.642	.018	26.263	.014
10.0	-1.772	.026	32.644	.023	26.265	.019
11.0	-1.773	.030	32.654	.052	26.273	.042
12.0	-1.776	.020	32.657	.061	26.275	.049
13.0	-1.778	.011	32.661	.060	26.279	.048
14.0	-1.779	.009	32.666	.071	26.283	.058
15.0	-1.777	.015	32.669	.079	26.286	.064
16.0	-1.776	.032	32.681	.090	26.295	.074
17.0	-1.774	.034	32.685	.082	26.299	.067
18.0	-1.775	.033	32.691	.075	26.303	.062
19.0	-1.778	.034	32.697	.066	26.308	.054
20.0	-1.780	.033	32.702	.060	26.312	.050

SALINITY

32.0

32.5

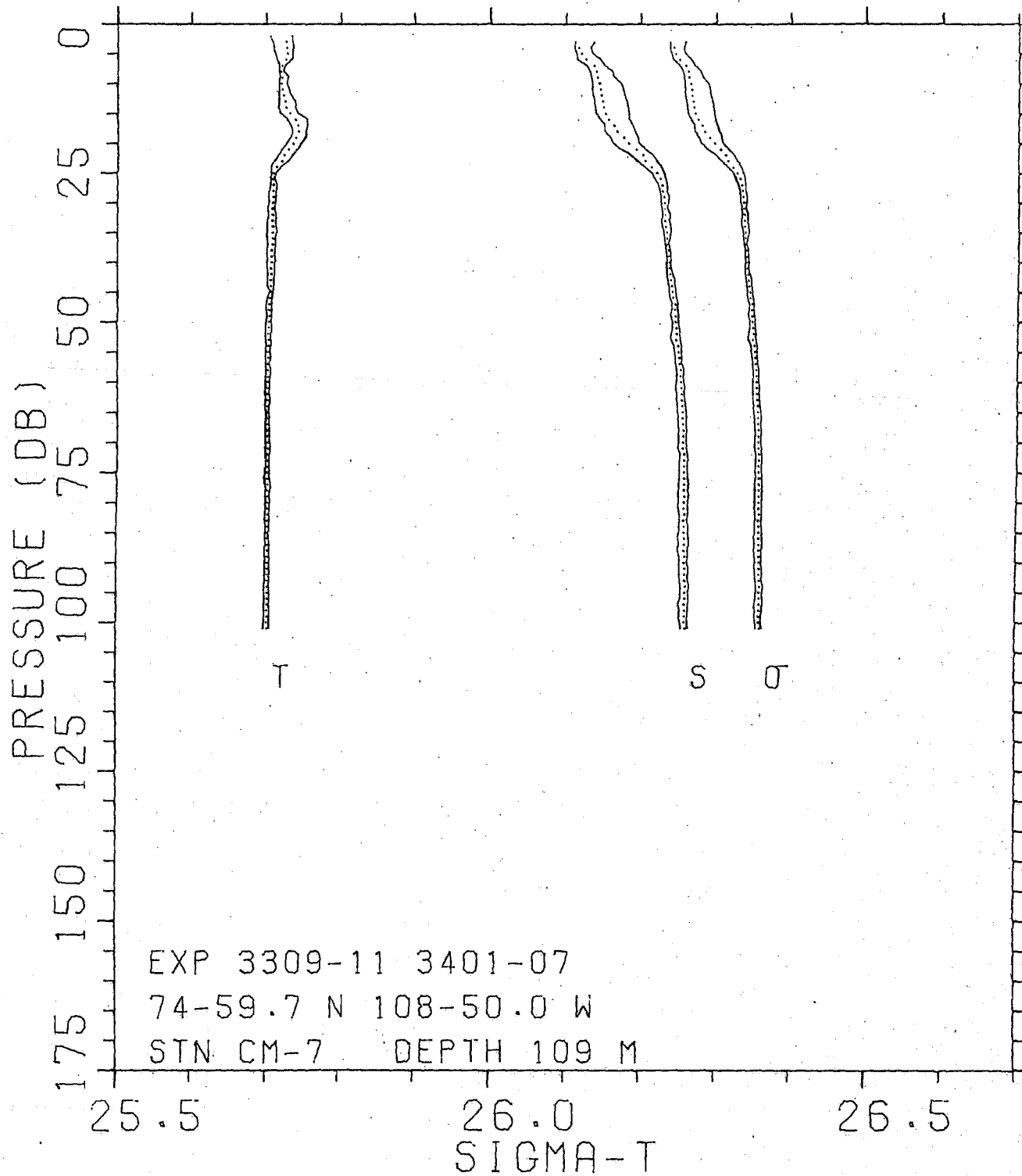
33.0

TEMPERATURE (DEG. C)

-2.0

-1.5

-1.0



CRUISE 15-80-020 BRIDPORT INLET-80
 STATION CM-7 EXPERIMENT NO.S 3309-11,3401-07
 LAT. 74-59.7 N LONG. 108-50.0 W
 WATER DEPTH 109.0 M

PRESSURE (DBARS)	T MEAN (DEG.C)	T RANGE (DEG.C)	S MEAN	S RANGE	SIGMAT MEAN	SIGMAT RANGE
2.0	-1.783	.028				
3.0	-1.775	.025	32.618	.025	26.244	.021
4.0	-1.774	.025	32.616	.021	26.242	.018
5.0	-1.773	.022	32.620	.022	26.245	.018
6.0	-1.775	.019	32.626	.031	26.250	.025
7.0	-1.780	.006	32.637	.024	26.259	.020
8.0	-1.781	.005	32.640	.029	26.262	.024
9.0	-1.780	.012	32.641	.031	26.263	.025
10.0	-1.781	.010	32.644	.039	26.265	.031
11.0	-1.780	.013	32.645	.042	26.266	.034
12.0	-1.778	.016	32.646	.042	26.267	.034
13.0	-1.776	.022	32.648	.043	26.268	.035
14.0	-1.775	.023	32.649	.044	26.269	.035
15.0	-1.770	.023	32.652	.044	26.271	.036
16.0	-1.763	.027	32.656	.038	26.275	.031
17.0	-1.759	.022	32.663	.037	26.280	.030
18.0	-1.758	.017	32.668	.041	26.284	.033
19.0	-1.762	.020	32.676	.037	26.291	.031
20.0	-1.765	.019	32.683	.035	26.296	.028
21.0	-1.771	.020	32.693	.033	26.305	.027
22.0	-1.778	.019	32.702	.029	26.312	.024
23.0	-1.781	.018	32.705	.025	26.314	.021
24.0	-1.787	.012	32.713	.022	26.321	.018
25.0	-1.792	.005	32.720	.016	26.327	.013
26.0	-1.792	.004	32.725	.014	26.331	.012
27.0	-1.792	.008	32.727	.012	26.333	.009
28.0	-1.791	.008	32.728	.009	26.333	.008
29.0	-1.792	.009	32.730	.011	26.335	.009
30.0	-1.792	.007	32.730	.010	26.335	.008
31.0	-1.793	.008	32.730	.007	26.335	.006
32.0	-1.793	.009	32.731	.010	26.336	.008
33.0	-1.792	.010	32.731	.010	26.336	.008
34.0	-1.792	.011	32.732	.011	26.337	.009
35.0	-1.792	.012	32.733	.010	26.338	.008
36.0	-1.792	.010	32.734	.007	26.338	.006
37.0	-1.792	.009	32.733	.004	26.338	.003
38.0	-1.793	.010	32.736	.006	26.340	.005
39.0	-1.793	.009	32.736	.005	26.340	.005
40.0	-1.793	.010	32.737	.005	26.341	.004
41.0	-1.794	.009	32.737	.006	26.341	.005
42.0	-1.794	.008	32.738	.008	26.341	.006
43.0	-1.795	.007	32.739	.009	26.343	.007
44.0	-1.795	.008	32.740	.008	26.343	.007

PRESSURE (DBARS)	T MEAN (DEG.C)	T RANGE (DEG.C)	S MEAN	S RANGE	SIGMAT MEAN	SIGMAT RANGE
45.0	-1.793	.002	32.742	.009	26.345	.007
46.0	-1.796	.006	32.742	.009	26.345	.008
47.0	-1.796	.006	32.745	.008	26.348	.006
48.0	-1.796	.007	32.744	.008	26.347	.006
49.0	-1.796	.005	32.746	.011	26.348	.009
50.0	-1.797	.006	32.746	.008	26.348	.006
51.0	-1.797	.008	32.747	.009	26.349	.008
52.0	-1.797	.006	32.748	.012	26.350	.010
53.0	-1.797	.005	32.747	.013	26.349	.010
54.0	-1.797	.006	32.749	.010	26.351	.008
55.0	-1.798	.004	32.750	.009	26.352	.008
56.0	-1.797	.007	32.751	.009	26.352	.007
57.0	-1.798	.003	32.752	.008	26.353	.006
58.0	-1.798	.006	32.753	.011	26.354	.008
59.0	-1.798	.005	32.753	.008	26.354	.006
60.0	-1.798	.005	32.754	.009	26.355	.007
61.0	-1.798	.004	32.754	.013	26.355	.010
62.0	-1.798	.005	32.755	.010	26.355	.008
63.0	-1.798	.005	32.755	.011	26.356	.009
64.0	-1.799	.005	32.756	.011	26.356	.009
65.0	-1.798	.003	32.756	.012	26.356	.009
66.0	-1.798	.004	32.756	.011	26.356	.009
67.0	-1.798	.005	32.757	.010	26.357	.008
68.0	-1.799	.005	32.757	.010	26.357	.008
69.0	-1.799	.005	32.757	.010	26.357	.008
70.0	-1.798	.005	32.756	.010	26.357	.008
71.0	-1.798	.006	32.757	.012	26.357	.009
72.0	-1.799	.005	32.758	.009	26.358	.008
73.0	-1.799	.004	32.758	.012	26.358	.010
74.0	-1.799	.005	32.758	.010	26.358	.008
75.0	-1.798	.005	32.758	.011	26.358	.009
76.0	-1.799	.006	32.759	.011	26.359	.009
77.0	-1.798	.007	32.758	.013	26.358	.011
78.0	-1.798	.005	32.759	.012	26.359	.009
79.0	-1.798	.005	32.759	.013	26.359	.011
80.0	-1.798	.005	32.759	.012	26.358	.010
81.0	-1.798	.005	32.759	.013	26.359	.010
82.0	-1.799	.005	32.760	.011	26.359	.009
83.0	-1.798	.006	32.759	.009	26.359	.008
84.0	-1.798	.004	32.759	.013	26.359	.011
85.0	-1.798	.004	32.760	.012	26.359	.009
86.0	-1.798	.004	32.760	.015	26.360	.012
87.0	-1.798	.005	32.760	.013	26.359	.010
88.0	-1.798	.006	32.760	.013	26.359	.011
89.0	-1.798	.006	32.760	.011	26.360	.009
90.0	-1.798	.005	32.760	.010	26.359	.008
91.0	-1.798	.006	32.761	.012	26.360	.010
92.0	-1.798	.006	32.760	.012	26.360	.009

PRESSURE (DBARS)	T MEAN (DEG.C)	T RANGE (DEG.C)	S MEAN	S RANGE	SIGMAT MEAN	SIGMAT RANGE
93.0	-1.798	.005	32.761	.010	26.360	.008
94.0	-1.798	.006	32.762	.012	26.361	.010
95.0	-1.798	.007	32.761	.010	26.360	.008
96.0	-1.798	.006	32.761	.011	26.361	.009
97.0	-1.798	.006	32.761	.014	26.360	.011
98.0	-1.798	.007	32.761	.010	26.360	.008
99.0	-1.797	.007	32.761	.011	26.360	.009
100.0	-1.798	.007	32.761	.009	26.360	.007
101.0	-1.797	.007	32.762	.009	26.361	.007

SALINITY

32.0

32.5

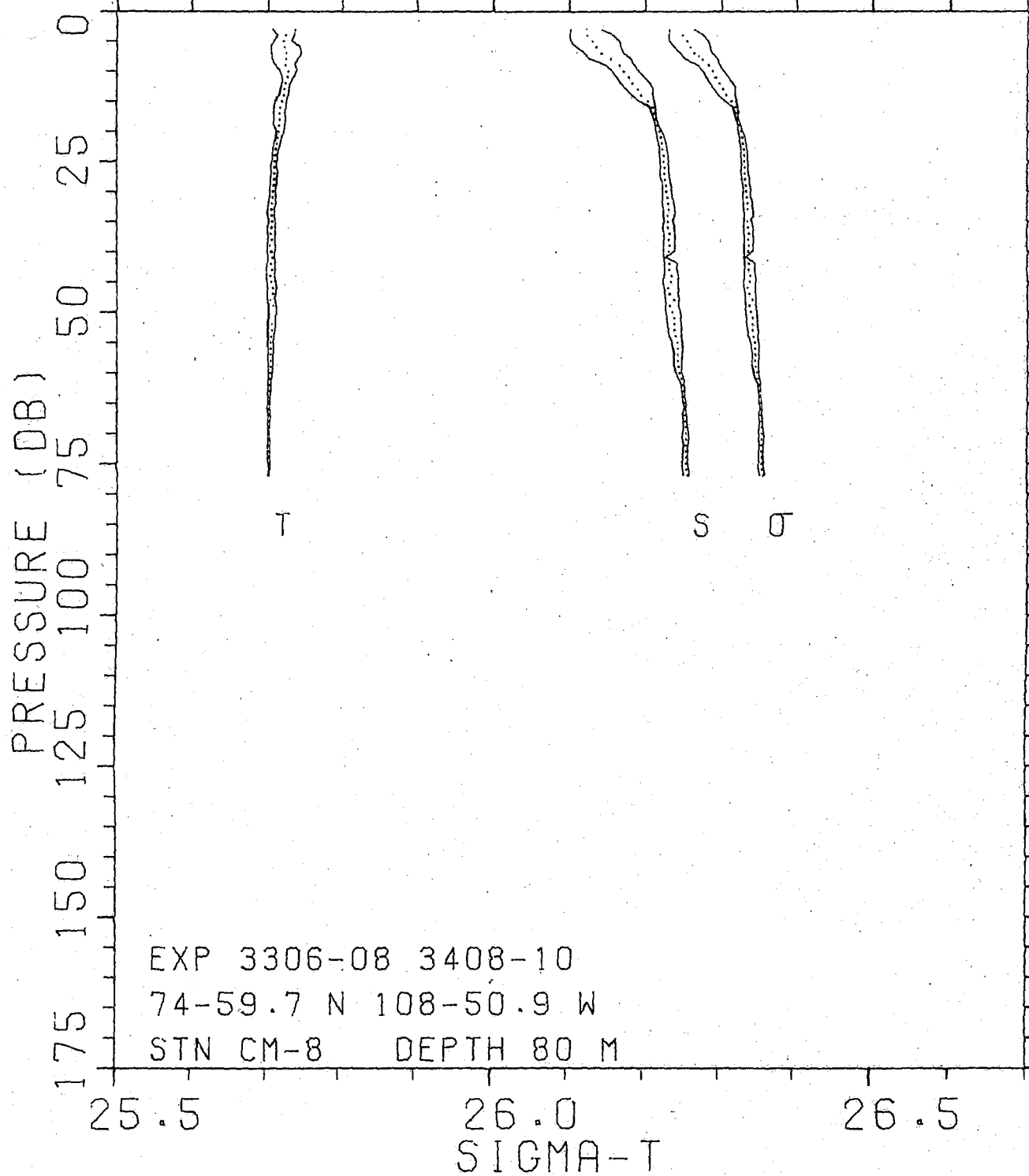
33.0

TEMPERATURE (DEG. C)

-2.0

-1.5

-1.0



CRUISE 15-80-020 BRIDPORT INLET-80
 STATION CM-8 EXPERIMENT NO.S 3306-08,3408-10
 LAT. 74-59.7 N LONG. 108-50.9 W
 WATER DEPTH 80.0 M

PRESSURE (DBARS)	T MEAN (DEG.C)	T RANGE (DEG.C)	S MEAN	S RANGE	SIGMAT MEAN	SIGMAT RANGE
3.0	-1.781	.029	32.618	.041	26.244	.033
4.0	-1.777	.020	32.623	.058	26.248	.047
5.0	-1.780	.023	32.630	.064	26.253	.052
6.0	-1.779	.039	32.635	.058	26.258	.047
7.0	-1.777	.040	32.642	.051	26.263	.041
8.0	-1.777	.034	32.655	.055	26.274	.044
9.0	-1.778	.025	32.665	.037	26.282	.030
10.0	-1.773	.022	32.672	.034	26.288	.027
11.0	-1.774	.015	32.678	.037	26.292	.030
12.0	-1.777	.010	32.683	.038	26.297	.031
13.0	-1.779	.011	32.690	.036	26.302	.029
14.0	-1.780	.012	32.694	.027	26.306	.022
15.0	-1.782	.015	32.703	.020	26.313	.016
16.0	-1.785	.015	32.709	.006	26.318	.005
17.0	-1.785	.014	32.711	.005	26.319	.005
18.0	-1.785	.015	32.712	.003	26.321	.002
19.0	-1.786	.014	32.716	.004	26.324	.003
20.0	-1.787	.010	32.718	.008	26.325	.006
21.0	-1.787	.007	32.720	.009	26.327	.007
22.0	-1.788	.008	32.722	.010	26.328	.009
23.0	-1.789	.007	32.723	.009	26.329	.008
24.0	-1.791	.006	32.724	.011	26.330	.009
25.0	-1.791	.006	32.724	.010	26.330	.008
26.0	-1.792	.007	32.725	.011	26.331	.009
27.0	-1.791	.008	32.725	.012	26.331	.010
28.0	-1.792	.008	32.726	.012	26.332	.010
29.0	-1.793	.007	32.727	.011	26.333	.009
30.0	-1.793	.007	32.728	.013	26.333	.010
31.0	-1.794	.007	32.729	.013	26.334	.010
32.0	-1.794	.010	32.730	.015	26.335	.013
33.0	-1.796	.008	32.730	.014	26.335	.012
34.0	-1.795	.009	32.729	.015	26.335	.013
35.0	-1.795	.007	32.729	.010	26.334	.009
36.0	-1.795	.010	32.730	.016	26.335	.013
37.0	-1.796	.009	32.732	.014	26.337	.012
38.0	-1.795	.008	32.731	.015	26.336	.012
39.0	-1.797	.010	32.732	.014	26.337	.012
40.0	-1.796	.010	32.731	.015	26.336	.013
41.0	-1.795	.007	32.726	.001	26.332	.001
42.0	-1.796	.010	32.732	.018	26.337	.015
43.0	-1.795	.011	32.732	.015	26.337	.013
44.0	-1.798	.010	32.734	.018	26.339	.015
45.0	-1.796	.011	32.734	.020	26.338	.016

PRESSURE (DBARS)	T MEAN (DEG.C)	T RANGE (DEG.C)	S MEAN	S RANGE	SIGMAT MEAN	SIGMAT RANGE
46.0	-1.795	.011	32.730	.018	26.335	.015
47.0	-1.794	.010	32.732	.017	26.337	.014
48.0	-1.798	.009	32.738	.018	26.342	.015
49.0	-1.793	.010	32.733	.016	26.337	.013
50.0	-1.795	.011	32.736	.019	26.340	.016
51.0	-1.796	.008	32.738	.018	26.342	.015
52.0	-1.796	.010	32.738	.018	26.341	.015
53.0	-1.795	.009	32.738	.017	26.341	.014
54.0	-1.797	.008	32.740	.016	26.343	.013
55.0	-1.797	.006	32.742	.013	26.345	.010
56.0	-1.797	.008	32.742	.013	26.345	.011
57.0	-1.797	.006	32.742	.010	26.345	.009
58.0	-1.797	.007	32.742	.011	26.345	.009
59.0	-1.797	.006	32.743	.010	26.346	.009
60.0	-1.797	.005	32.745	.007	26.347	.006
61.0	-1.799	.004	32.747	.007	26.349	.006
62.0	-1.799	.003	32.749	.004	26.351	.003
63.0	-1.799	.004	32.750	.004	26.352	.003
64.0	-1.800	.003	32.750	.002	26.352	.002
65.0	-1.800	.002	32.752	.004	26.353	.003
66.0	-1.800	.004	32.753	.002	26.354	.001
67.0	-1.799	.002	32.752	.006	26.353	.005
68.0	-1.800	.003	32.753	.005	26.354	.004
69.0	-1.800	.002	32.753	.006	26.354	.005
70.0	-1.799	.001	32.753	.008	26.354	.006
71.0	-1.799	.002	32.753	.009	26.354	.007
72.0	-1.800	.003	32.753	.005	26.354	.004
73.0	-1.799	.003	32.754	.007	26.354	.005
74.0	-1.799	.003	32.754	.007	26.354	.005
75.0	-1.799	.003	32.754	.007	26.355	.006
76.0	-1.799	.001	32.754	.009	26.355	.007
77.0	-1.799	.001	32.756	.007	26.357	.006

This page is blank.

122

SALINITY

32.0

32.5

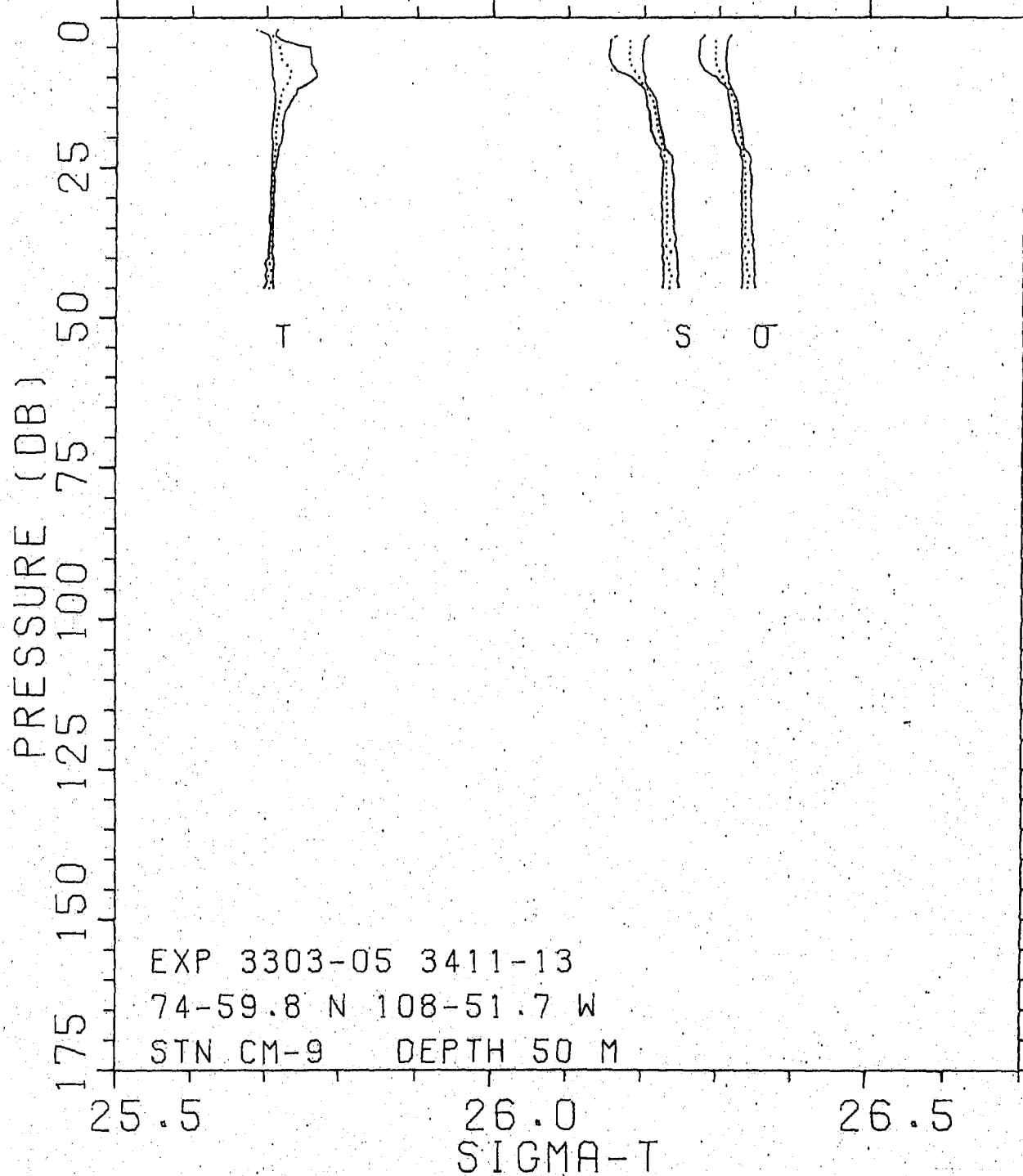
33.0

TEMPERATURE (DEG. C)

-2.0

-1.5

-1.0



CRUISE 15-80-020 BRIDPORT INLET-80
 STATION CM-9 EXPERIMENT NO.S 3303-05,3411-13
 LAT. 74-59.8 N LONG. 108-51.7 W
 WATER DEPTH 50.0 M

PRESSURE (DBARS)	T MEAN (DEG.C)	T RANGE (DEG.C)	S MEAN	S RANGE	SIGMAT MEAN	SIGMAT RANGE
2.0	-1.807	.028				
3.0	-1.793	.007	32.691	.042	26.304	.035
4.0	-1.789	.017	32.679	.045	26.294	.037
5.0	-1.784	.055	32.680	.044	26.294	.036
6.0	-1.782	.054	32.679	.044	26.293	.036
7.0	-1.781	.055	32.679	.043	26.294	.036
8.0	-1.774	.053	32.681	.040	26.295	.034
9.0	-1.768	.059	32.686	.034	26.299	.028
10.0	-1.770	.061	32.691	.019	26.303	.016
11.0	-1.774	.046	32.696	.010	26.307	.009
12.0	-1.780	.031	32.703	.007	26.313	.005
13.0	-1.782	.026	32.706	.010	26.315	.008
14.0	-1.784	.022	32.710	.013	26.319	.011
15.0	-1.785	.018	32.712	.013	26.321	.011
16.0	-1.787	.014	32.714	.010	26.322	.009
17.0	-1.788	.013	32.715	.012	26.323	.010
18.0	-1.788	.013	32.716	.012	26.323	.010
19.0	-1.789	.016	32.718	.015	26.326	.012
20.0	-1.789	.014	32.721	.012	26.328	.010
21.0	-1.788	.010	32.722	.011	26.329	.009
22.0	-1.789	.007	32.725	.005	26.331	.004
23.0	-1.791	.008	32.726	.017	26.332	.014
24.0	-1.792	.005	32.729	.013	26.334	.010
25.0	-1.792	.005	32.728	.011	26.333	.009
26.0	-1.793	.002	32.728	.013	26.334	.011
27.0	-1.792	.005	32.728	.016	26.334	.013
28.0	-1.793	.004	32.729	.015	26.335	.013
29.0	-1.794	.005	32.729	.015	26.334	.013
30.0	-1.793	.003	32.729	.014	26.334	.011
31.0	-1.794	.004	32.731	.016	26.336	.013
32.0	-1.794	.003	32.730	.014	26.335	.012
33.0	-1.794	.005	32.730	.013	26.336	.011
34.0	-1.794	.004	32.729	.017	26.335	.014
35.0	-1.794	.003	32.730	.014	26.335	.012
36.0	-1.794	.004	32.730	.018	26.335	.014
37.0	-1.794	.004	32.734	.018	26.339	.015
38.0	-1.793	.005	32.729	.017	26.334	.014
39.0	-1.796	.005	32.736	.018	26.340	.014
40.0	-1.793	.006	32.731	.021	26.336	.017
41.0	-1.797	.013	32.733	.019	26.338	.015
42.0	-1.794	.007	32.733	.020	26.338	.016
43.0	-1.799	.011	32.737	.020	26.341	.016
44.0	-1.795	.007	32.735	.018	26.339	.015

PRESSURE (DBARS)	T MEAN (DEG.C)	T RANGE (DEG.C)	S MEAN	S RANGE	SIGMAT MEAN	SIGMAT RANGE
45.0	-1.797	.013	32.734	.022	26.338	.018

This page is blank.

126

SALINITY

32.0

32.5

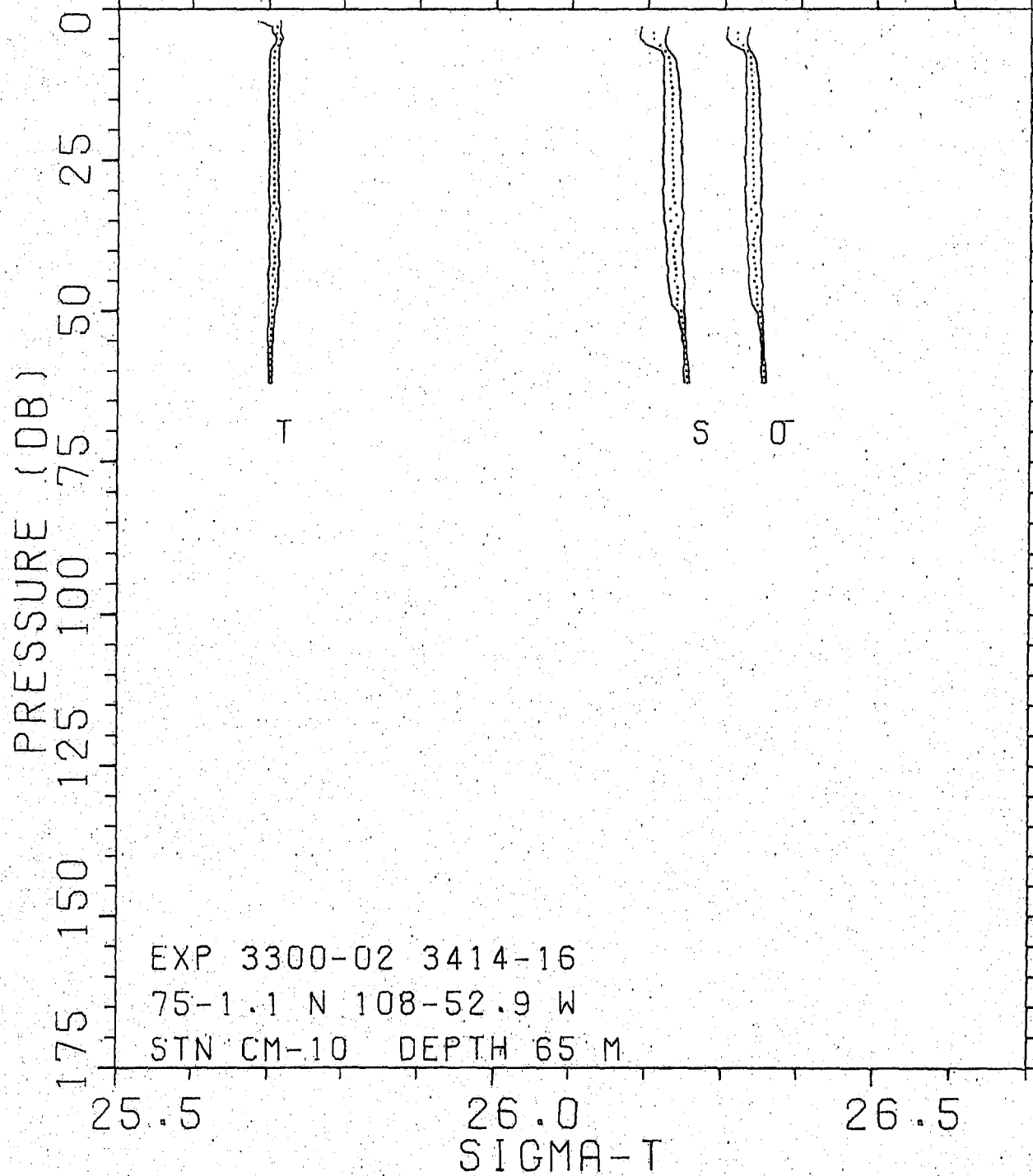
33.0

TEMPERATURE (DEG. C)

-2.0

-1.5

-1.0



CRUISE 15-80-020 BRIDPORT INLET-80
 STATION CM-10 EXPERIMENT NO.5 3300-02,3414-16
 LAT. 75-01.1 N LONG. 108-52.9 W
 WATER DEPTH 65.0 M

PRESSURE (DBARS)	T MEAN (DEG.C)	T RANGE (DEG.C)	S MEAN	S RANGE	SIGMAT MEAN	SIGMAT RANGE
2.0	-1.805	.029				
3.0	-1.791	.010	32.708	.035	26.317	.029
4.0	-1.791	.010	32.706	.034	26.316	.028
5.0	-1.787	.008	32.707	.032	26.316	.026
6.0	-1.790	.006	32.714	.024	26.322	.020
7.0	-1.794	.012	32.721	.009	26.328	.008
8.0	-1.795	.012	32.726	.013	26.332	.011
9.0	-1.795	.012	32.727	.016	26.333	.013
10.0	-1.795	.012	32.728	.017	26.333	.014
11.0	-1.795	.012	32.728	.019	26.334	.016
12.0	-1.795	.013	32.729	.020	26.334	.017
13.0	-1.795	.011	32.730	.019	26.335	.016
14.0	-1.795	.013	32.731	.020	26.336	.017
15.0	-1.795	.011	32.730	.021	26.336	.018
16.0	-1.795	.011	32.730	.020	26.335	.017
17.0	-1.795	.013	32.731	.021	26.336	.018
18.0	-1.795	.012	32.731	.022	26.336	.018
19.0	-1.795	.012	32.732	.023	26.336	.019
20.0	-1.794	.013	32.730	.024	26.336	.020
21.0	-1.795	.012	32.732	.023	26.337	.019
22.0	-1.795	.010	32.731	.022	26.336	.018
23.0	-1.794	.011	32.731	.025	26.336	.020
24.0	-1.794	.012	32.730	.024	26.335	.020
25.0	-1.794	.011	32.731	.024	26.336	.020
26.0	-1.795	.011	32.732	.024	26.337	.020
27.0	-1.795	.013	32.732	.025	26.337	.020
28.0	-1.794	.011	32.732	.024	26.337	.020
29.0	-1.794	.013	32.733	.025	26.337	.021
30.0	-1.794	.014	32.731	.027	26.336	.022
31.0	-1.795	.012	32.733	.024	26.337	.020
32.0	-1.795	.013	32.734	.023	26.339	.019
33.0	-1.791	.013	32.728	.023	26.334	.019
34.0	-1.796	.013	32.737	.025	26.341	.021
35.0	-1.792	.014	32.729	.025	26.335	.020
36.0	-1.797	.016	32.739	.022	26.343	.019
37.0	-1.795	.015	32.735	.021	26.339	.018
38.0	-1.793	.013	32.733	.021	26.338	.017
39.0	-1.794	.012	32.733	.019	26.337	.016
40.0	-1.795	.013	32.736	.020	26.340	.017
41.0	-1.794	.013	32.734	.022	26.338	.018
42.0	-1.794	.013	32.735	.020	26.339	.016
43.0	-1.795	.013	32.736	.020	26.340	.016
44.0	-1.796	.013	32.738	.020	26.341	.017

PRESSURE (DBARS)	T MEAN (DEG.C)	T RANGE (DEG.C)	S MEAN	S RANGE	SIGMAT MEAN	SIGMAT RANGE
45.0	-1.793	.013	32.735	.022	26.339	.018
46.0	-1.795	.013	32.738	.021	26.342	.017
47.0	-1.796	.011	32.739	.018	26.343	.015
48.0	-1.795	.012	32.738	.017	26.342	.014
49.0	-1.795	.011	32.739	.017	26.343	.014
50.0	-1.797	.008	32.744	.008	26.347	.007
51.0	-1.796	.007	32.745	.007	26.347	.006
52.0	-1.798	.007	32.746	.007	26.348	.006
53.0	-1.798	.007	32.746	.005	26.348	.004
54.0	-1.798	.007	32.748	.003	26.349	.003
55.0	-1.799	.007	32.748	.005	26.350	.004
56.0	-1.799	.004	32.749	.003	26.351	.002
57.0	-1.799	.005	32.749	.004	26.351	.003
58.0	-1.799	.005	32.750	.004	26.351	.003
59.0	-1.799	.004	32.751	.006	26.352	.005
60.0	-1.799	.004	32.750	.008	26.352	.006
61.0	-1.799	.004	32.751	.007	26.352	.005
62.0	-1.798	.003	32.752	.006	26.353	.005

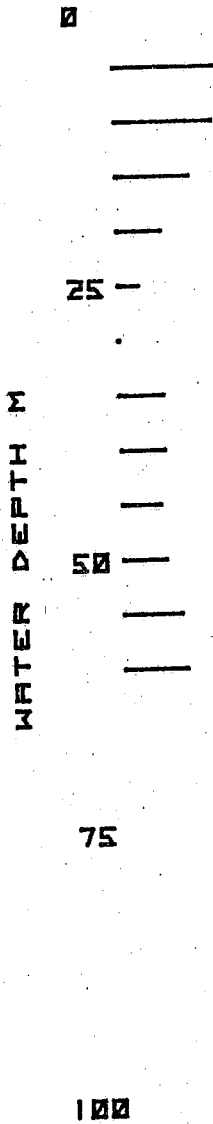
APPENDIX B
ULTRA SONIC CURRENT METER PROFILES

BRIDPORT INLET SITE: 80-5

12 APR 1981

19: 53 - 20: 0 GMT

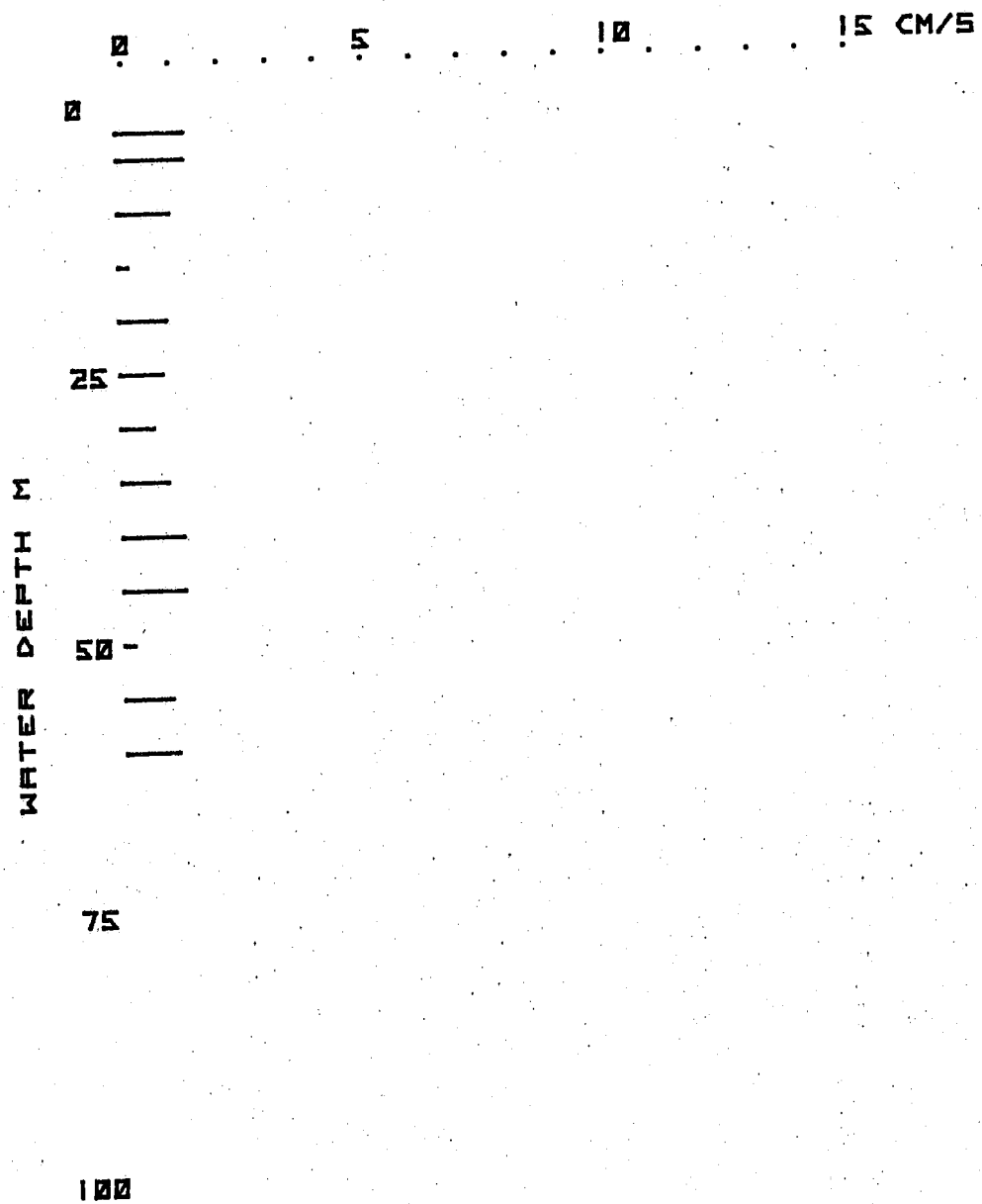
0 5 10 15 CM/S



BRIDPORT INLET SITE: 80-5

12 APR 1981

20:20 - 20:28 GMT



BRIDPORT INLET SITE: 80-5

12 APR 1981

21:00 - 22:00 GMT

0 5 10 15 CM/S

0

|||||

25

Σ
I
T
E
M
S
O
B
S
E
R
V
E
D

50

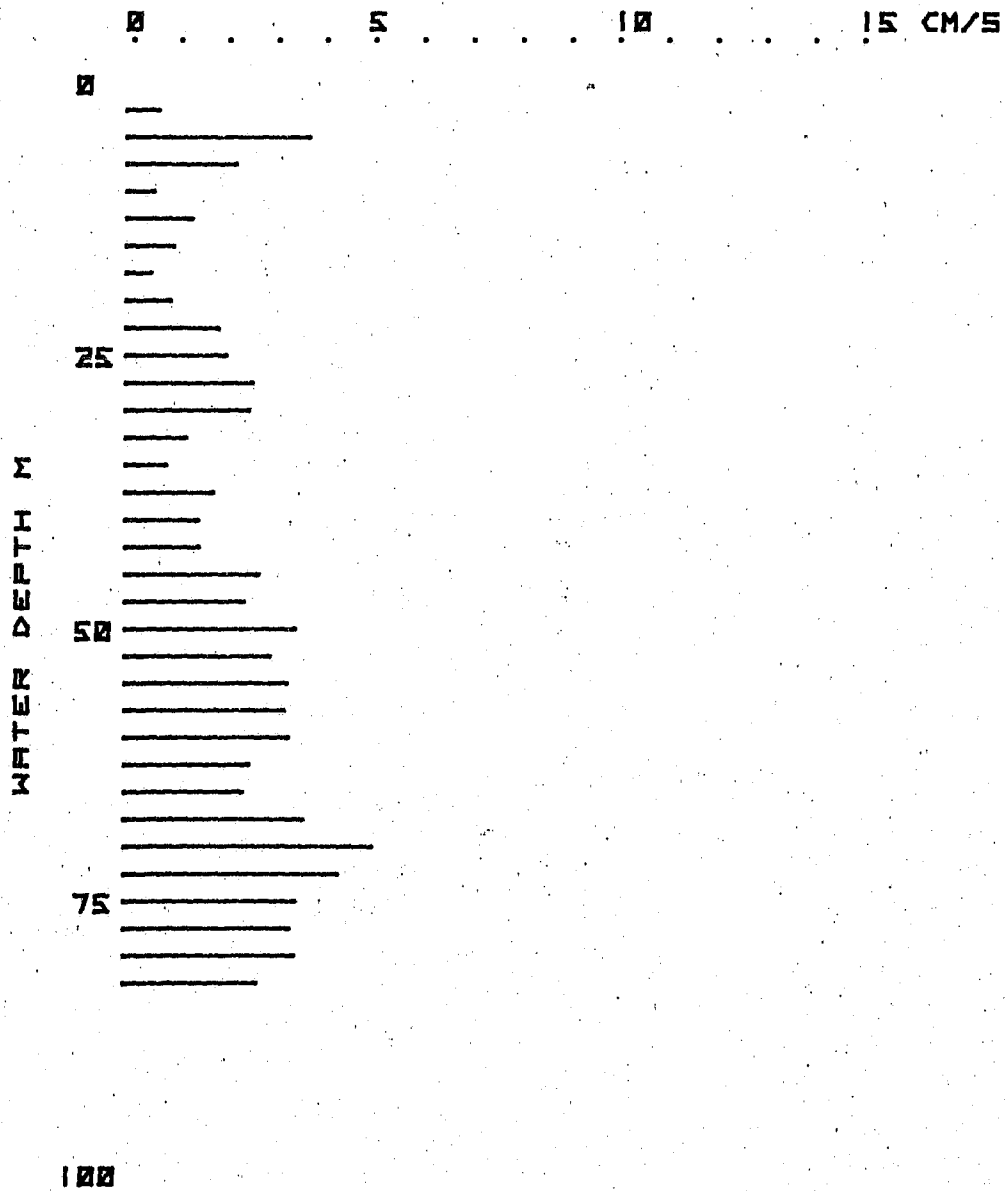
75

100

BRIDPORT INLET SITE: UCM-1

17 APR 1980

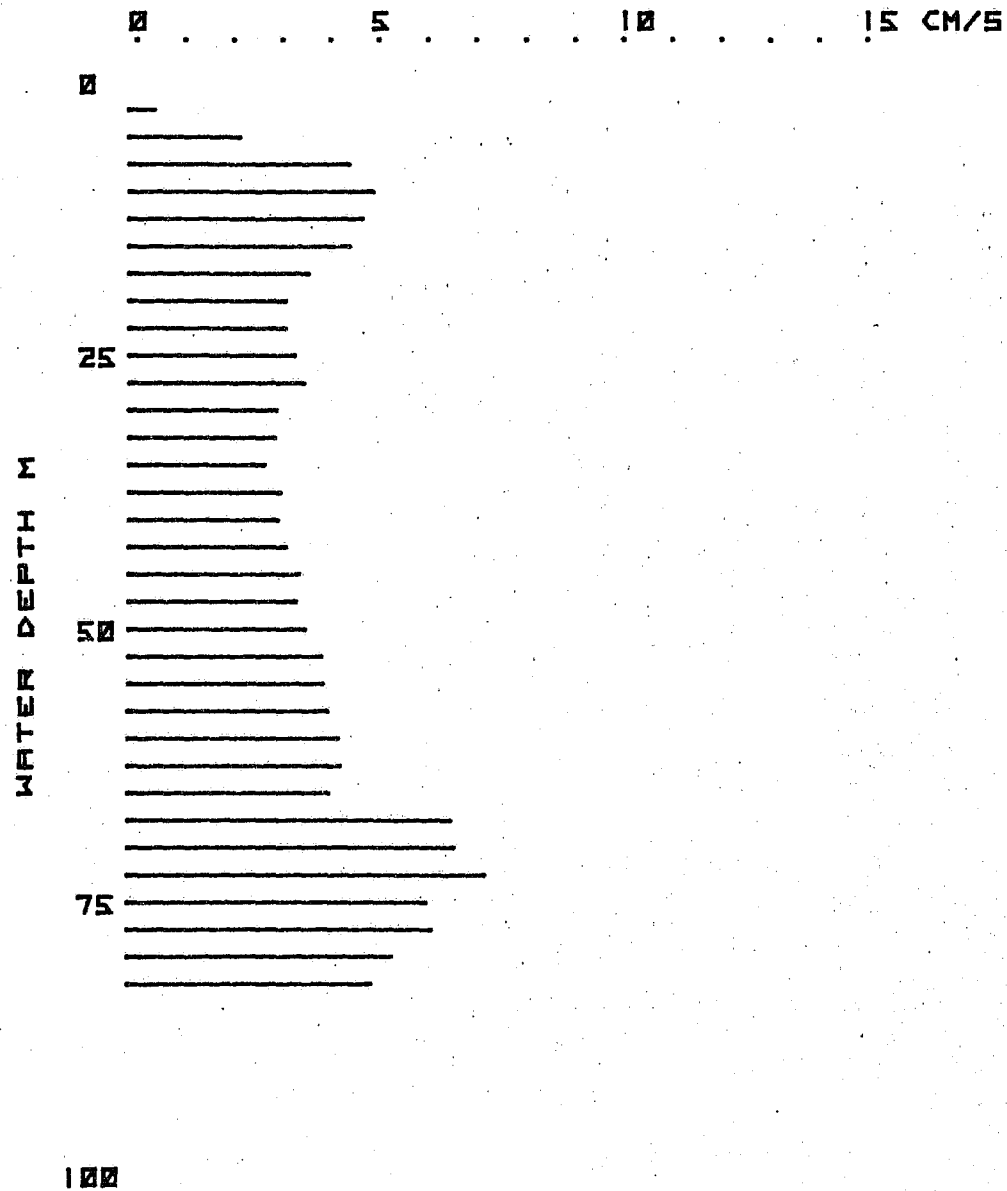
21: 8 - 22: 8 GMT



BRIDPORT INLET SITE: UCM-1

18 APR 1980

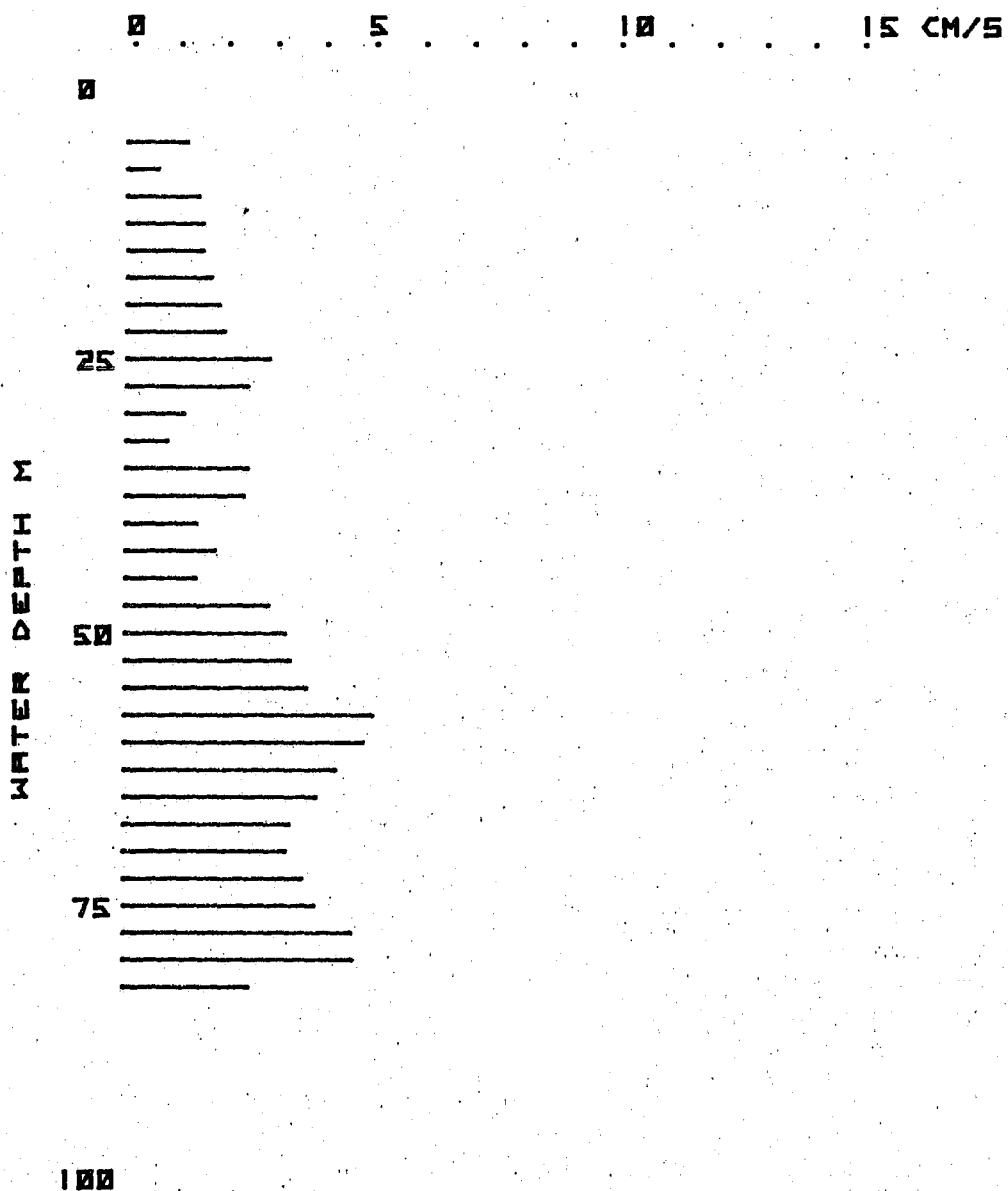
1:50 - 2:7 GMT



BRIDPORT INLET SITE: UCM-2

19 APR 1980

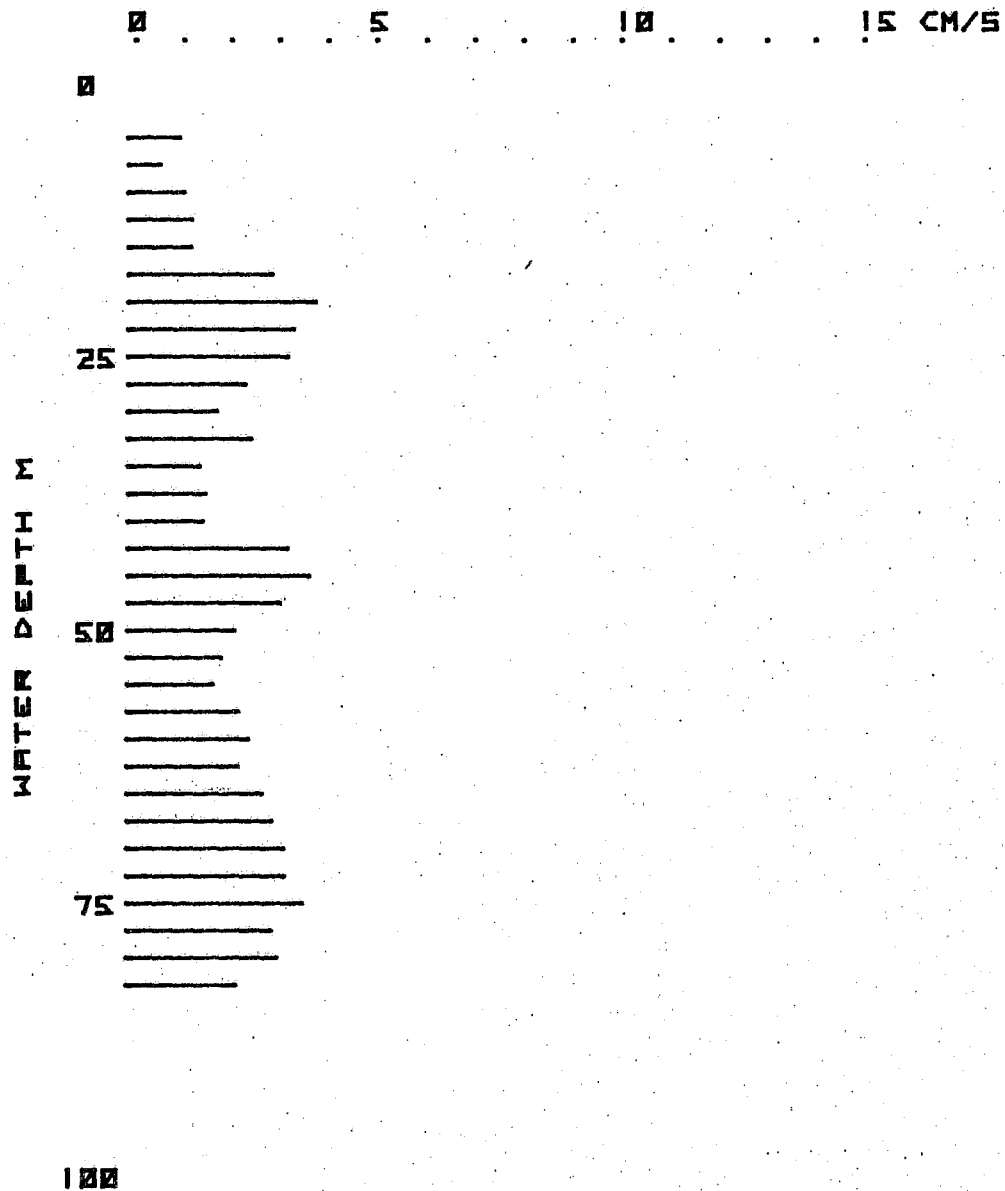
15: 50 - 16: 2 GMT



BRIDPORT INLET SITE: UCM-2

19 APR 1980

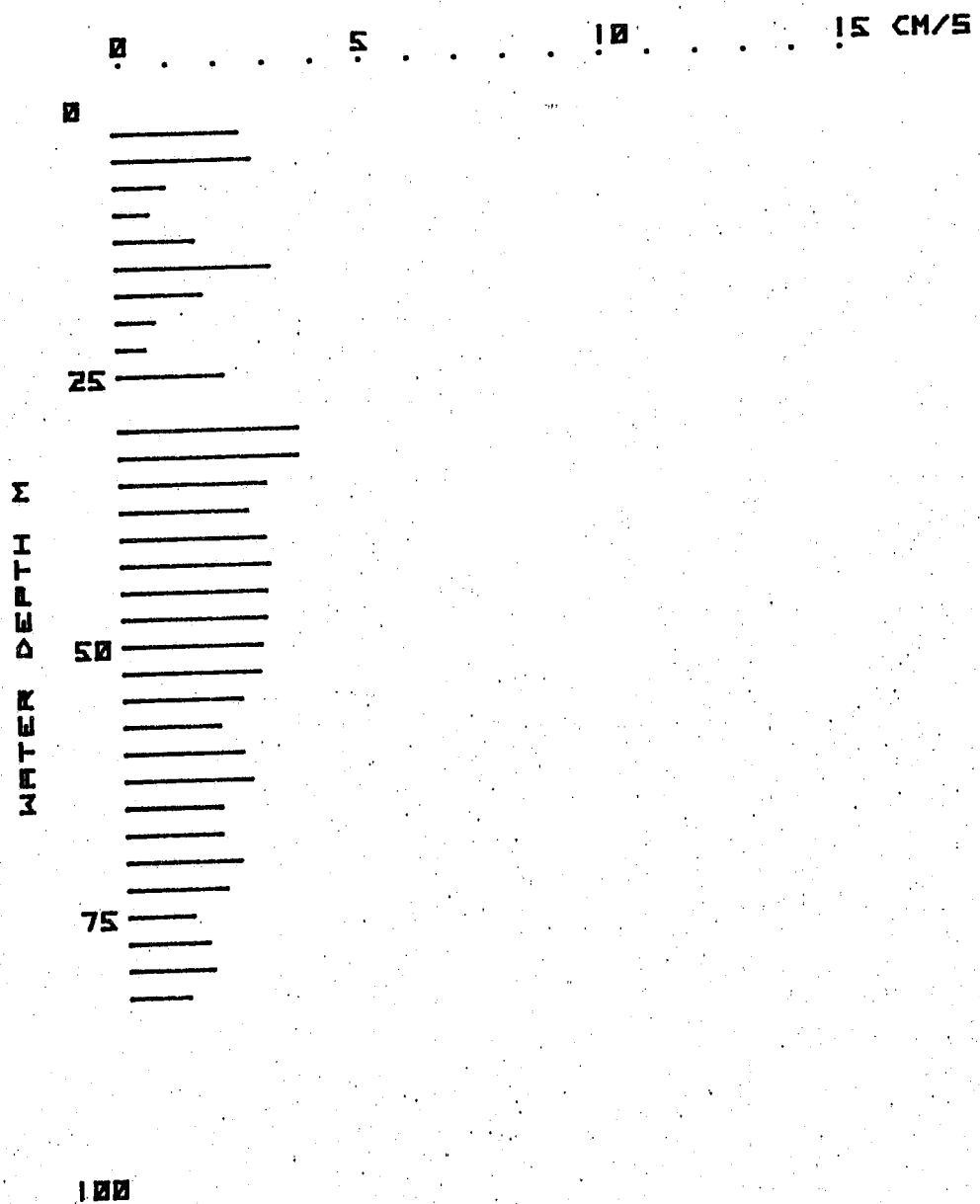
16:54 - 17:06 GMT



BRIDPORT INLET SITE: UCM-2

19 APR 1980

19: 12 - 19: 27 GMT

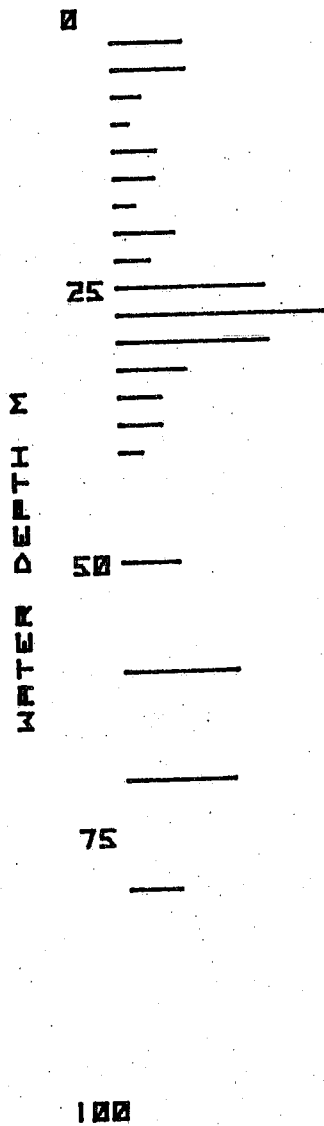


BRIDPORT INLET SITE: UCM-2

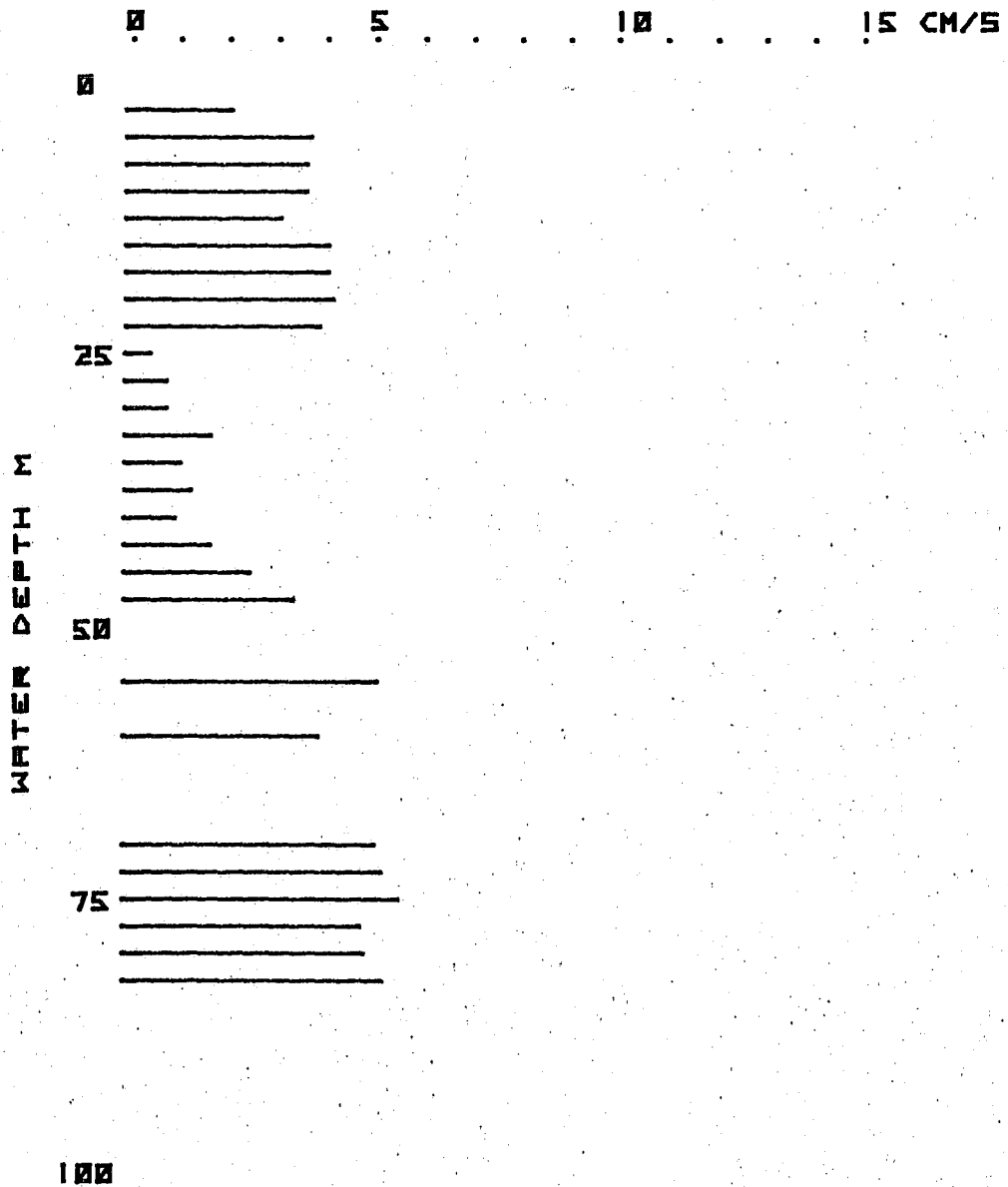
19 APR 1980

21:5 - 21:21 GMT

0 5 10 15 CM/S



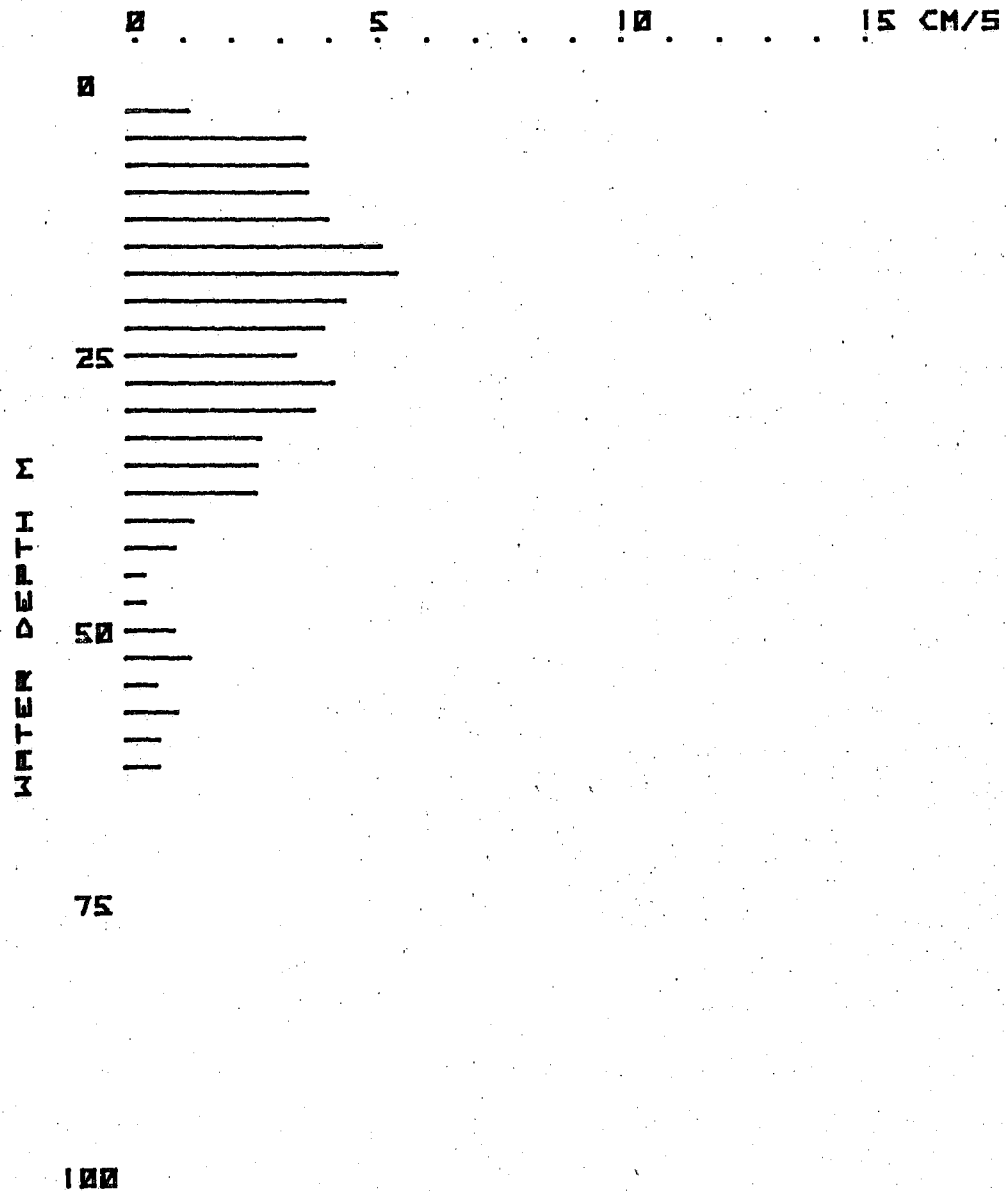
BRIDPORT INLET SITE: UCM-2
19 APR 1980 22: 30 - 22: 40 GMT



BRIDPORT INLET SITE: UCM-3

21 APR 1980

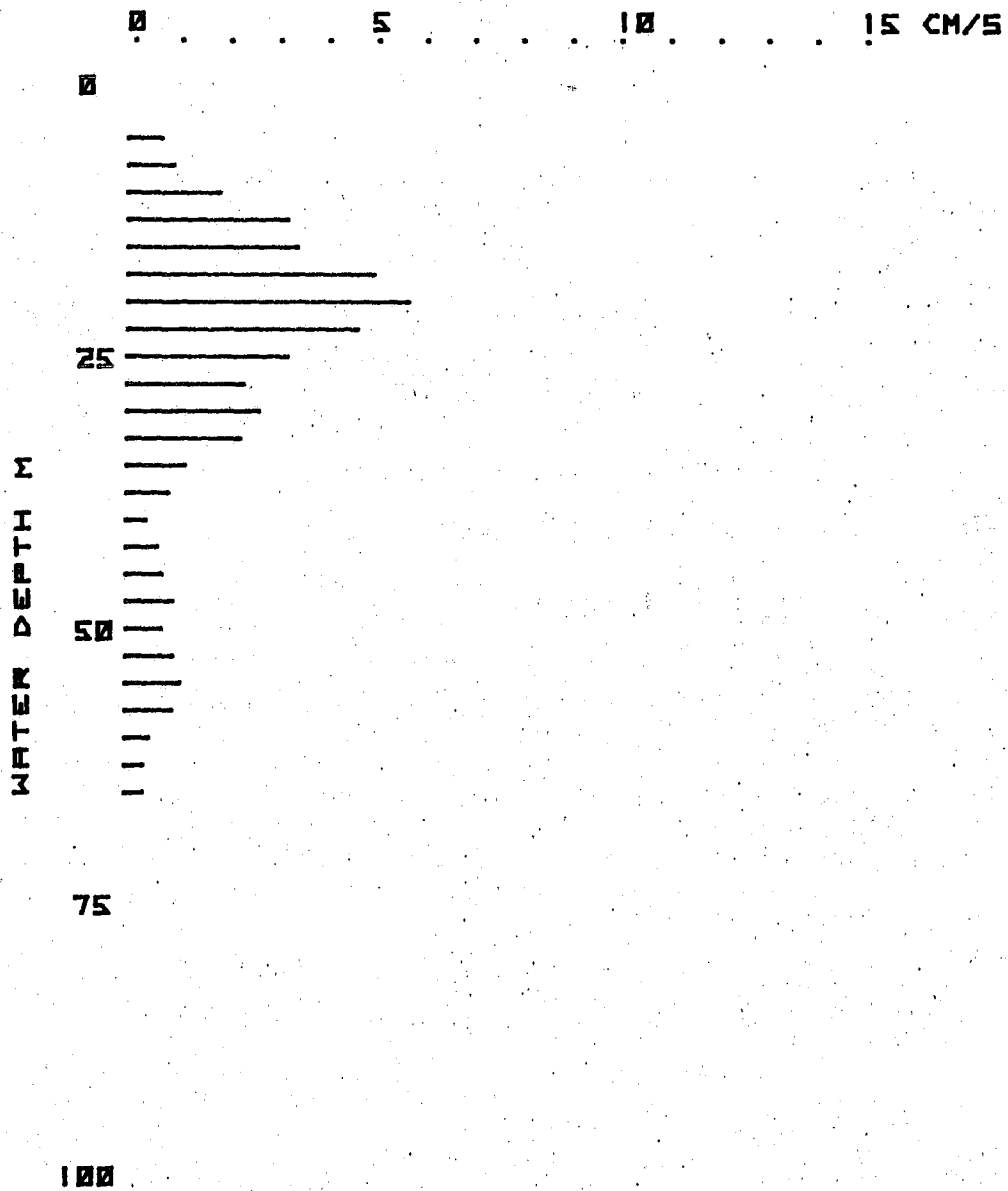
16:15 - 16:28 GMT



BRIDPORT INLET SITE: UCM-3

21 APR 1980

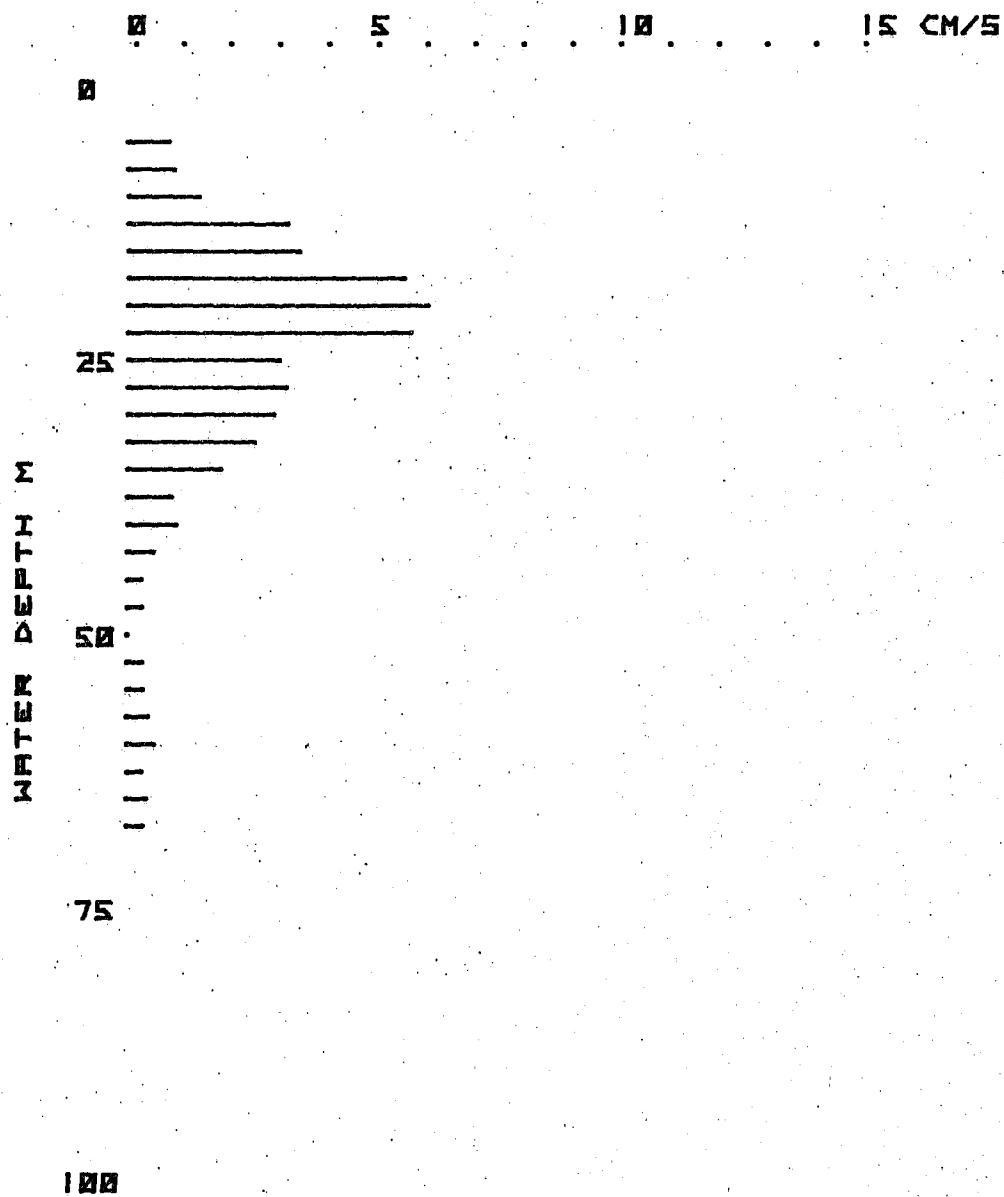
17: 25 - 17: 37 GMT



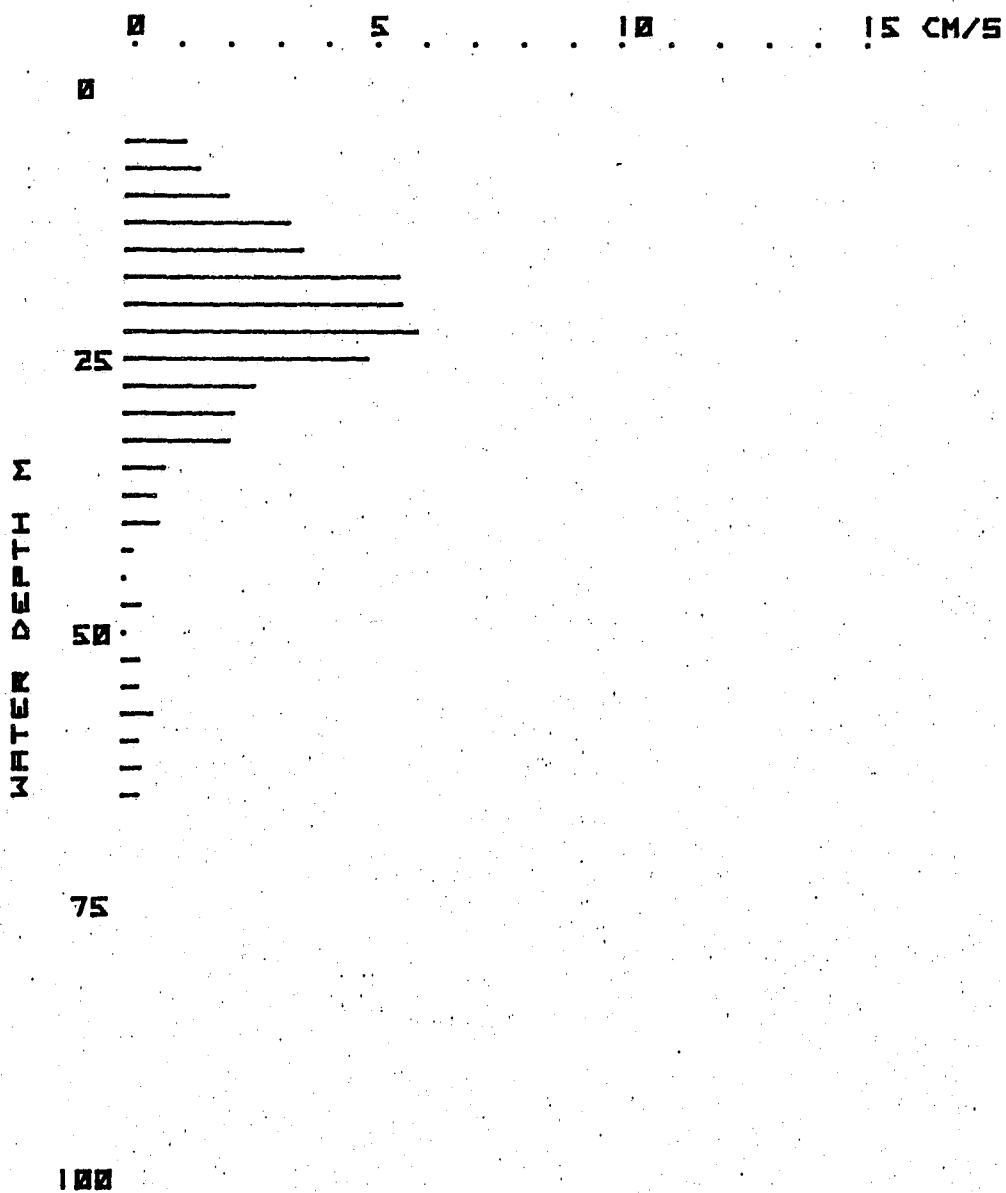
BRIDPORT INLET SITE: UCM-3

21 APR 1980

18: 1 - 18: 13 GMT



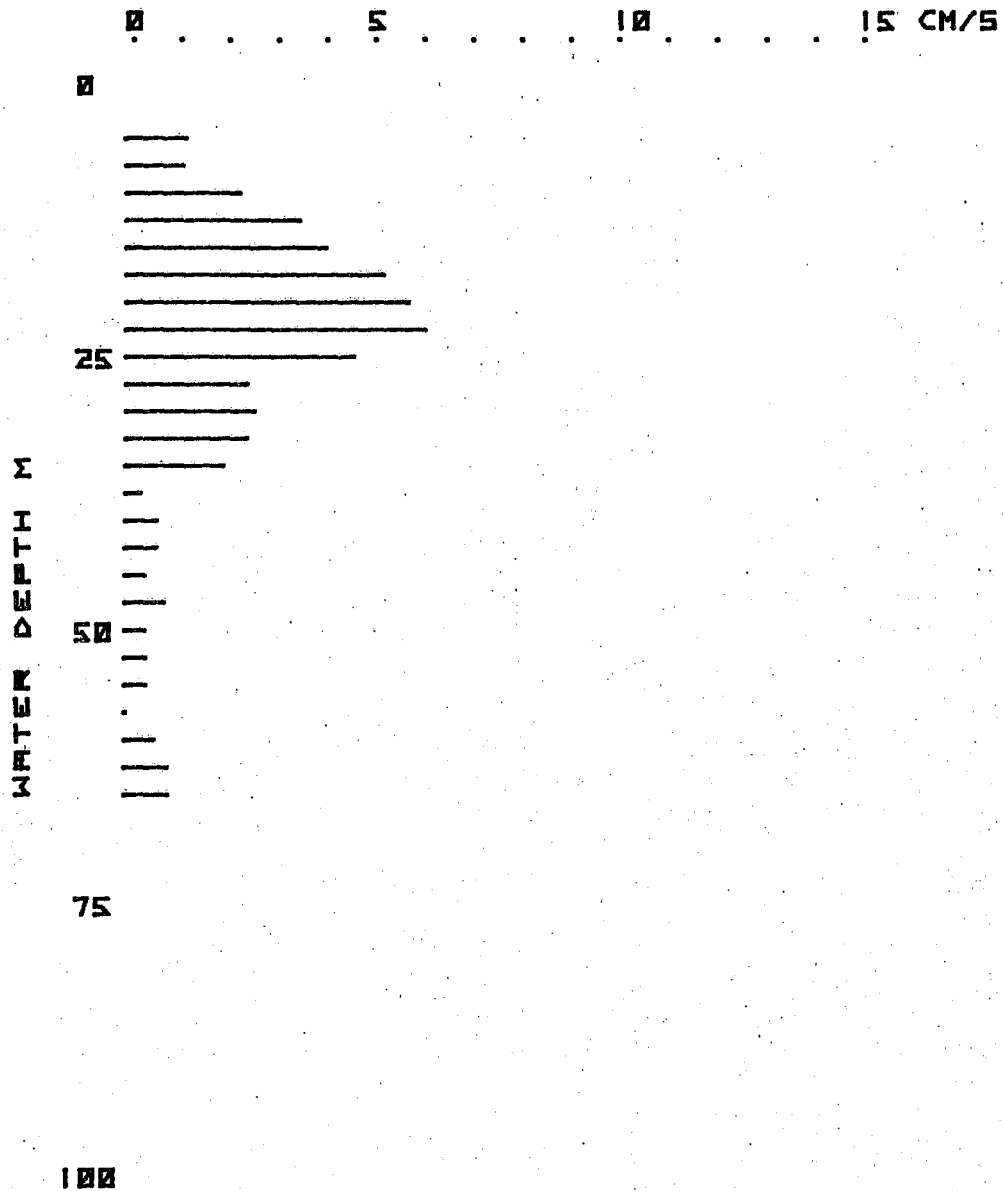
BRIDPORT INLET SITE: UCM-3
21 APR 1980 20: 5 - 20: 17 GMT



BRIDPORT INLET SITE: UCM-3

21 APR 1980

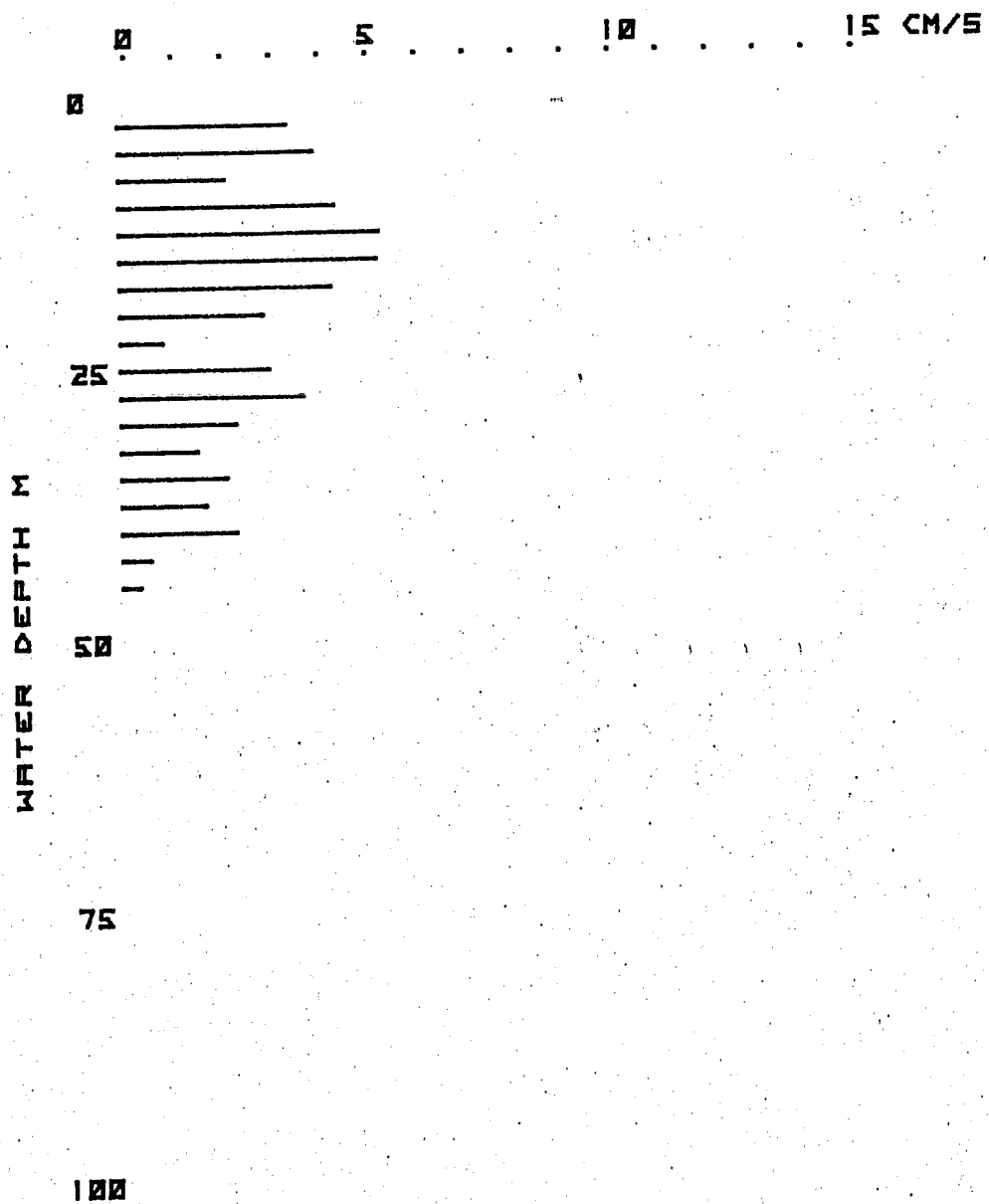
21. 18 - 21. 29 GMT



BRIDPORT INLET SITE: CM-9

18 APR 1980

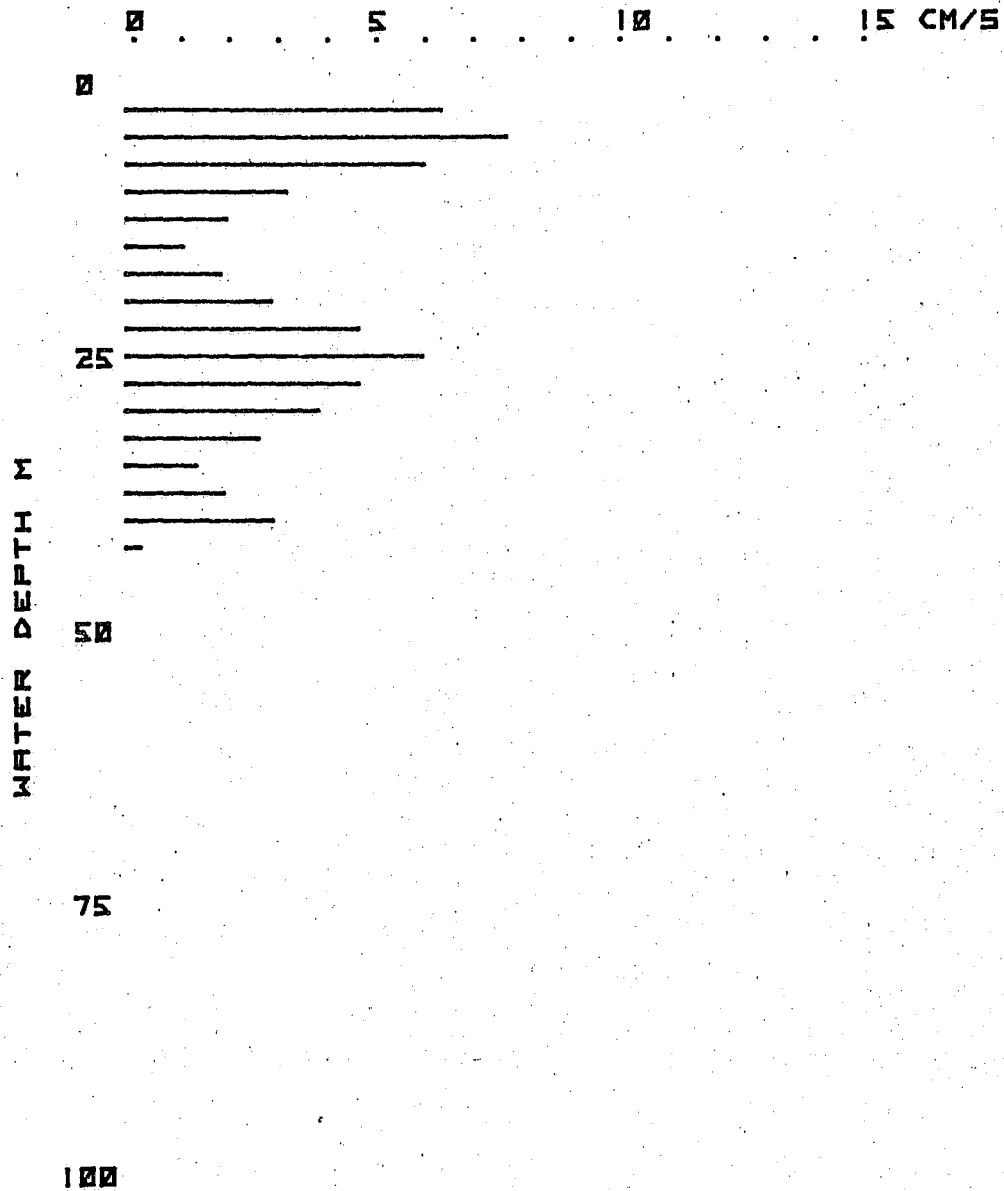
15: 8 - 15: 16 GMT



BRIDPORT INLET SITE: CM-9

18 APR 1980

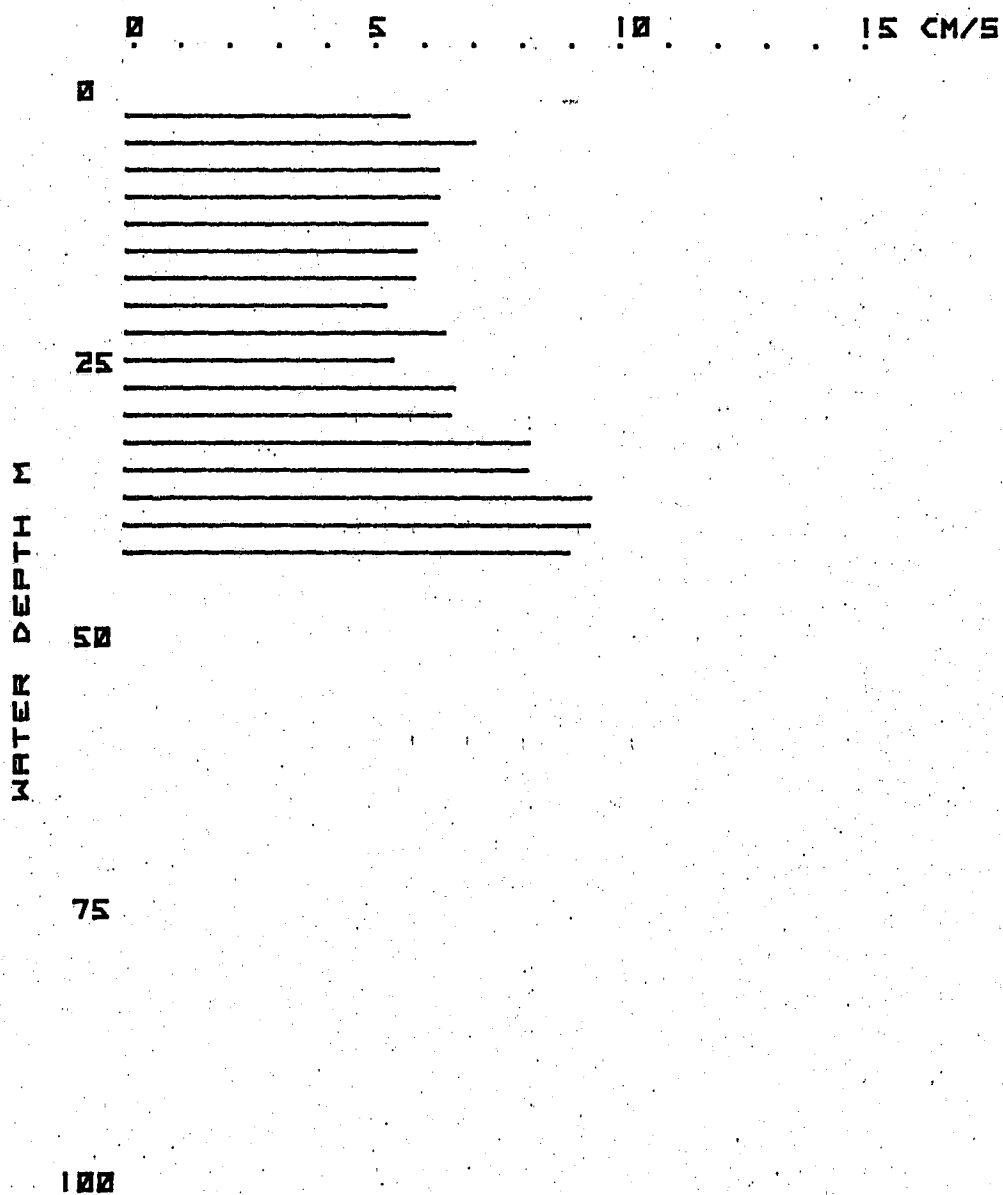
15:30 - 15:36 GMT



BRIDPORT INLET SITE: CM-9

18 APR 1980

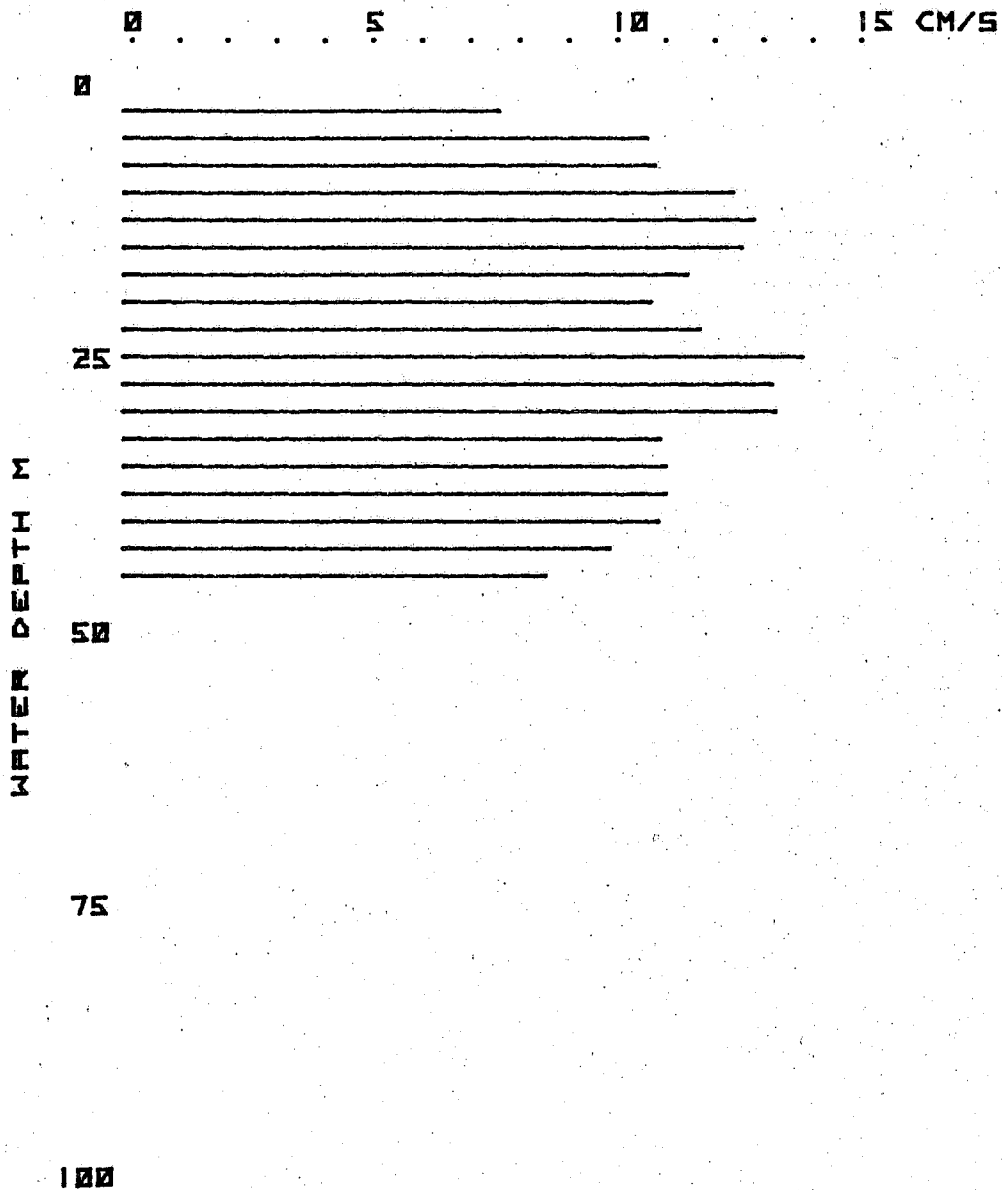
17: 3 - 17: 16 GMT



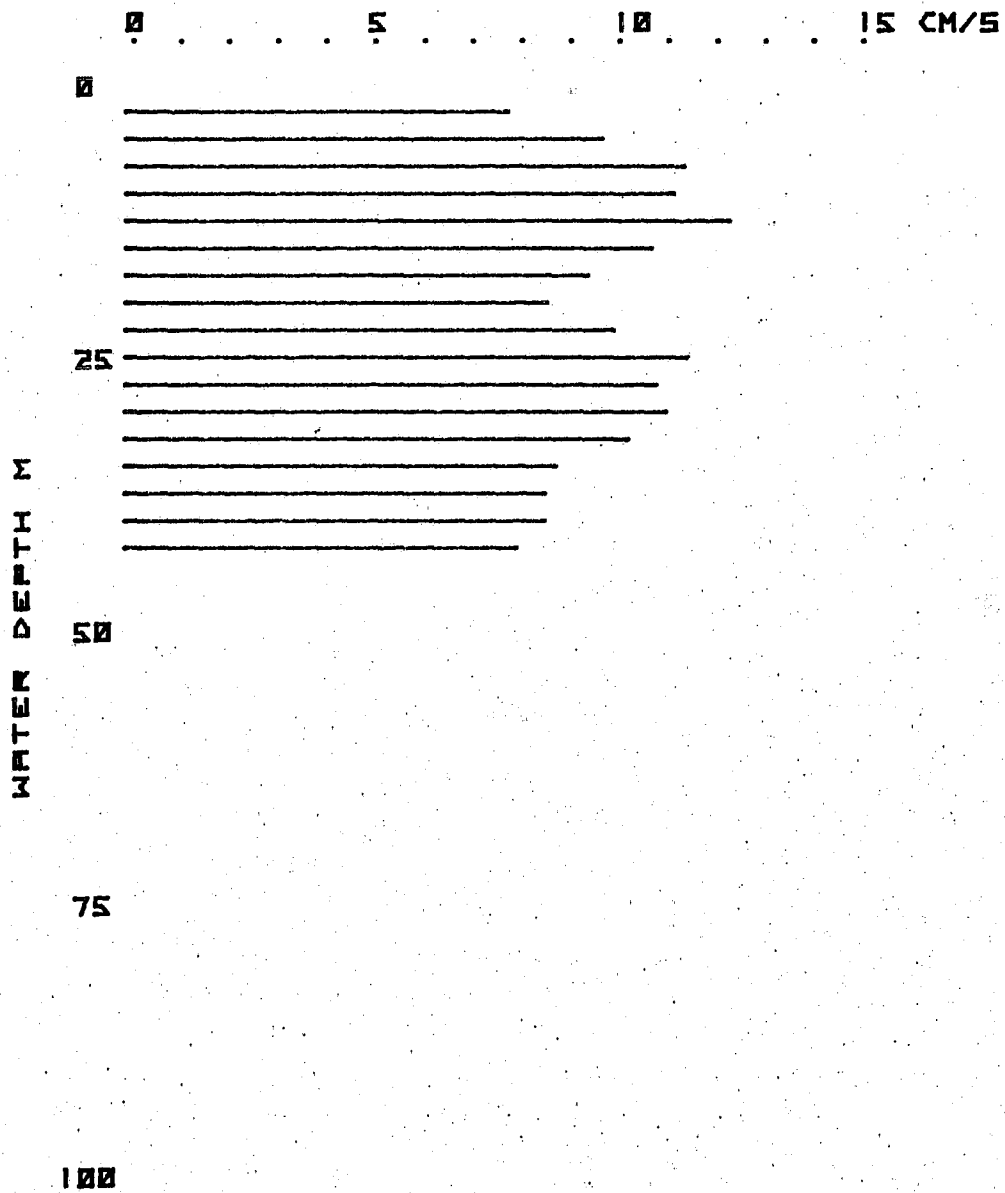
BRIDPORT INLET SITE: CM-9

18 APR 1980

19: 0 - 19: 11 GMT



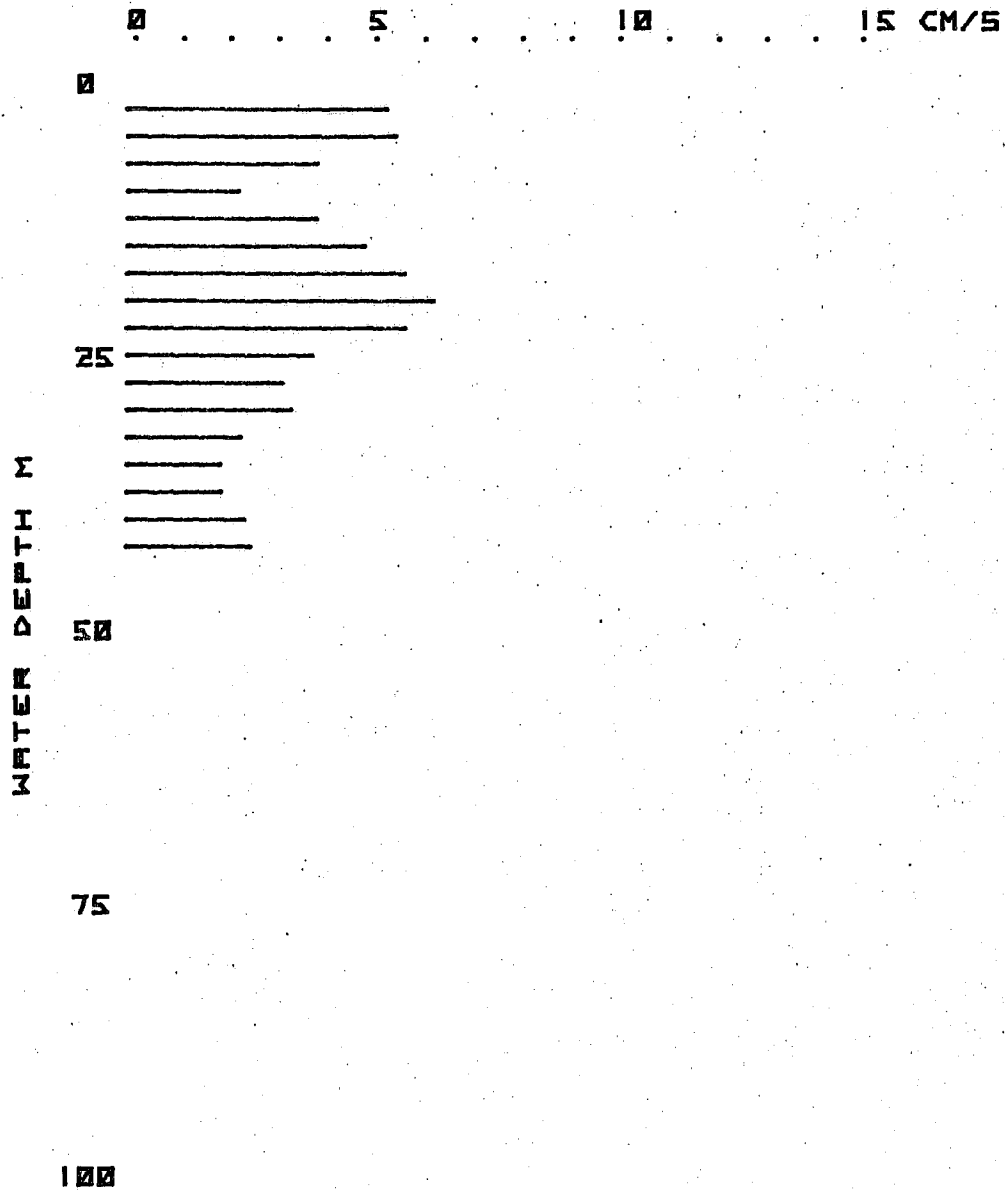
BRIDPORT INLET SITE: CM-9
18 APR 1980 21: 0 - 21: 8 GMT



BRIDPORT INLET SITE: CM-9

19 APR 1980

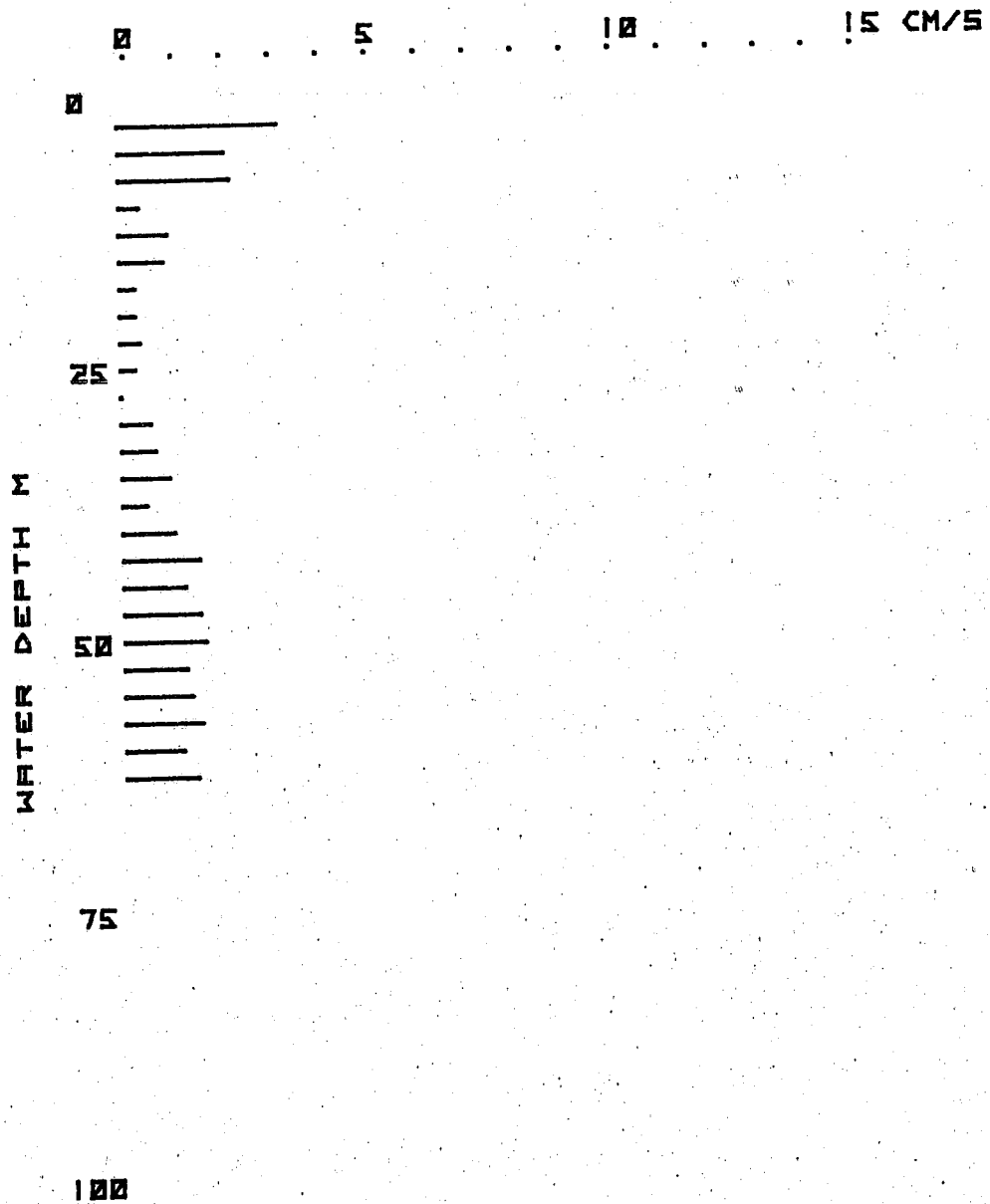
1:20 - 1:29 GMT



BRIDPORT INLET SITE: CM-10

15 APR 1981

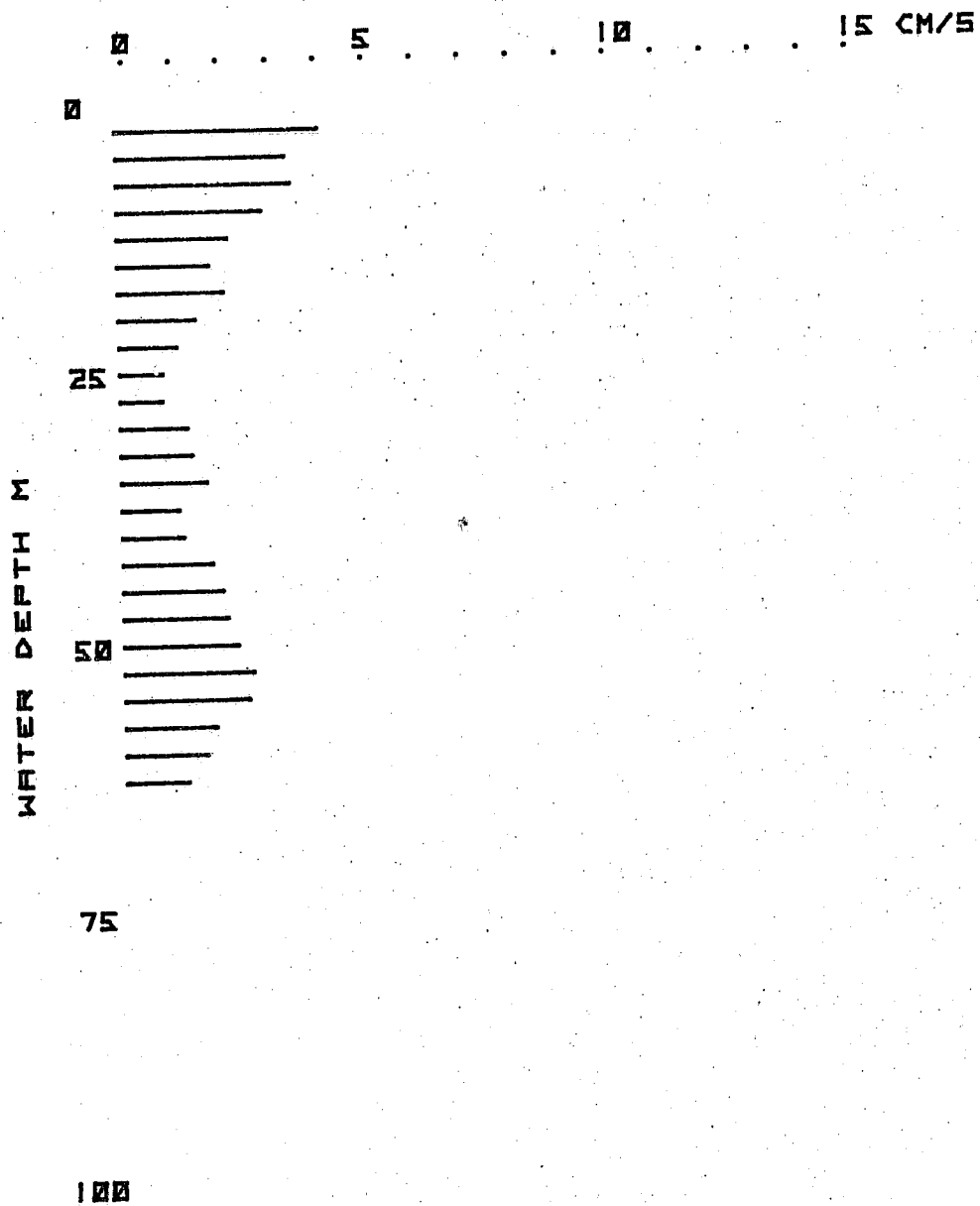
16: 54 - 17: 37 GMT



BRIDPORT INLET SITE: CM-10

15 APR 1980

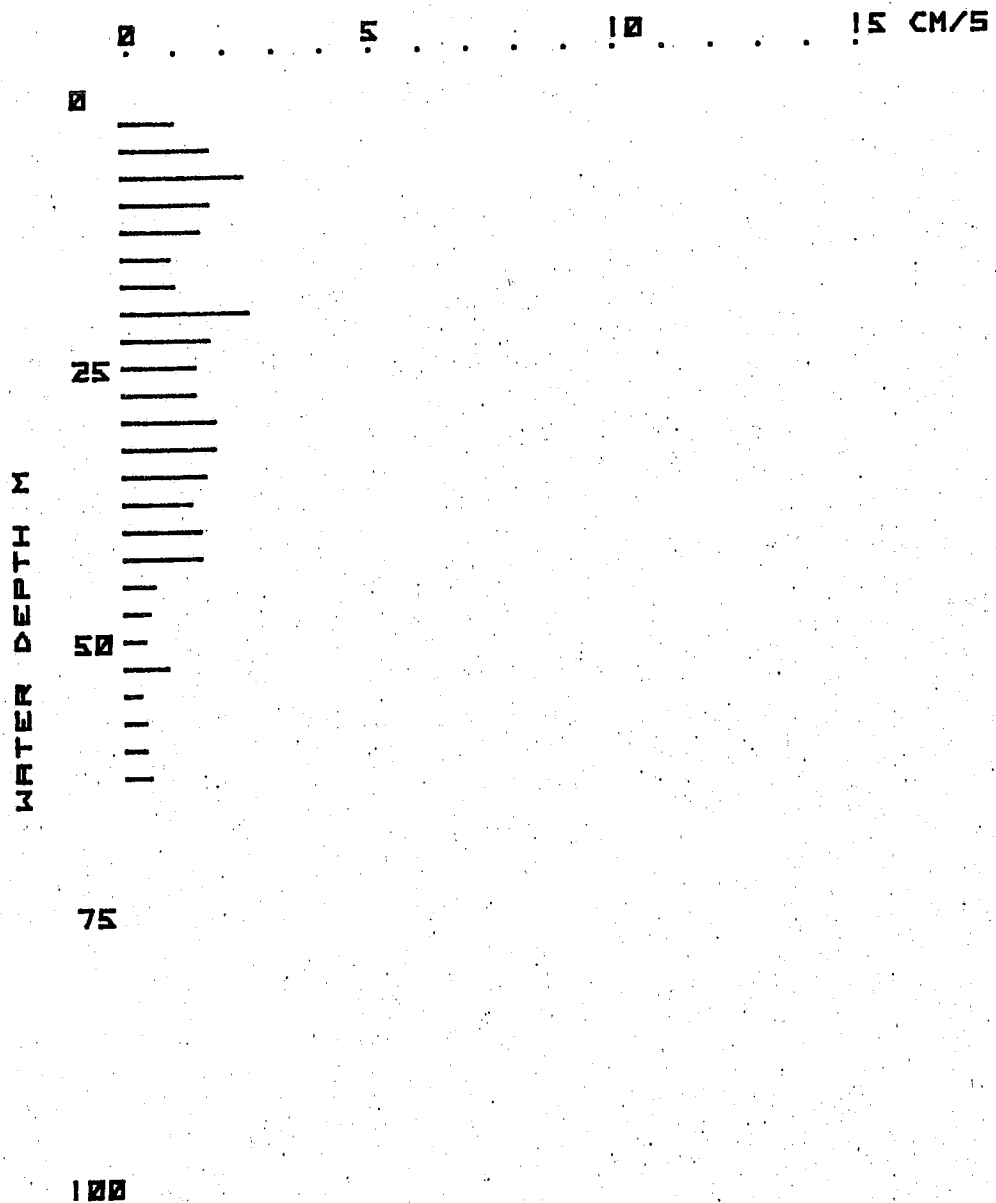
18:58 - 19:34 GMT



BRIDPORT INLET SITE: CM-10

16 APR 1980

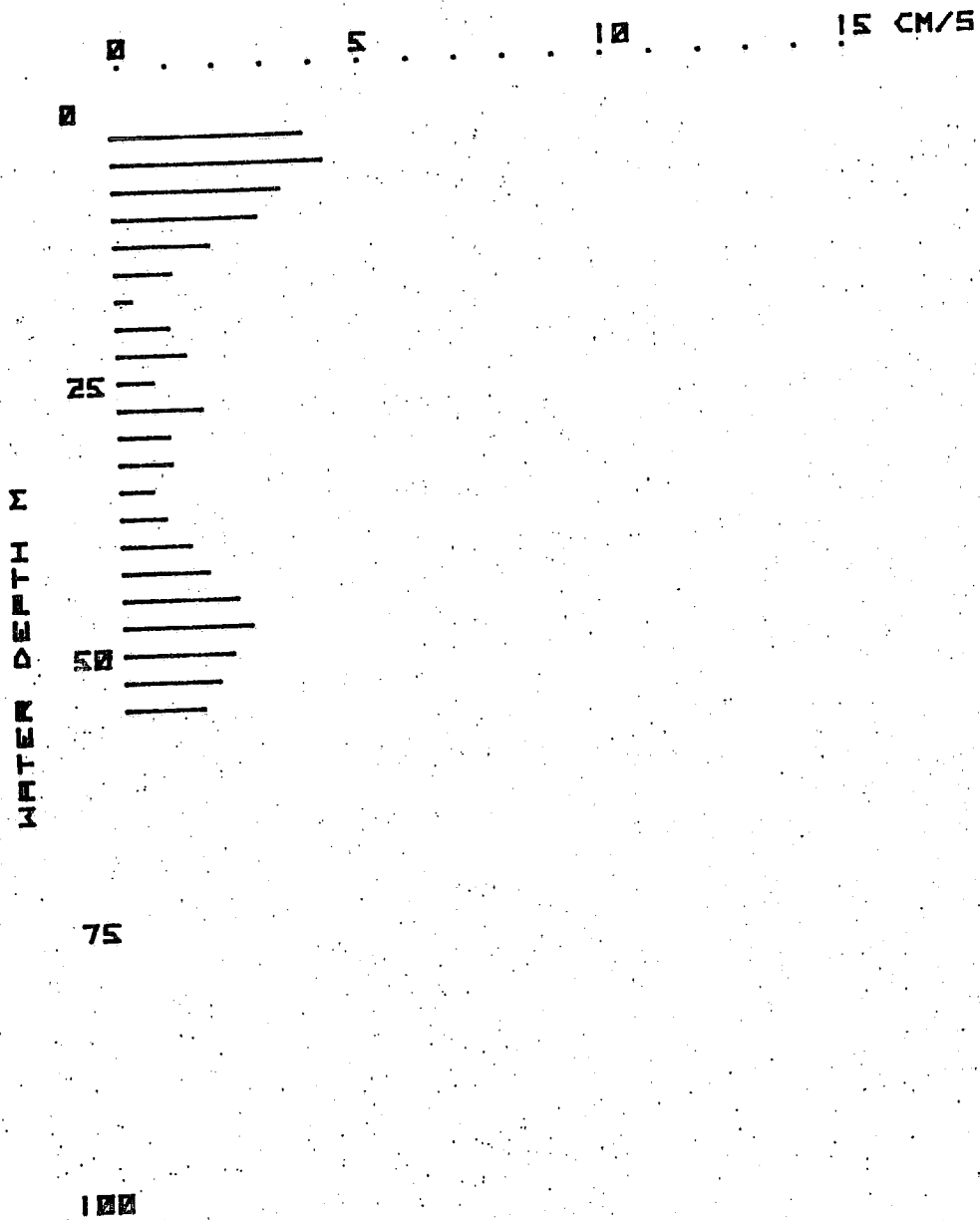
11 55 - 21 33 GMT



BRIDPORT INLET SITE: CM-4

22 APR 1980

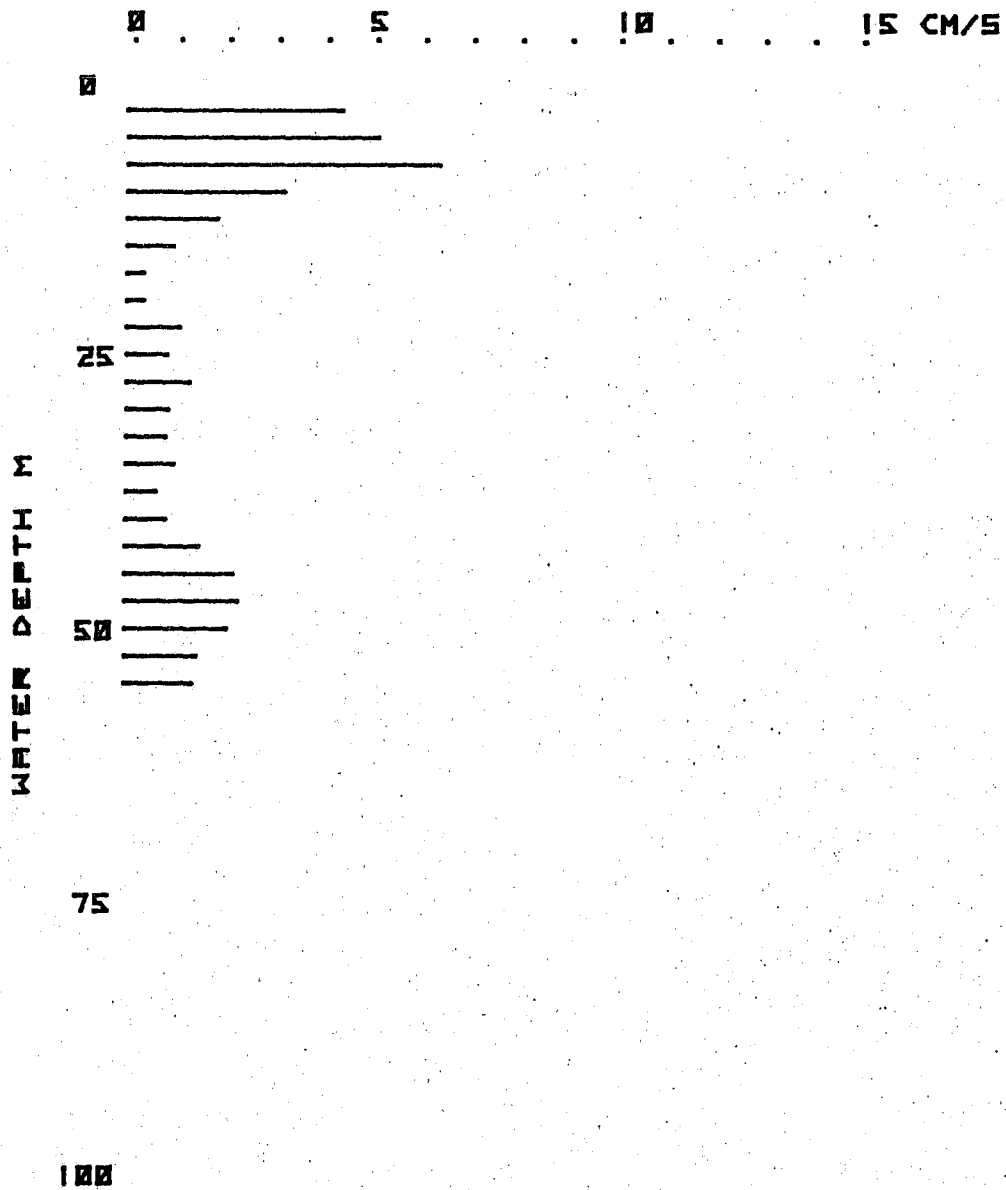
18:25 - 18:34 GMT



BRIDPORT INLET SITE: CM-4

22 APR 1980

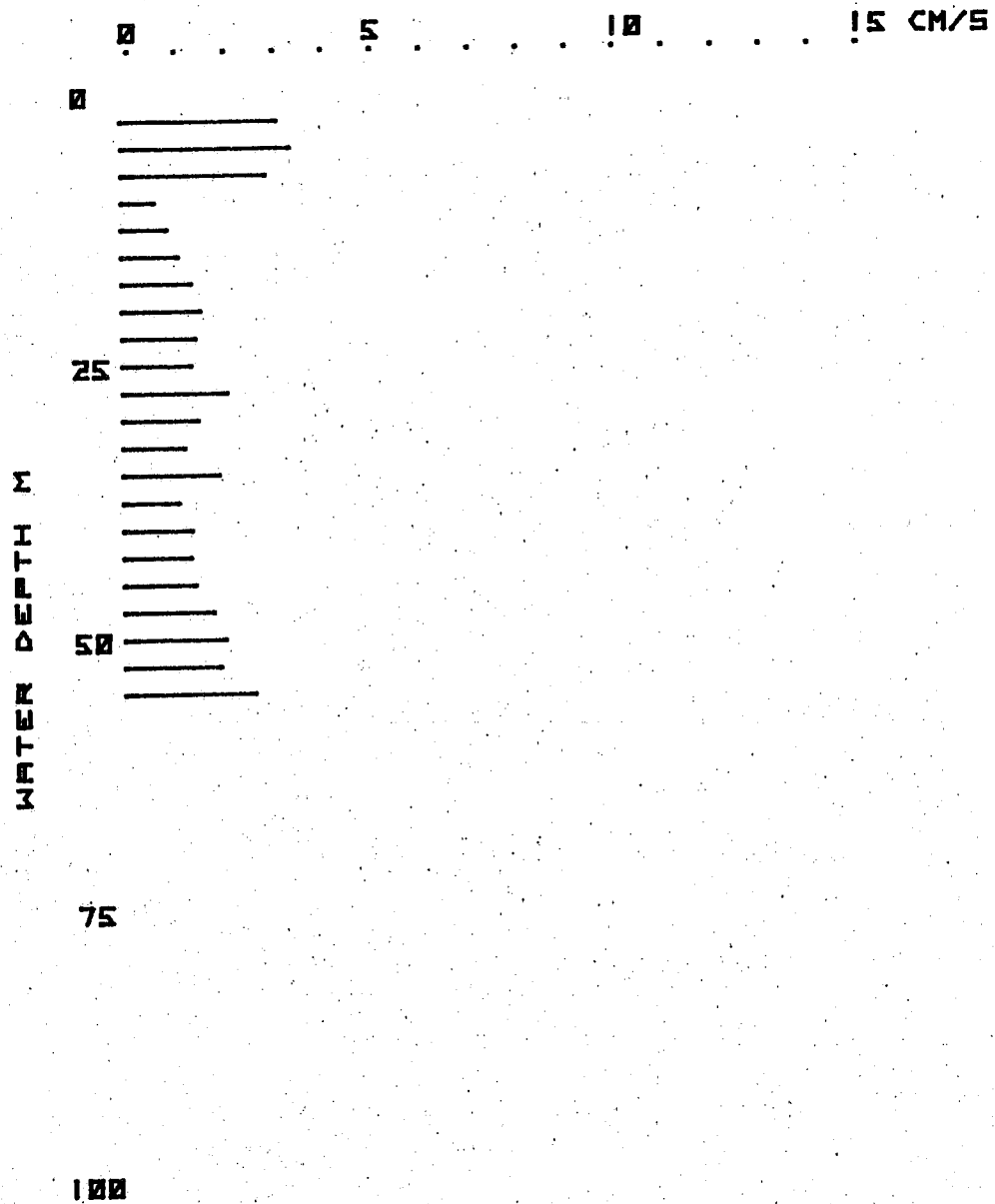
19: 36 - 19: 45 GMT



BRIDPORT INLET SITE: CM-4

22 APR 1980

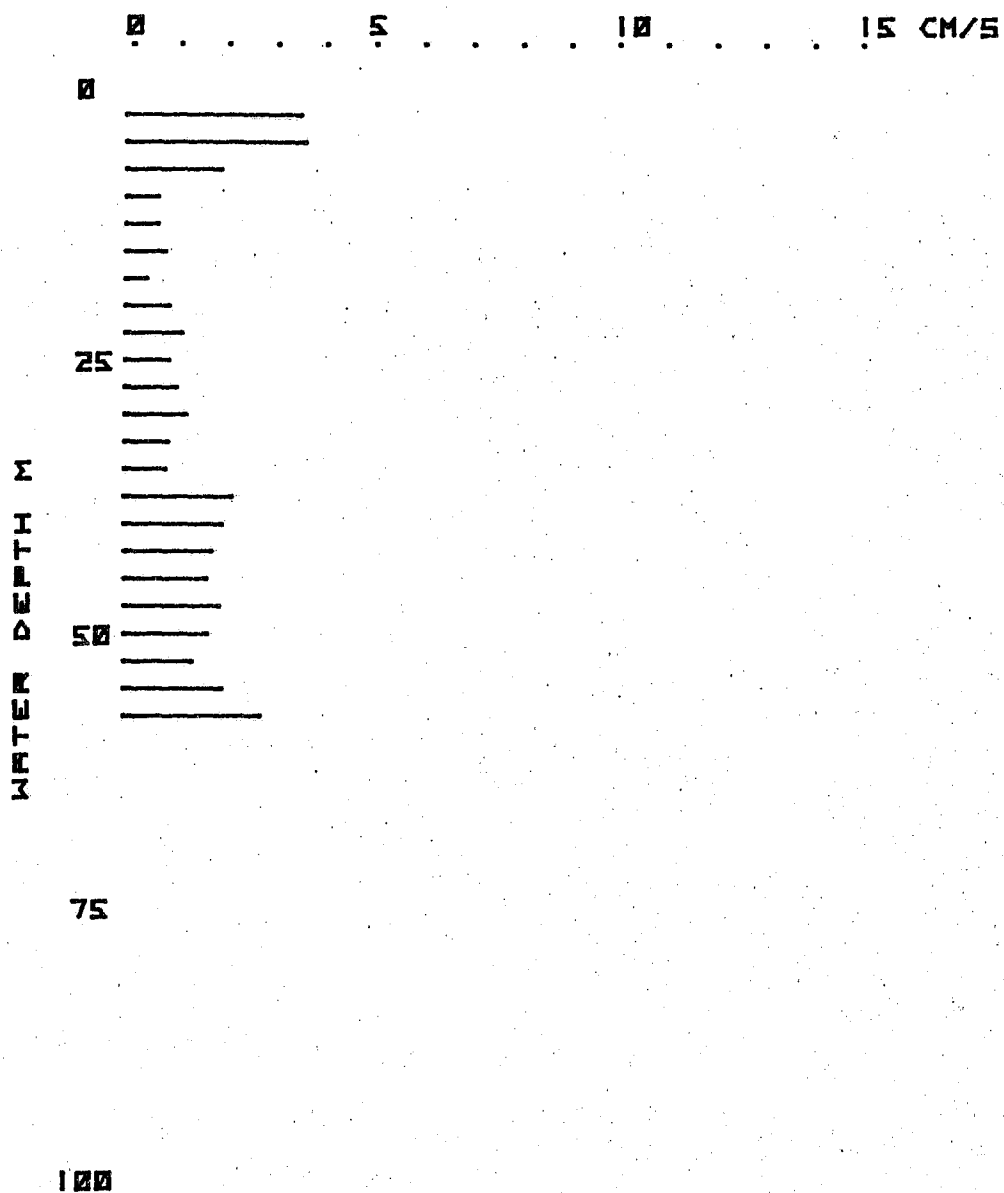
22: 44 - 22: 55 GMT



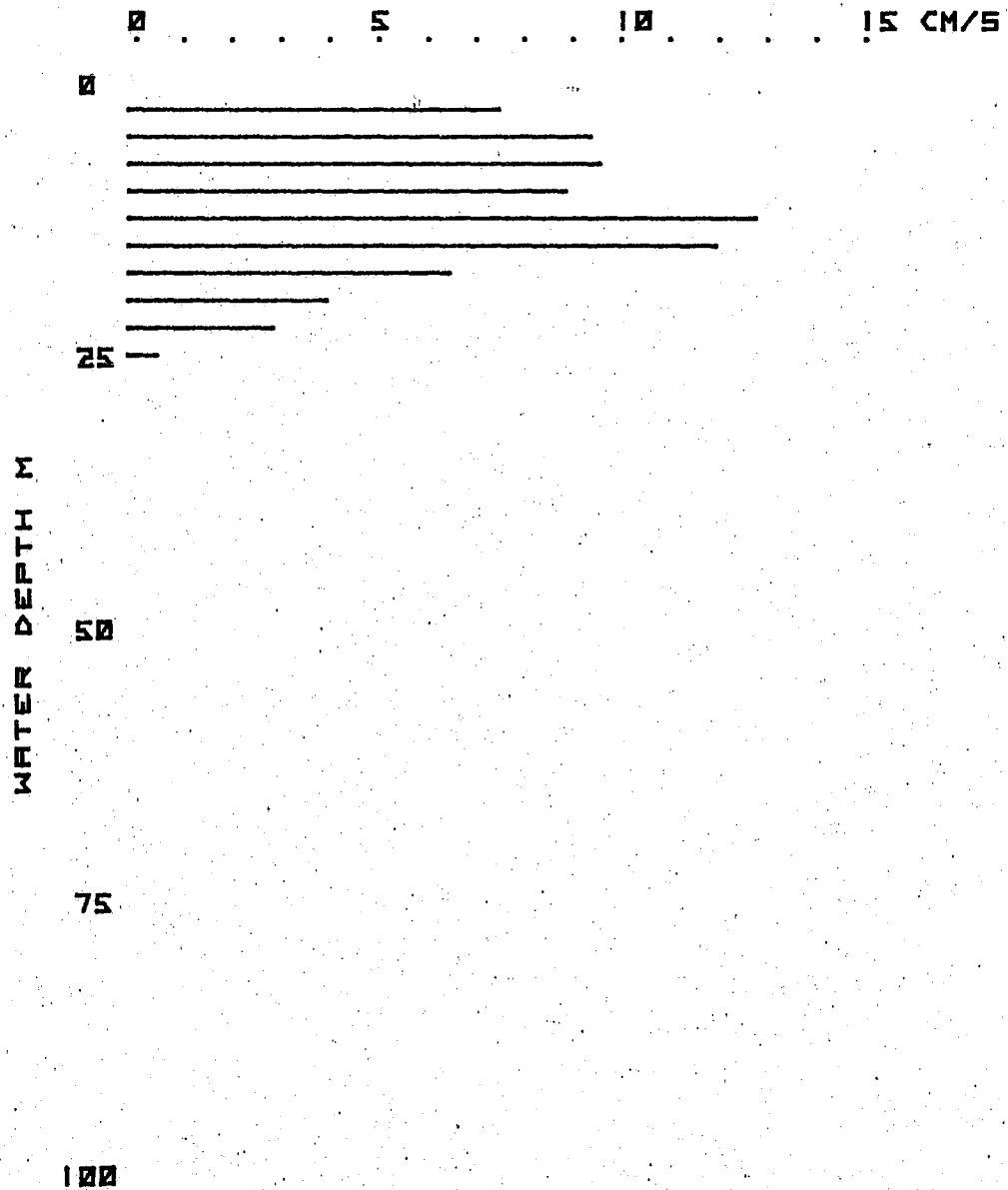
BRIDPORT INLET SITE: CM-4

22 APR 1980

24: 32 - 24: 44 GMT



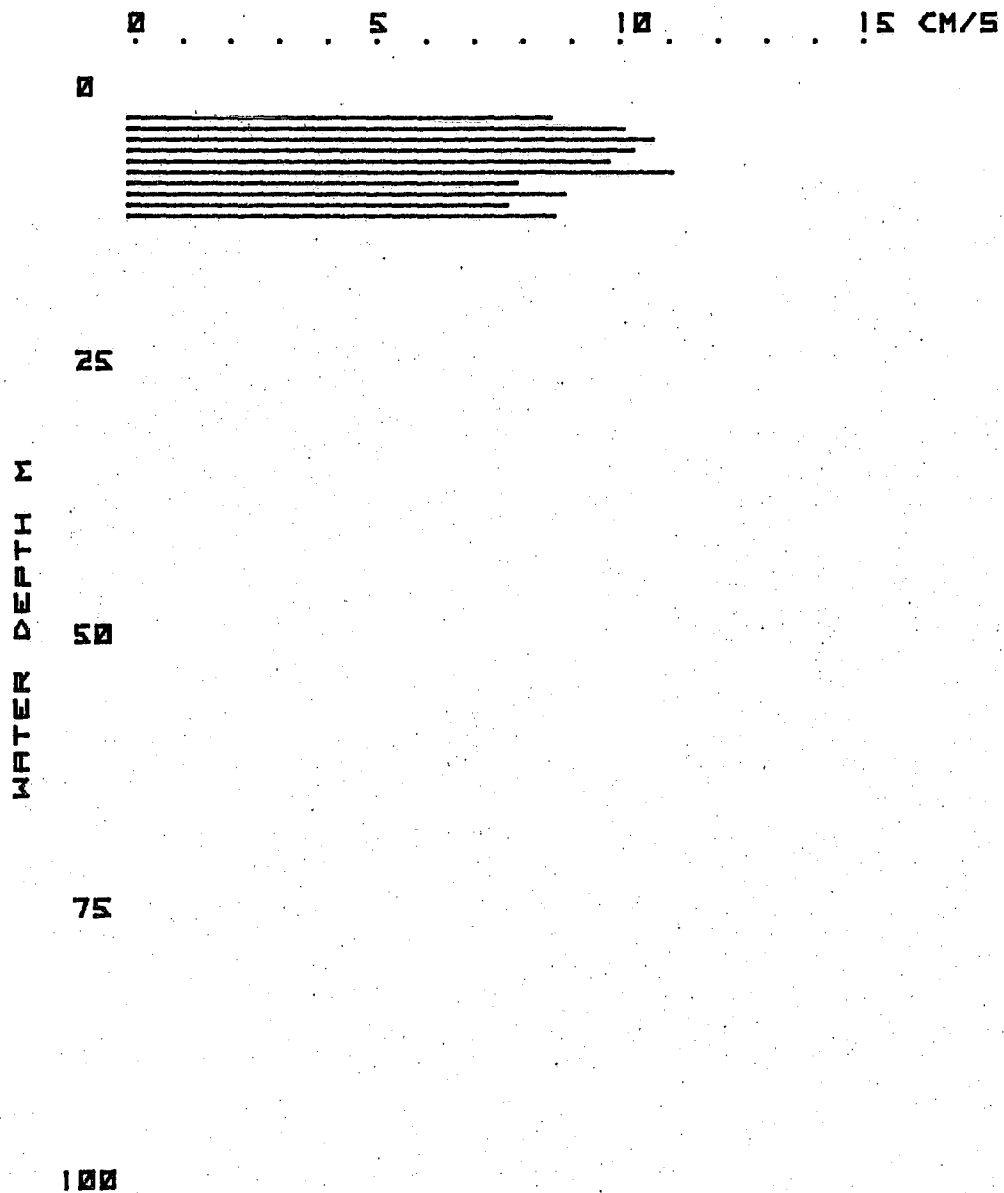
BRIDPORT INLET SITE: CM-5
13 APR 1981 16: 20 - 16: 50 GMT



BRIDPORT INLET SITE: CM-5

13 APR 1981

17: 8 - 17: 32 GMT

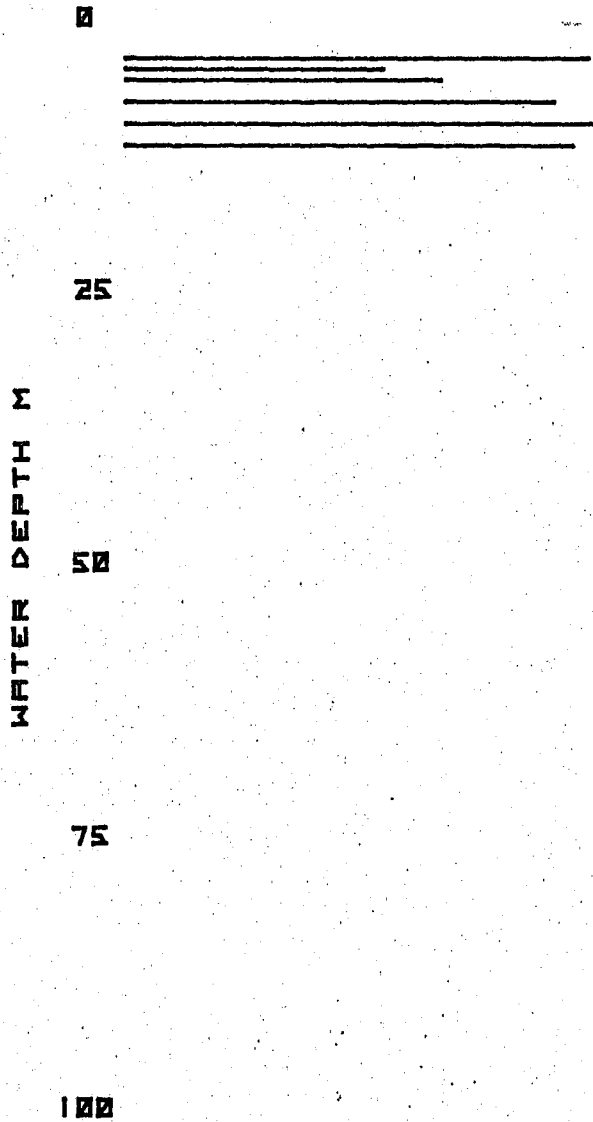


BRIDPORT INLET SITE: CM-5

13 APR 1981

18:5 - 18:50 GMT

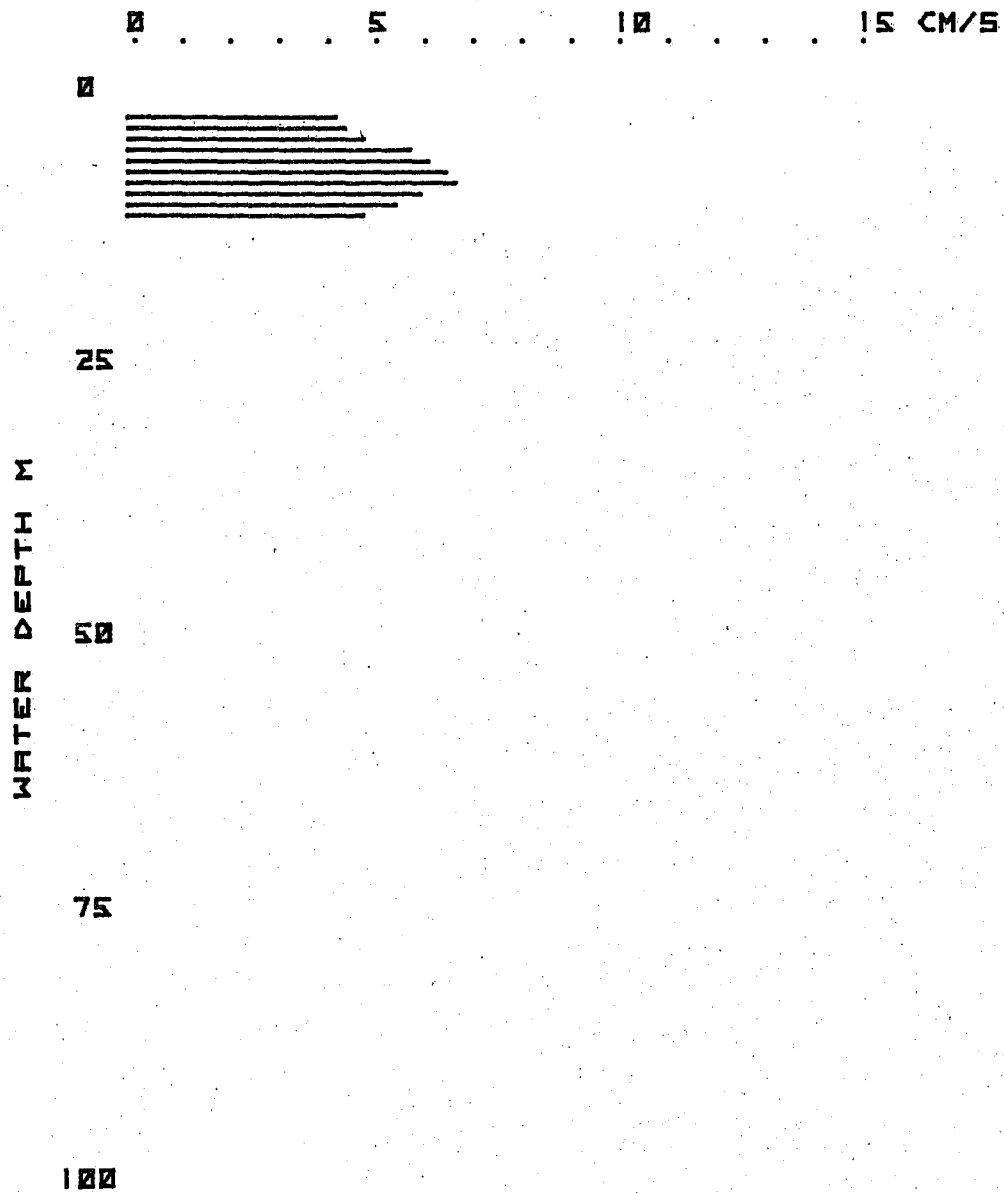
0 5 10 15 CM/S



BRIDPORT INLET SITE: CM-5

13 APR 1981

21: 52 - 22: 17 GMT



BRIDPORT INLET SITE: CM-5

13 APR 1981

22: 30 - 22: 52 GMT

